**Zeitschrift:** IABSE reports of the working commissions = Rapports des commissions de travail AIPC = IVBH Berichte der Arbeitskommissionen

**Band:** 29 (1979)

**Rubrik:** Session I: Constitutive equations - yield criteria

# SESSION I

## Constitutive Equations – Yield Criteria

## Equations de base – Limites d'écoulement

## Fliessbedingungen und Fliessgesetze

Chairman: Prof. K.H. Gerstle, USA

Introductory Lectures: „Constitutive Equations for Concrete"
Prof. W.F. Chen, USA

„Yield Criteria for Elements of Reinforced Concrete Slabs"
Dr. C.T. Morley, Great Britain

(The Introductory Lectures are published in the Introductory Report, Volume AK 28)

Leere Seite
Blank page
Page vide

I

**Failure Criteria for Concrete under Multiaxial Stress States**

Un critère de rupture du béton sous l'effet de contraintes multiaxiales

Bruchbedingungen für Beton unter mehrachsigen Spannungszuständen

J. WASTIELS
Assistant Professor of Civil Constructions
Vrije Universiteit Brussel
Brussels, Belgium

**SUMMARY**
Various failure criteria for multiaxial compression available in literature are compared with selected experimental data. It appears that the biaxial degenerations of some criteria proposed for triaxial compression yield an unexpected shape, while the results obtained in the use of other criterial accord with expectations. Since none of the investigated criteria corresponds completely to the experimental data in the studied triaxial stress range, a failure criterion for multiaxial stress states is proposed.

**RESUME**
Différents critères de rupture du béton sous l'effet d'une compression multiaxiale proposés dans la littérature sont comparés à des résultats expérimentaux. Il s'avère que les dégénérations biaxiales de certains critères pour compression triaxiale présentent une forme inattendue, en désaccord avec les résultats expérimentaux, tandis que d'autres sont satisfaisantes. Parce qu'aucun des critères considérés ne concorde pour tous les états de contraintes triaxiales étudiés avec les résultats expérimentaux, un nouveau critère de rupture du béton sous l'effet de contraintes multiaxiales est proposé.

**ZUSAMMENFASSUNG**
Verschiedene in der Literatur für mehrachsige Druckbeanspruchung vorgeschlagene Bruchbedingungen werden mit ausgelesenen Versuchsergebnissen verglichen. Es zeigt sich, dass gewisse für dreiachsigen Druck aufgestellte Bruchbedingungen für den ebenen Spannungszustand zu einer unerwarteţ schlechten Übereinstimmung mit Versuchsergebnissen führen. Da keine der untersuchten Bedingungen für die betrachteten dreiachsigen Spannungszustände völlig mit den Versuchsergebnissen übereinstimmt, wird eine neue Bruchbedingung für mehrachsige Spannungszustände vorgeschlagen.

## 1. EXPERIMENTAL DATA

Since the beginning of the century, a lot of experimental investigations were performed to determine the strength of concrete under multiaxial stress states. However, the behaviour of concrete being very complex [1], the experimental conditions often are not those one wants or supposes to obtain. The occuring problems, lying outside the subject of this paper, are treated profoundly by HILSDORF [2] and KUPFER [3]. Only recently these problems were solved in a more or less satisfying manner. A critical attitude towards experimental data is indispensable, and leads to elimination of many of them. A comprehensive study of experimental investigations available in literature was made in [4], without claiming completeness. The retained compressive data, represented on the figures, were extracted from references [5] to [9].

## 2. EXISTING CRITERIA

Following conventions are used : $\sigma_1 \geqslant \sigma_2 \geqslant \sigma_3$ are the principal stresses, compression being negative. Three invariants of the stress tensor are used : the octahedral normal stress $\sigma_{oct}$, the octahedral shear stress $\tau_{oct}$, and the Lode angle $\theta$, defined as follows :

$$\sigma_{oct} = \frac{1}{3}(\sigma_1 + \sigma_2 + \sigma_3)$$

$$\tau_{oct} = \frac{1}{3}\left[(\sigma_1-\sigma_2)^2 + (\sigma_2-\sigma_3)^2 + (\sigma_3-\sigma_1)^2\right]^{1/2} \qquad (1)$$

$$\cos\theta = (2\sigma_1 - \sigma_2 - \sigma_3) / (3\sqrt{2}\,\tau_{oct}) \qquad 0° \leqslant \theta \leqslant 60°$$

The stress ratios are defined as $k_1 = \sigma_1/\sigma_3$ and $k_2 = \sigma_2/\sigma_3$.
The investigated failure criteria were drawn using a proportional stress increase (constant $k_1$ and $k_2$) up to the point where failure is predicted by the criterion. This technique seemed the most logical one : it is the only way of obtaining a unique solution for all criteria and for all stress states. Moreover, the criteria in question are almost exclusively used in finite element applications, where an incremental force (or displacement) technique is used in nonlinear computations, so that the stress increase is roughly proportional. The loading path of a proportional stress increase is represented both in principal stress and in octahedral stress coordinates by a straight line through the origin, the slope being a function of $k_1$ and $k_2$, as follows from (1).

### 2.1. Biaxial compression

Seventeen criteria are drawn on figures 1 and 2, together with the biaxial experimental data from refs. [5] to [9], in principal stress coordinates normalised by $R'_{br}$, the absolute value of the uniaxial compressive strength. When parameters need to be determined, it is assumed that the uniaxial strength equals $-R'_{br}$, that in compression the equibiaxial strength equals $\beta = 1.16$ times the uniaxial strength and that the ratio between $R'_{br}$ and the tensile strength $R_{br}$ equals 10. The comparison of a criterion to the experimental data is done through the values MRSD (Mean Relative Square Deviation) and RDEV (Relative DEViation) :

$$MRSD = \frac{1}{n}\sum_{i=1}^{m} n_i \frac{(OP-OQ)^2}{OQ^2}$$

$$RDEV = \frac{1}{n}\sum_{i=1}^{m} n_i \frac{OP-OQ}{OQ} \qquad (2)$$

where m is the number of different values of $k_2$ in the experiments, $n_i$ is the number of experiments for one value of $k_2$, and $n = \sum_{i=1}^{m} n_i$ is the total number of experiments. The point P represents failure during the experiment, while Q, laying on the straight line OP through the origin O, represents the failure predicted by the criterion. It can be seen that P and Q share the same stress ratio $k_2$. A criterion gives a good approximation to the experimental data when MRSD and RDEV are small, and a safe one when RDEV is positive. The values of MRSD and RDEV are given in Table 1.

| Criterion | MRSD.$10^3$ | RDEV.$10^3$ |
|---|---|---|
| [10] | 1.34 | + 10 |
| [11] | 3.57 | + 33 |
| [7] | 0.99 | - 2.2 |
| [12] | 1.18 | + 12 |
| [13] | 1.29 | + 10 |
| [14] | 2.30 | + 19 |
| [15] | 2.15 | - 18 |
| [17] | 3.92 | + 41 |
| [18] (3p) | 3.28 | - 26 |
| [18] (5p) | 1.61 | - 14 |
| [19] | 37.10 | + 186 |
| [20] | 75.10 | - 197 |
| [22] | 79.36 | - 200 |
| [23] | 143.03 | - 208 |
| Author | 0.89 | + 1.4 |

Table 1 Correspondence between experimental data and criteria for biaxial compression.

The conclusion can be drawn that all the criteria presented on figure 1 behave in a more or less satisfying manner, with [19] on the safe side (the definition of admissible stress is more stringent), and [15] and [18] on the unsafe side. The choice of a criterion can thus be guided by additional requirements, such as continuity of the slope for equibiaxial stresses, or simplicity of the analytical formulation. The criterion of DRUCKER - PRAGER [10] with adapted parameters offers a good and simple approximation.

The four criteria represented on figure 2 are striking by their strong deviation from the experimental data. For [21] the reason herefore is evident : it is based upon not retained (because unreliable) experimental data. For the remaining three, which were proposed for triaxial compression, the reason can be found in the ambiguity of representing a triaxial stress state in octahedral coordinates, as will be mentioned in next section. On the other hand, one can easily check that wen these criteria are computed in a different way, the correspondence to the experimental data is much better : when the experimental values of $\sigma_{oct}$ and $\theta$ at failure during an experiment are substituted in the criterion, the value of $\tau_{oct}$ for which the criterion predicts failure is considerably nearer to the experimental one than the value which would be obtained by proportional stress increase. Unfortunately, this way of reasoning is completely erroneous : indeed, the stress state for which failure is predicted is not a biaxial one, as can be easily computed by inverting (1), and comparison to experiment has no sense.

## 2.2. Triaxial compression

Inspection of the experimental data leads to the conclusion that the failure criterion must be dependent upon all three stress invariants of (1). Representing the criterion in octahedral axes implies the use of $\theta$ as a parameter. On figures 3 to 9, the criteria are drawn for the values $\theta = 0°$, 30° and 60° (from the bottom upwards), together with the corresponding experimental data, respectively marked by squares, circles and asterisks. The stress region studied is limited to $|\sigma_{oct}| \leq 1.5\ R'_{br}$. Following conclusions can be drawn :

- criterion [13] is represented on figure 3 by a unique curve, since it contains only two invariants. It becomes more and more conservative with increasing values of $\sigma_{oct}$ and $\theta$.

- the other criteria all give a good approximation for $\theta = 0$ (lower curve). Criterion [19] lies below the experiments since the definition of admissible stress is more stringent.

- for $\theta = 60°$ however (upper curve), only a few criteria do correspond to the experiments, namely [19] (figure 4) and [18] (5 parameters, figure 5 - the parameters given by the authors were however changed). All the other criteria are lying above the experimental data. Although the difference does not seem to be critical, it really is. This is demonstrated on figure 10 : suppose a proportional loading path OA with a certain value of $\theta$, and the corresponding trace in octahedral stresses of the failure criterion for that value of $\theta$. Consider three proportional stress states A, B and C of different magnitude, as indicated on figure 10, where B is the failure stress predicted by the criterion. When the slope of the criterion is nearly equal to that of the loading path, as is the case in figure 10, and also for $\theta = 60°$ for most criteria, the "corresponding" points A' and C' do not differ much in ordinate from a respectively C. Suppose now that A is the failure stress state experimentally obtained, instead of B. The one would conclude from the fact of A' being near to A, that the criterion describes well failure, although it only predicts failure at the double magnitude (point B). It can thus be concluded, that the presented experimental results for $\theta = 60°$ (asterisks) are much more "distant" from the failure criteria [15], [18] (3 parameters), [20], [22] and [23] than would be expected from the figures. As an example, [18] (3p) and [23] do not predict failure for $\theta = 60°$ for a proportional stress increase with $k_1 = k_2 \geqslant 0.099$, [20] and [22] for $k_1 = k_2 \geqslant 0.184$, while experimentally [9] failure occurs already at $\sigma_{oct} = -1.5\ \bar{R}'_{br}$ for $k_1 = k_2 = 0.205$ .

- for $\theta = 30°$, the corresponding of the criteria to experimental data is somewhat intermediate between the corresponding for $\theta = 0$ and $\theta = 60°$. This means that the dependence of the criteria upon $\theta$ is good, but also for [15] and [18] (3p) that the predicted failure stresses are too high, as can be seen on figures 7 and 6. Exceptions to this are criteria [20], [22] and [23], for which the interpolation function is not satisfying. Besides the fact that the predicted failure stresses are too high, the meridian is only represented for $|\sigma_{oct}| > 1.44\ R'_{br}$ on figure 8, ([20] and [22] share the same meridians for $\theta = 0$, 30° and 60°) and it is traced in dotted line on figure 9 for [23]. The reason for this is that the region in octahedral coordinates, where triaxial stresses can exist, is limited, so that the criterion for triaxial compression is a bounded curve. This is a fact that is often overlooked. Space limitations are preventing a complete analysis, but it can be said that the region where triaxial compression with a certain value of $\theta$ can exist is limited by a straight line through the origin, the slope of which is depending upon $\theta$. The intersection of this line with the meridian of the criterion for that value of $\theta$ is a point of biaxial compression, and the section of the meridian with $|\sigma_{oct}|$ lower than this "limit point" represents stress states of compression-compression-tension ! Now if the criterion is not supposed to be valid for other stress states than triaxial compression, this section has no sense. The problem is that the "limit point" is not apparent in octahedral coordinates, as it would be in principal stress coordinates. The extremity on the right of the meridians represented on the figures is precisely this "limit point". On figure 8, the abscis of the "limit point" for $\theta = 30°$ is approximately - 1.44, and the meridian is limited to that point since criteria [20] and [22] are not assumed to be valid for tension-compression stress states. This is well assumed for [23], but the abscis of the "limit point" for $\theta = 30°$ is approximately - 2.57, so that the complete section on figure 9 represents tension-compression stress states, and is traced in dotted line. Anyhow, it is lying well above the experimental data. It is hoped that a more comprehensive study of these phenomena will be published in the near future.

- the locus of the "limit points" represents the failure criterion for biaxial compression. It can be suspected from figures 8 and 9 that for the criteria in question, this will have a bulged shape in octahedral coordinates (and also in principal stress coordinates). This is confirmed by figure 2.

## 3. PROPOSED CRITERION FOR MULTIAXIAL STRESS STATES

Since none of the investigated criteria correspond to the experimental data for the complete stress region studied, a criterion is proposed, based on the experimental data [5] to [9] and taking into account following conditions :

- a regression is made of the experimental octahedral stresses, for $\theta = 0$ and $\theta = 60°$. A linear regression seems appropriate, due to the good linearity of the data in the studied stress region ($|\sigma_{oct}| \leq 1.5\ R'_{br}$). The regression needs to be performed in polar coordinates, with the angle as independent coordinate (cfr. the dangers mentioned in 2.2).

- the meridians must pass through the points of uniaxial and equibiaxial compressive strength. The latter equals $\beta = 1.16$ times the former.

- the interpolation function in $\theta$ must be continuous and convex. The elliptic function proposed by WILLAM and WARNKE [18] is used. Considering this, following criterion is proposed for multiaxial compression :

$$\frac{\tau_{oct}}{R'_{br}} = \frac{2C(C^2-T^2)\cos\theta + C(2T-C)\left[4(C^2-T^2)\cos^2\theta + 5T^2 - 4TC\right]^{1/2}}{4(C^2-T^2)\cos^2\theta + (C-2T)^2}$$

$$\text{with} \quad T = 0.12051 - 0.55128\ \sigma_{oct}/R'_{br}$$
$$C = 0.25834 - 0.63917\ \sigma_{oct}/R'_{br} \qquad (3)$$
$$|\sigma_{oct}| \leq 1.5\ R'_{br}$$

C and T, the dimensionless octahedral shear stress values for the compressive ($\theta = 60°$) and tensile ($\theta = 0°$) meridians of the criterion, are determined by regression of the experimental data. This criterion has the same analytical formulation as [19], although it was drawn up independently. However, the parameters are not the same, thus yielding different results. The criterion is represented on figure 11. It can be noticed that also for $\theta = 30°$ the criterion corresponds very well to the experimental data, though no use of this data was made to construct the criterion. Its trace for biaxial compression is represented on figure 1, together with the other criteria. The correspondence to the experimental data is better than that of all other criteria, as appears in table 1, though no use of the biaxial data was made to construct the criterion, except uniaxial and equibiaxial strength. This proves that the elliptic interpolation function proposed in [18] is really the best one can choose, and suggests that also for triaxial compression there is good agreement with experimental results for all values of $\theta$.
For compression-tension stress states, the same interpolation function as (3) is proposed, but T and C are replaced by :

$$T = \frac{\sqrt{2}\,\alpha\beta}{2\beta+\alpha} - \frac{\sqrt{2}\,(\beta-\alpha)}{2\beta+\alpha}\,\sigma_{oct}/R'_{br}$$
$$C = \frac{\sqrt{2}\,\alpha\beta}{3\alpha\beta+\beta-\alpha} - \frac{\sqrt{2}\,(\beta-\alpha)}{3\alpha\beta+\beta-\alpha}\,\sigma_{oct}/R'_{br} \qquad (4)$$

with $\alpha = R_{br}/R'_{br}$ (= 0.1 on figure 11) ; $\beta = 1.16$ .
These meridians satisfy continuity with the triaxial compression criterion,

share the same intersection with the octahedral stress axis, and the first one satisfies the tensile strength $R_{br}$. Comparison to experimental data is difficult to check, due to the scarcity of reliable experimental data. Agreement with [8] is good for low tensile stresses, but not so well for low compressive stresses. Tensile strength $R_{br}$ was however not determined experimentally in [8], which may possibly explain the deviation.

REFERENCES


1. WASTIELS, J.: Behaviour of concrete under multiaxial stresses : a review. Cement and Concrete Research, V9, n°1, Jan. 1979, pp. 35-46.
2. HILSDORF, H.: Versuchstechnische Probleme beim Studium der zweiachsigen Festigkeit des Betons. Deutscher Ausschuss für Stahlbeton, Heft 173, Berlin 1965.
3. KUPFER, H.: Das verhalten des Betons under mehrachsiger Kurzzeitbelastung unter besonderer Berücksichtigung der zweiachsigen Beanspruchung. Deutscher Ausschuss für Stahlbeton, Heft 229, Berlin 1973.
4. WASTIELS, J.: Experimentele resultaten en breukcriteria voor beton onder multiaxiale belasting (in Dutch). Internal report, Vrije Universiteit Brussel, 1979.
5. KUPFER, H., HILSDORF, H., RUSCH, H.: Behaviour of concrete under biaxial stresses. ACI Journal, Proc. V66, n°8, Aug. 1969, pp. 656-666.
6. NELISSEN, L.: Biaxial testing of normal concrete. Heron, vol.18, n°1, 1972.
7. PANDIT, G., TANWANI, N.: Behaviour of concrete in biaxial compression. Indian Concrete Journal, V49, n°2, Feb. 1975, pp. 39-45.
8. BREMER, F., STEINSDORFER, F.: Bruchfestigkeiten und Bruchverformung von Beton unter Mehraxialer Belastung bei Raumtemperatur. Deutscher Ausschuss für Stahlbeton, Heft 263, Berlin 1976.
9. SCHICKERT, G., WINKLER, H.: Results of test concerning strength and strain of concrete subjected to multiaxial compressive stresses. Deutscher Ausschuss für Stahlbeton, Heft 277, Berlin 1977.
10. DRUCKER, D., PRAGER, W.: Soil mechanics and plastic analysis of limit design. Q. Appl. Math., 10, 1952, pp. 157-165.
11. RAJAGOPALAN, K.: Proc. of ASCE, V101, n°EM6, Dec. 1975, pp. 912-914 (discussion).
12. KUPFER, H., GERSTLE, K.: Behaviour of concrete under biaxial stresses. Proc. of ASCE, V99, n°EM4, Aug. 1973, pp. 853-866.
13. CHEN, A., CHEN, W.F.: Constitutive relations for concrete. Proc. of ASCE, V101, n°EM4, Aug. 1975, pp. 465-481.
14. LIU, T., NILSON, A., SLATE, F.: Biaxial stress-strain relations for concrete. Proc. of ASCE, V98, n°ST5, May 1972, pp. 1025-1034.
15. OTTOSEN, N.: A failure criterion for concrete. Proc. of ASCE, 103, n°EM4, Aug. 1977, pp. 527-535.
16. LINK, J., SCHAFER, H., MEHLHORN, G.: Eine formulierung des zweiachsigen bruch- und verformungsverhaltens von Beton. Beton- und Stahlbeton, 1974, n°9, pp.208-214.
17. BUYUKOZTURK, O.: Nonlinear analysis of reinforced concrete structures. Computers and Structures, V17, n°1, Feb. 1977, pp. 149-156.
18. WILLAM, K., WARNKE, E.: Constitutive model for the triaxial behaviour of concrete. Proc. IABSE, V19, Zurich 1975.
19. KOTSOVOS, M., NEWMAN, J.: Generalised stress-strain relations for concrete. Proc. of ASCE, V104, n°EM4, Aug. 1978, pp. 845-856.
20. MILLS, L., ZIMMERMAN, R.: Compressive strength of plain concrete under multiaxial loading conditions. ACI Journal, Proc. V67, n°10, Oct. 1970, pp.802-807.
21. MAGNAS,J.P., AUDIBERT, A.: Critères de résistance du béton sous sollicitations multiaxiales. Annales de l'Institut Technique du Bâtiment et des Travaux Publics, n°287, Nov. 1971, pp. 23-43.
22. CEDOLIN, L., CRUTZEN, Y., DEI POLI, S.: Triaxial stress-strain relationship for concrete. Proc. of ASCE, V103, n°EM3, June 1977, pp. 423-439.
23. ARGYRIS, J., FAUST, G., SZIMMAT, J., WARNKE, E., WILLAM, K.: Recent developments in the finite element analysis of prestressed concrete reactor vessels. Nuclear Engineering and Design, n°28, 1974, pp. 42-75.

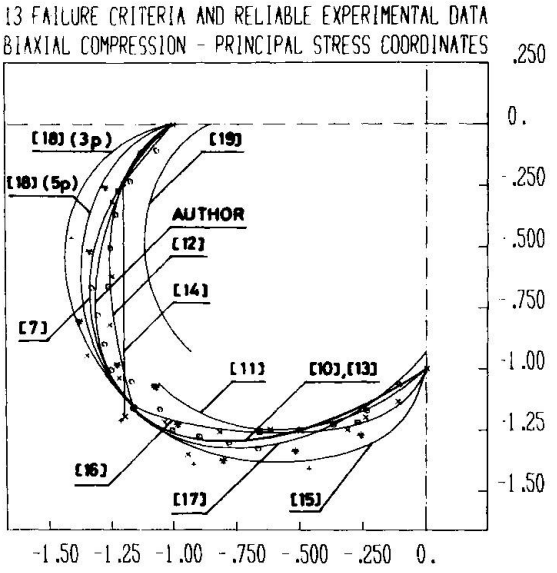


figure 1

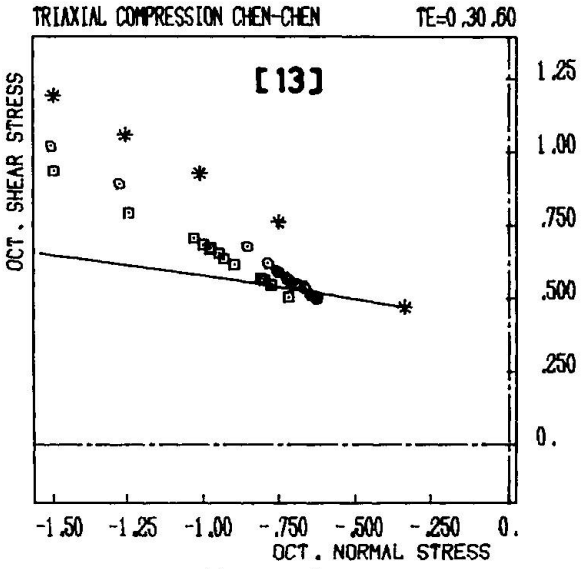


figure 3

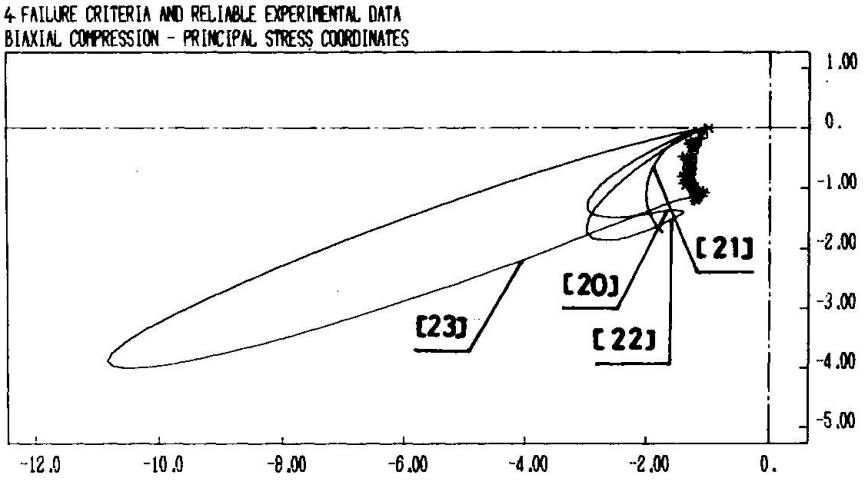


figure 2

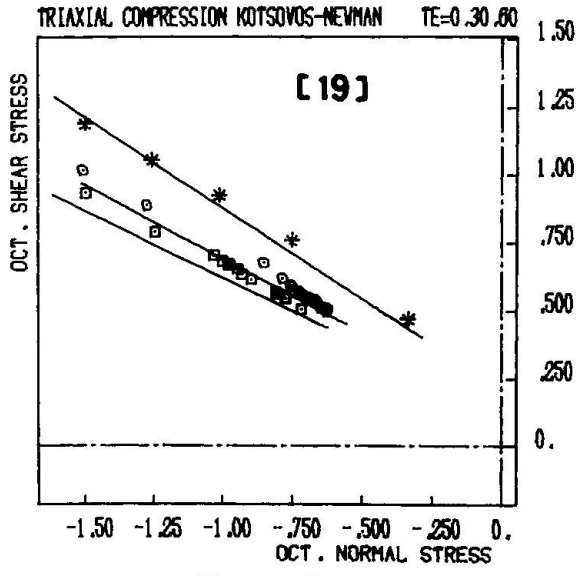


figure 4

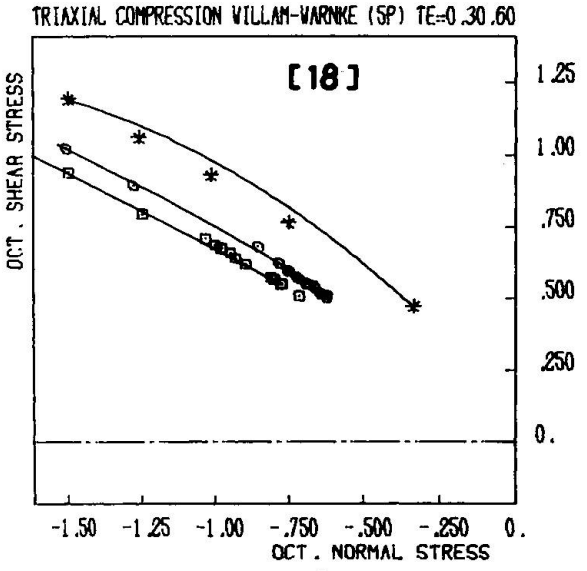


figure 5

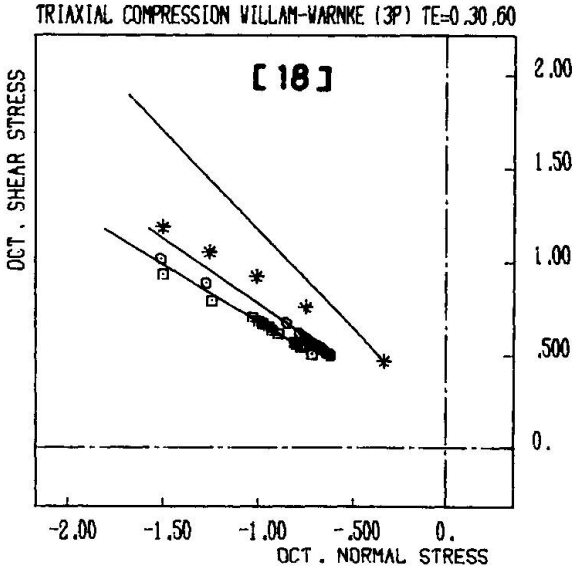


figure 6

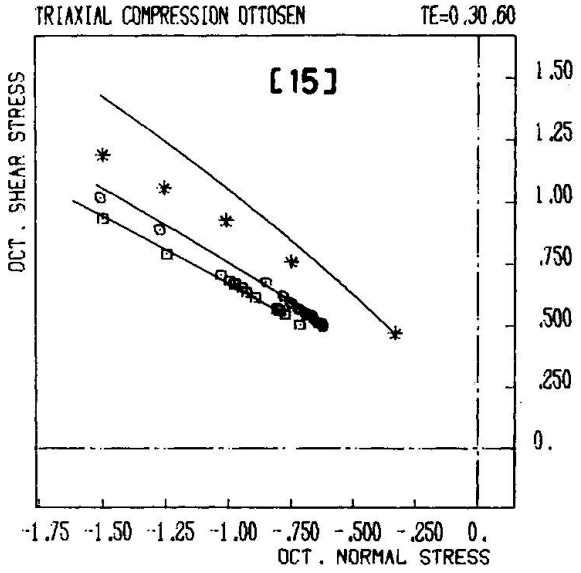


figure 7

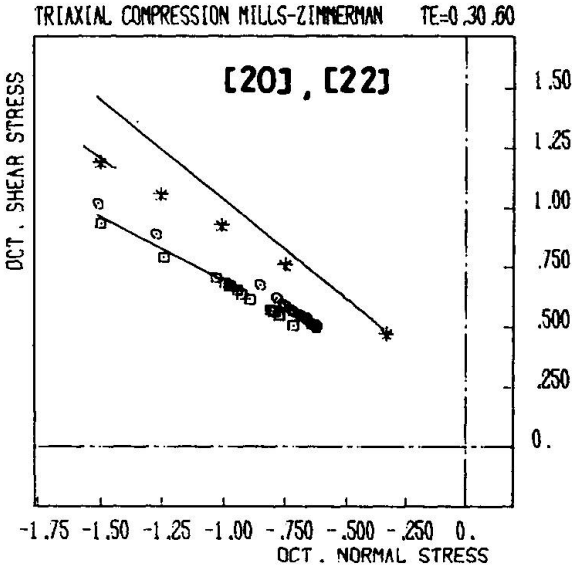


figure 8

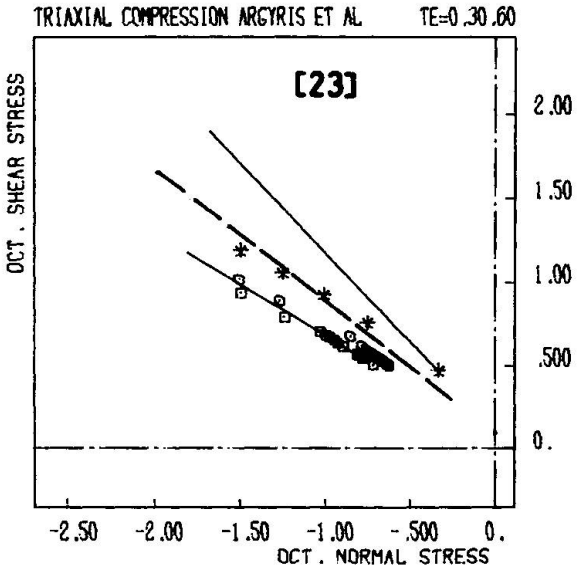


figure 9

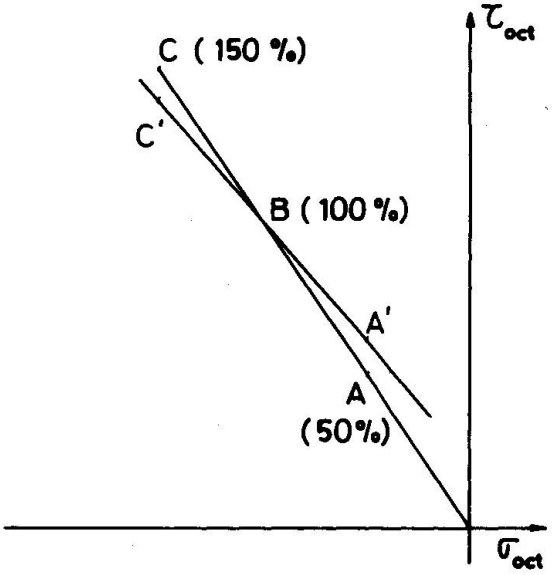


figure 10

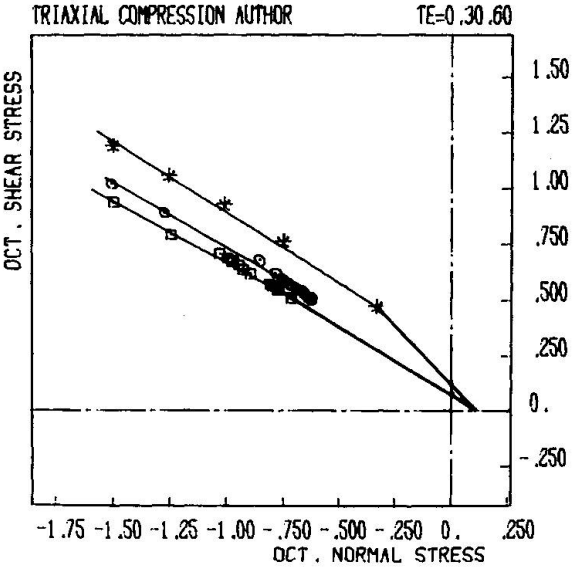


figure 11

I

# A Kinematic and Isotropic Hardening Plasticity Model for Plain Concrete under General Triaxial Stress Conditions

Modèle à écrouissage cinématique et isotrope du béton, dans des états de contraintes triaxiales

Kinematisch und Isotrop verfestigend-plastisches Modell für Beton unter allgemeinen räumlichen Spannungszuständen

B. HERMANN
Civil Engineer
Rambøll & Hannemann
DK 2830 Virum, Denmark

## SUMMARY
A new plastic model valid under general triaxial conditions is formulated and comparisons with experimental data are carried out. The model requires knowledge of only the elastic modulus, Poisson's ratio, and the compressive and tensile strengths.

## RESUME
Un nouveau modèle valable pour des états de contrainte généraux est décrit et comparé avec des résultats expérimentaux. Le modèle ne nécessite que la connaissance de quatre paramètres: le module d'élasticité, le coefficient de Poisson et les résistances à la compression et à la traction maximales.

## ZUSAMMENFASSUNG
Ein neues plastizitätstheoretisches Modell für allgemeine räumliche Spannungszustände wird beschrieben und mit Versuchsresultaten verglichen. Nur vier Parameter müssen bekannt sein, nämlich Elastizitätsmodul und Querdehnungszahl sowie einachsige Druck- und Zugfestigkeit.

## 1. INTRODUCTION

The purpose of this paper is to investigate the possibilities and limitations of a plasticity model based on Drucker's postulates [1] for plain concrete under general trixial conditions. This is done by proposing a new model with two sets of yield surfaces. The model involves both isotropic and kinematic work-hardening, but it requires knowledge only of the elastic modulus E, Poisson's ratio $\nu$, the uniaxial compressive strength $f_c$, and tensile strength $f_t$. The results of the model are compared to experimental data.

## 2. THE NEW PLASTICITY MODEL

The concrete is assumed to be isotropic in the initial state as well as after deformation, and therefore the formulation of the analytical equations will be given in principal strains $\varepsilon_i$ and stresses $\sigma_i$ only. The invariants are designated

$$\left.\begin{aligned} &I_1 = \sigma_1+\sigma_2+\sigma_3, \quad I_2 = \tfrac{1}{2}(\sigma_1^2+\sigma_2^2+\sigma_3^2), \quad I_3 = \tfrac{1}{3}(\sigma_1^3+\sigma_2^3+\sigma_3^3) \\ &I_2' = I_2 - \tfrac{1}{6} I_1^2 \text{ , the 2. deviatoric invariant} \end{aligned}\right\} \quad (1)$$

and

$$J_1 = \varepsilon_1+\varepsilon_2+\varepsilon_3 \text{ , } J_2 = \tfrac{1}{2}(\varepsilon_1^2+\varepsilon_2^2+\varepsilon_3^2), \quad J_3 = \tfrac{1}{3}(\varepsilon_1^3+\varepsilon_2^3+\varepsilon_3^3) \quad (2)$$

respectively.

The model is closely related to a failure criterion, and in this formulation a "parabolic" criterion proposed by N.S.Ottosen [2] is chosen.

The reason for this can be seen from the comparisons made in Figure 1. In this figure the intersection curves between some analytical failure surfaces and a plane containing the hydrostatic axis and one principal stress-axis in the principal stress space are shown. Also some results from experimental tests are shown.

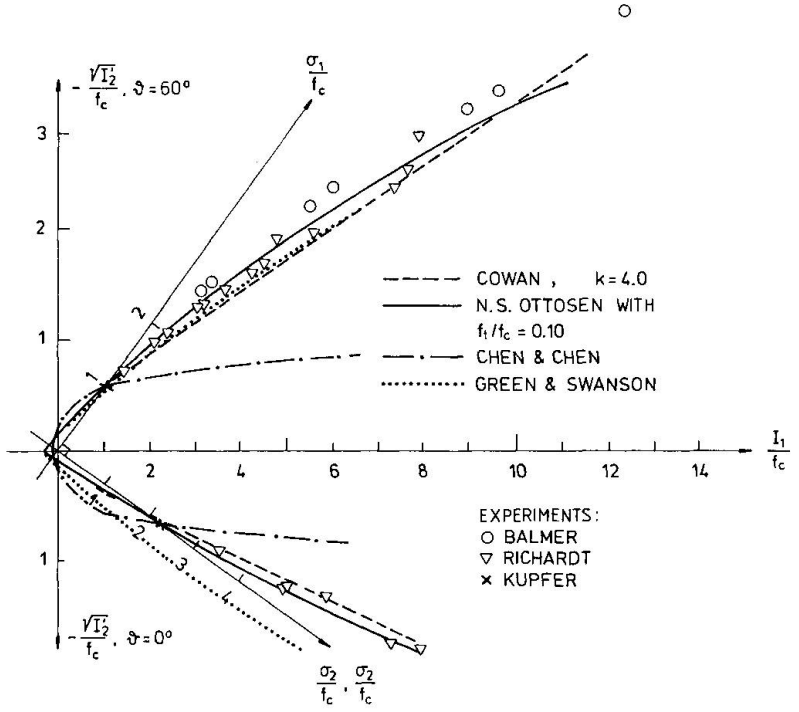


Fig. 1.

A test series performed by Launay et al. [3] indicates that the failure surface is not axisymmetric about the hydrostatic axis. Analytically this means that the third stress-invariant enters into the equation for the failure surface. The abovementioned analytical failure surface takes account on this dependence. See [2].

It is now assumed that in the principal stress-space the yield surfaces are of the shape indicated in Figure 2. One of the main characteristics of this figure is that the yield surfaces are all cut by the hydrostatic axis. The extension of the linear-elastic domain (the shaded area in Figure 2) implies that hydrostatic tension is

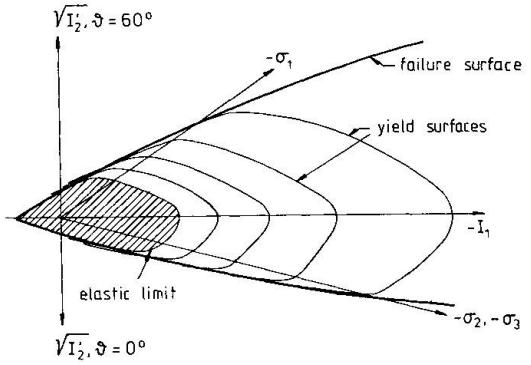


Fig. 2.

assumed to be linear-elastic until failure. Further it can be observed that the yield surfaces have relatively "sharp corners" in the vicinity of the failure surface in order to reflect the sudden volume-expansion that occurs in a compression test just before failure. This gives rise to a mathematical inconvenience that can be circumvented by using two different sets of yield surfaces as shown in Figure 3.

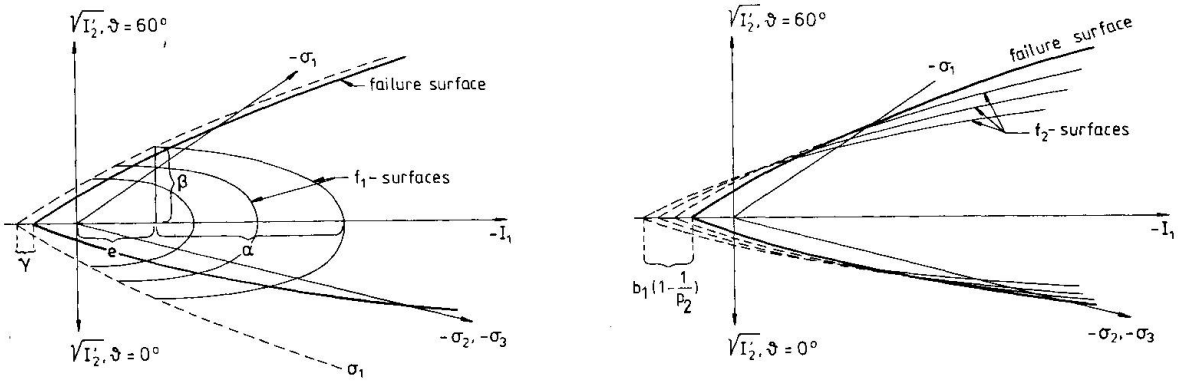


Fig. 3.

Analytically the surfaces can be expressed as

$$f_1 = \frac{(I_1 + p_1 - \alpha)^2}{\alpha^2} + \frac{I_2'}{\beta^2} - 1 = 0 \qquad (3)$$

and

$$f_2 = \frac{A}{f_c^2} \cdot \frac{I_2'}{p_2^2} - \frac{\lambda(\theta)}{f_c} \cdot \frac{I_2'}{p_2} + B \cdot (b_1 \cdot (1 - \frac{1}{p_2}) - \frac{I_1}{f_c}) - 1 = 0 \qquad (4)$$

The entering constants and the function $\lambda(\theta)$ are explained in the following.

$\theta$ is used instead of $I_3$ . The relationship is

$$\theta = \frac{1}{3} \text{ Arccos } (\frac{3\sqrt{3}}{2} \cdot \frac{I_3 - \frac{2}{3} I_1 I_2 + \frac{2}{27} I_1^3}{(I_2')^{3/2}}) \qquad (5)$$

$p_1$ and $p_2$ are the two parameters whereby the instantaneous yield surfaces are uniquely determined. $b_1$ and the ratio $\frac{\alpha}{\beta}$ are chosen to be constants that must be determined empirically. For each value of $p_1$ eq. (3) is the equation of an ellipsoid. $\alpha$ is now determined so that the circle of toppoints of the ellipsoid are common with the surface

$$g_1 = \frac{A}{f_c^2} \cdot I_2' - \frac{\lambda_c}{f_c} \cdot \sqrt{I_2'} + B \cdot (\gamma - \frac{I_1}{f_c}) - 1 = 0 \qquad (6)$$

A, B, $\lambda_c$ and $\lambda(\theta)$ are determined as for the failure criterion adopted herein. For each value of $p_2$ and constant $\theta$ eq. (3) is the equation of a parabola.

The two sets of yield surfaces are treated entirely separate. The contributions to the plastic strain-increments when the stress-point is moving outside the $f_1$-surface respectively the $f_2$-surface are superposed, i.e.

$$d\varepsilon_i^{pl} = d\varepsilon_i^{pl(1)} + d\varepsilon_i^{pl(2)} \qquad (7)$$

When the stress-point moves outside or on the instantaneous $f_1$-surface $p_1$ is determined so that the stress-point is always lying on the instantaneous $f_1$-surface which implies $dp_1 \geq 0$ .

When the stress-point moves inside the instantaneous $f_1$-surface $dp_1 = 0$. $p_2$ is determined in a similar way. The initial values of $p_1$ and $p_2$ are designated $p_1'$ and $p_2'$ .

The total plastic strain-increments can now be written as

$$d\varepsilon_i^{pl} = d\varepsilon_i^{pl(1)} + d\varepsilon_i^{pl(2)} = G_1 \cdot \frac{\partial f_1}{\partial \sigma_i} \cdot dp_1 + G_2 \cdot \frac{\partial f_2}{\partial \sigma_i} \cdot dp_2 \ , \qquad (8)$$

where $G_1$ and $G_2$ are functions of the stresses, the strain-history and the hydrostatic plastic work $W_{e(hyd)}^{pl}$. This amount of work can be determined from hydrostatic compression tests, but because of lack of data from such experiments it is proposed to put

$$G_1 = \begin{cases} \dfrac{\dfrac{dW_{e(hyd)}^{pl}}{dp_1}}{\sigma_i \dfrac{\partial f_1}{\partial \sigma_i}} & \text{for } dp_1 > 0 \\ 0 & \text{for } dp_1 = 0 \end{cases} \qquad (9)$$

with

$$W_{e(hyd)}^{pl} = \begin{cases} -\dfrac{p_1}{3} \cdot c_1 \cdot \dfrac{E}{f_c} \cdot \dfrac{a_1^{t_1}}{\left(\dfrac{p_1 - p_1'}{3}\right)^{t_1} + a_1^{t_1}} & \text{for } -I_1 = p_1 > p_1' \\ 0 & \text{for } -I_1 \leq p_1 = p_1' \end{cases} \qquad (10)$$

$a_1$, $c_1$ and $t_1$ are constants to be determined empirically. In an analogous way it is proposed to put

$$G_2 = \frac{H_2(I_2', p_2)}{\sigma_i \frac{\partial f_2}{\partial \sigma_i}} \tag{11}$$

with

$$H_2 = \begin{cases} a_2 \cdot \frac{E}{f_c} \cdot I_2' \cdot \left( c_2 \cdot \frac{p_2 - p_2'}{1 - p_2} \right)^{t_2} & \text{for } dp_2 > 0 \\ 0 & \text{for } dp_2 = 0 \end{cases} \tag{12}$$

$a_2$, $c_2$ and $t_2$ are constants to be determined empirically.

Now it is possible to give most of the constants, that remain to be determined, a physical interpretation. For further details see [4].

After having studied some available experimental data it is suggested to put

$$\frac{\alpha}{\beta} = 2.4 \ , \ \gamma = -0.15 \ f_c \ , \ p_1' = -0.57 \ f_c \ , \ p_2' = 0.70 \ , \ a_1 = -6.5 \ f_c^{-0.8} \ , \ b_1 = 1.1,$$

$$c_1 = 7 \times 10^{-5} \ , \ t_1 = 1.8 \ , \ a_2 = -3.5 \times 10^{-6} / f_c \ , \ c_2 = 0.8 \ , \ t_2 = 1.6$$

With these values for the constants the results of the model are compared to experimental data in Figures 4-14 reproduced from [4]. The only variables in these comparisons are E, $\nu$, $f_c$ and $f_t$. The first eight figures show comparisons with plane stress-experiments performed by Kupfer et al. The following ones show comparisons with various triaxial experimental results in which two principal stresses are kept at constant values different from zero. Even though the correspond-

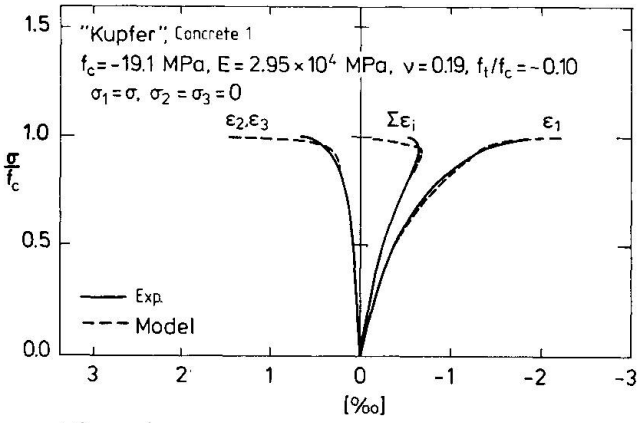


Fig. 4.

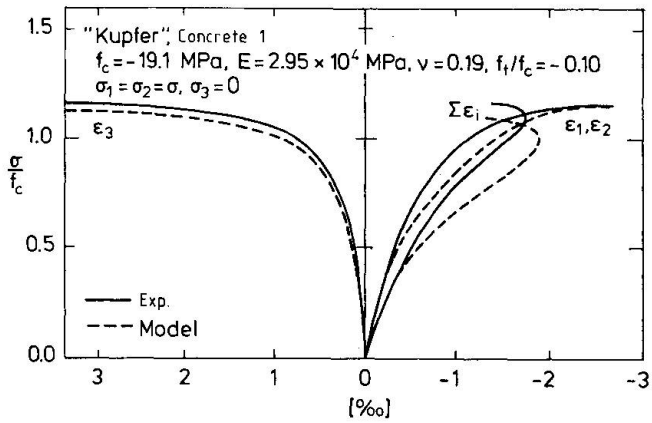


Fig. 5.

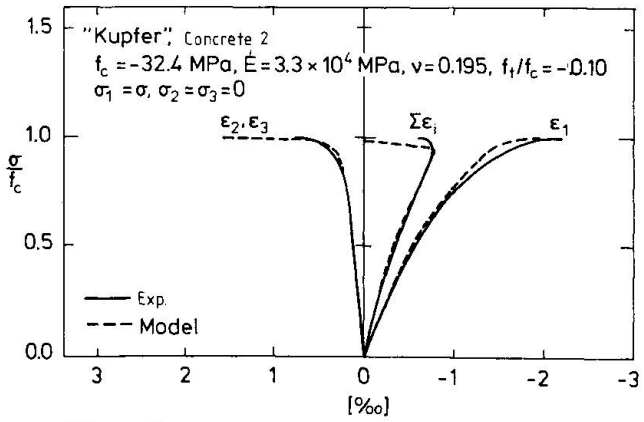


Fig. 6.

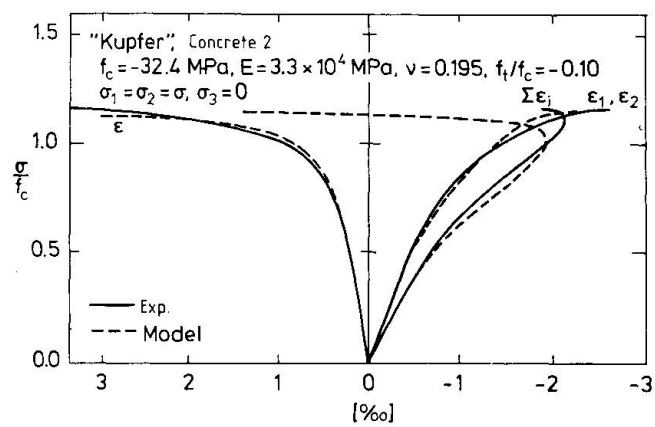


Fig. 7.

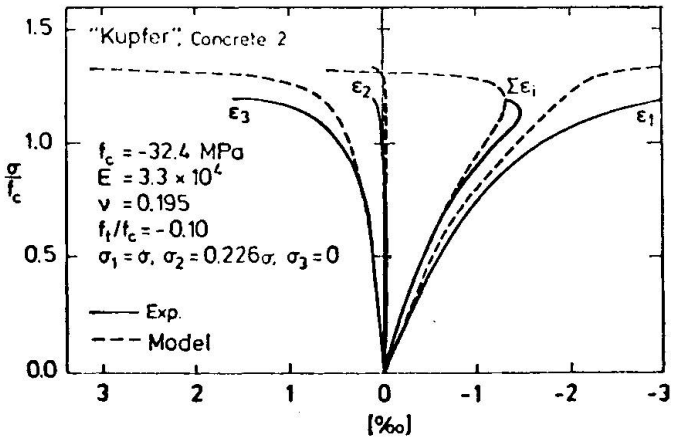


Fig. 8.

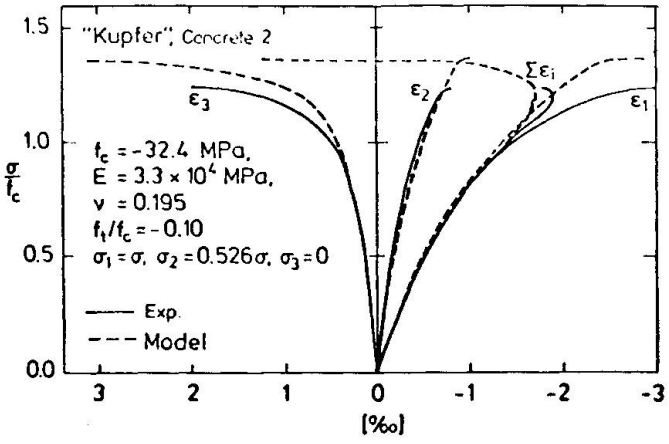


Fig. 9.

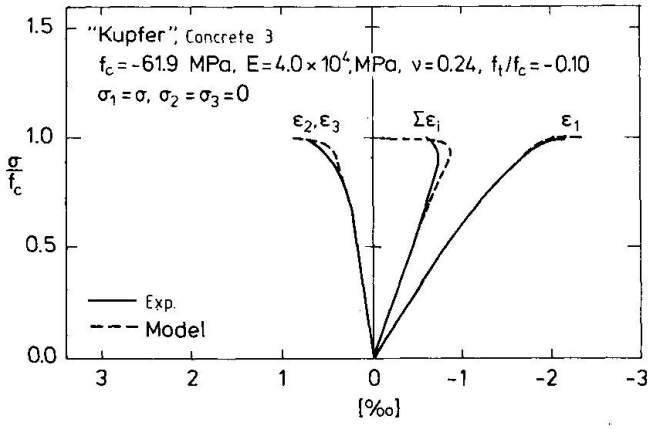


Fig. 10

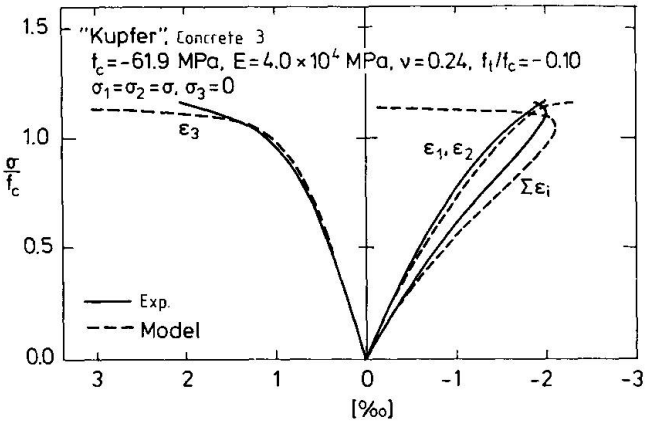


Fig. 11.

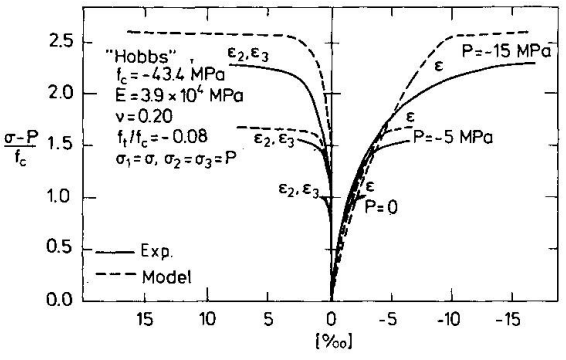


Fig. 12.

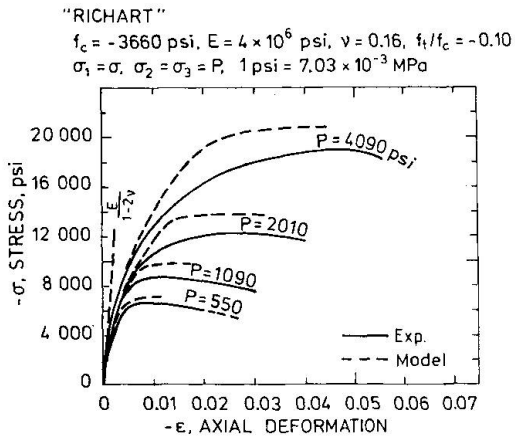


Fig. 13.

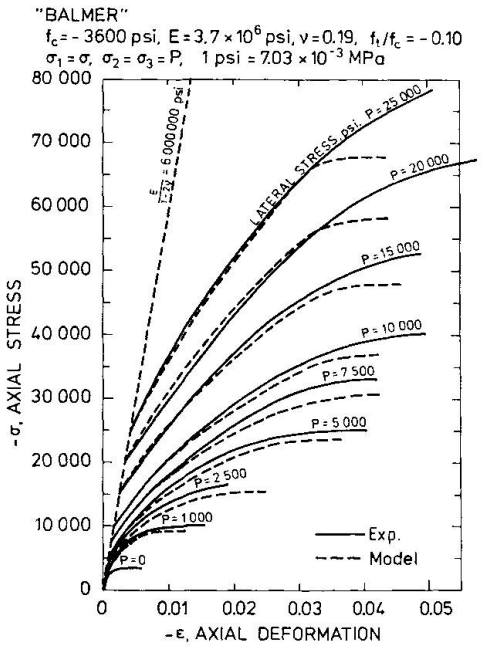


Fig. 14.

ance between model and experiments is quite fair attention should be drawn towards two inherent limitations in traditional plasticity models like the one just outlined above.

## 3. TWO IMPORTANT LIMITATIONS IN A TRADITIONAL PLASTICITY MODEL

The first limitation to be pointed out in connection with a traditional plasticity model based on Drucker's postulates concerns the normality condition. Both the normality and the convexity conditions are derived by Drucker under the assumption that the elastic proporties of the material remain constant under plastic deformation. Experimental tests indicate that for plain concrete this condition is fairly well fulfilled as long as the stress-state is not too near failure. But when the stress-state is near failure then the condition is no longer fulfilled. See Figure 15.

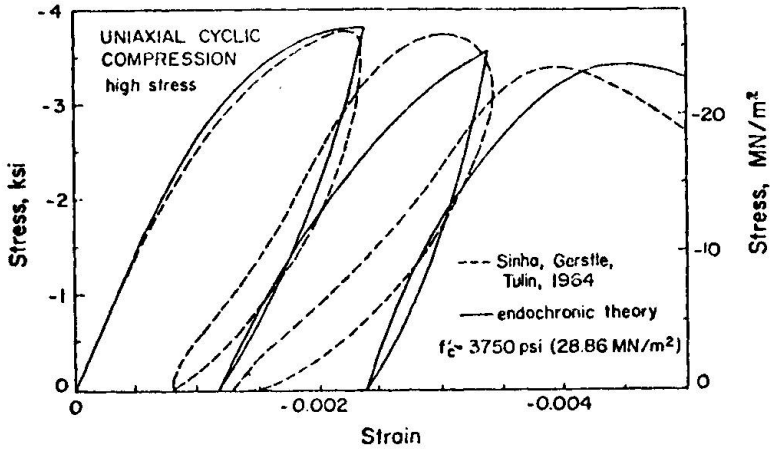


Fig. 15. (Reproduced after [8]).

The second limitation concerns the softening after failure. If, in an uniaxial compression test, the strain is controlled, a stress-strain relationship as shown on Figure 16 can be obtained. For failure calculations this must be of importance in statically indeterminate structures. The importance of this effect has among others been examined by N.S.Ottosen and S.I. Andersen (see [5]. A plasticity model

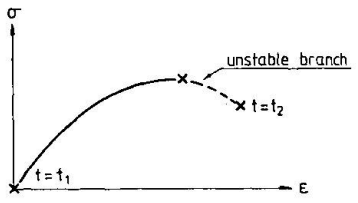


Fig. 16.

based on Drucker's postulates is not able to reflect this softening-effect, simply because one of the postulates requires that the material is not unstable in this way.

On this background it seems natural to look for other theoretical bases for the constitutive equations to be used especially for failure calculations.

## 4. OTHER THEORETICAL BASES FOR CONSTITUTIVE EQUATIONS FOR CONCRETE

Two other kinds of models that are both closely related to a traditional plasticity theory shall be mentioned. The first kind of model is based on Il'iushin's postulate of plasticity. See [6]. When startpoint is taken in this postulate it is possible to model softening.

The constitutive equations in an endochronic theory are derived from thermodynamic conditions. The basic equations are the 1. and 2. laws of thermodynamics with the usual time "t" measured with a clock replaced by an endochronic time measure "z" depending both on time "t" and a strain measure "$\zeta$".

"$\zeta$" is related to the arc-length of the path followed by the strain-point in a six-dimensional strain-space during deformation. With this kind of model it is possible to reflect softening as well as non-linearity at unloading. A formulation of the theory is given by Valanis [7]. Bazant et al. [8] and Argyris et al. [9] have formulated specific constitutive equations for plain concrete based on the principles suggested by Valanis.

## 5. CONCLUSIONS

As a conclusion it can be said that although a traditional plasticity model can be a better approximation than a linear elastic model, it seems probable that other theoretical bases are even better suited for describing the stress-strain relationship for plain concrete. This seems especially to be true in the vicinity of failure i.e. for failure calculations. For reinforced concrete members the situation is different because of the interaction with the steel.

## REFERENCES

[1] Drucker, D.C.: "A more fundamental approach to plastic stress-strain relations".
First U.S. National Cong. of Appl. Mech. ASME 1951.

[2] Ottosen, N.S.: "A failure criterion for concrete".
Journ. of the Eng. Mechn. Div. EM4 Aug. 1977.

[3] Launay, P., Gachon, H., Poitevin, P.: "Déformation et résistance ultime du béton sous étreinte triaxiale". Annales de l'Institut technique du Batiment et du Travaux Publics. No. 269. Mai 1970.

[4] Herrmann, B.: "Konstitutive ligninger for beton ved fleraksede spændingstilstande". Risø M-2121. Risø National Laboratory. Denmark. Aug. 1978.

[5] Ottosen, N.S., Andersen, S.I.: "Structural failure of thick-walled concrete elements". Conf. on structural mech. in reactor technology. San Francisco. Aug. 1977.

[6] Dafalias, Y.F.: "Il'iushin's postulate and resulting thermodynamic conditions on elasto-plastic coupling".
Int. Journ. Solid Structures. Vol. 13. 1977.

[7] Valanis, K.C.: "A theory of viscoplasticity without a yield surface".
Archives of mech. 23,4. Warzawa 1971.

[8] Bazant, Z.P., Bhat, P.D., Shieh, C.L.: "Endochronic theory for inelasticity and failure analysis of concrete structures".
Structural Eng. Report No. 1976-12/259. Northwestern Univ. Evanston, Ill. 60201. Dec. 1976.

[9] Argyris, J.H., Pister, K.S., Szimmat, J., Willam, K.J.: "Unified concepts of constitutive modelling and numerical solution methods for concrete creep problems". Computer methods in Appl. Mech. and Eng. 10. North-Holland Publishing Company. 1977.

I

## A Model of Concrete Behaviour under Generalised Stress

Modèle de comportement du béton dans des états de contrainte généraux

Modell für das Verhalten von Beton unter allgemeinen Spannungszuständen

M. KOTSOVOS
DIC, PhD
Civil Engineering Department, Imperial College
London, U.K.

J.B. NEWMAN
PhD, BSc(Eng), AGGI, DIC, CEng, MIStructE.
Civil Engineering Dept, Imperial College
London, U.K.

**SUMMARY**
The paper presents a description of the effect of internal fracture processes on the deformational behaviour of concrete under increasing load and introduces the fundamental concepts which have formed the basis for expressing mathematically the stress-strain relationship of the material under short-term generalised states of stress.

**RESUME**
L'article présente l'effet des processus de rupture interne sur le comportement du béton sous l'effet d'une augmentation de la charge. Les concepts fondamentaux ici décrits permettent d'exprimer mathématiquement les relations entre les contraintes et les déformations du matériau sous une sollicitation quelconque à court terme.

**ZUSAMMENFASSUNG**
Der Einfluss innerer Bruchvorgänge auf das Verformungsverhalten von Beton bei Laststeigerung wird beschrieben. Grundlegende Konzepte werden eingeführt, welche die Basis für die mathematische Formulierung der Spannungs-Dehnungs-Beziehung unter kurzzeitig wirkenden allgemeinen Spannungszuständen bilden.

## 1. INTRODUCTION

It is generally accepted that the nonlinear deformational behaviour of concrete is dictated by internal fracture processes occurring under increasing stress. It is considered, therefore, that any mathematical expression of the deformation -al properties of concrete must essentially describe the effect of the fracture processes on deformation. Such a description has led to the formulation of a mathematical model describing the deformational behaviour of concrete under generalised stress increasing up to [1,2] and beyond [3] the ultimate strength level.

The present paper presents a detailed description of the effect of the fracture processes on deformation and introduces the fundamental concepts which have formed the basis for modelling the deformational behaviour of concrete under short-term generalised stress states.

## 3. EFFECT OF FRACTURE PROCESSES ON DEFORMATION

The fracture processes of concrete under increasing stress take the form of crack extension and propagation in the direction of the maximum principal compressive stress (or orthogonal to the direction of the maximum principal tensile stress) [4]. The extension and propagation of cracks reduces the high tensile stress concentrations which exist near crack tips and causes void formation within the body of the material [4].

The reduction of the high tensile stress concentrations may be considered equivalent to the application of an effective internal compressive stress state which tends to reduce the volume of concrete. On the other hand, void formation tends to increase it. The combined effect on deformation, therefore, may be either a decrease or increase of overall volume depending on whether the effect of the internal stress state or that of void formation predominates.

### 2.1 Effect of Internal Stress State

Each internal stress state may be resolved into a hydrostatic and a deviatoric component.

Under a pure hydrostatic stress applied to the boundaries of an element of concrete, the effect of the hydrostatic component of the internal stress state on deformation is superimposed on that of the applied hydrostatic stress and, for a compressive applied hydrostatic stress, the combined effect is expressed by the variation of the volumetric strain ($\varepsilon_o$) with increasing applied hydrostatic stress ($\sigma_o$) shown in Figure 1. In contrast to the hydrostatic component of the internal stress state, the deviatoric component of internal stress is insignificant since the measured deviatoric strain ($\gamma_o$) has been found by experiment to be negligible.

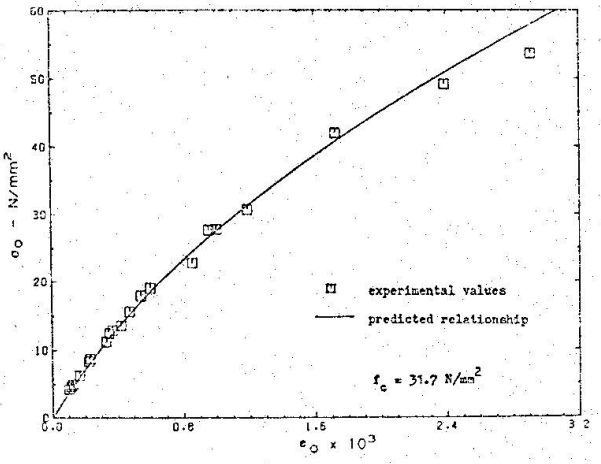


Fig. 1 Typical variation of $\varepsilon_o$ with $\sigma_o$

Under a pure deviatoric stress applied to the boundaries of an element of concrete, the hydrostatic component of the internal

stress state causes a volume decrease up to a stress level which has been termed onset of unstable fracture propagation (OUFP)[4](see Figure 2). Beyond this stress level, which marks the transition from the 'consolidation' to the 'volume dilation' stage, the material behaviour is dictated by the void formation processes and this is discussed in section 2.2.

Nominal values for the hydrostatic component of the internal stress state ($\sigma_{int}$) for given levels of applied stress may be evaluated by using the relationships shown in Figures 1 and 2. For a value of volumetric strain ($\varepsilon_o$) corresponding to a given level of applied stress ($\sigma_o$,$\tau_o$) below OUFP (see Figure 2), a value of hydrostatic stress which represents a nominal value for the hydrostatic component of the internal stress state ($\sigma_{int}$) may be obtained from Figure 1. In this mode , for stress levels up to OUFP, the $\tau_o$-$\varepsilon_o$ relationships of Figure 2 may be transformed into the $\sigma_{int}$-$\tau_o$ relationships of Figure 4.

Contrasting with the effect of the hydrostatic component of the internal stress state on deformation, the effect of the deviatoric component is superimposed on that of the applied deviatoric stress and the combined effect is reflected in the nonlinear variation of the deviatoric strain ($\gamma_o$) with increasing applied deviatoric stress ($\tau_o$) shown in Figure 3.

## 2.2 Effect of Void Formation

Although void formation may start at low levels of applied stress, its effect on deformation becomes significant when OUFP is exceeded. The void formation process dictates both the 'volume dilation' portion of the $\tau_o$-$\varepsilon_o$ relationship (see Figure 2) as well as the faster rate of increase of $\gamma_o$ with $\tau_o$ exhibited by the $\tau_o$-$\gamma_o$ relationship for stress levels beyond OUFP (see Figure 3). Furthermore, void formation increases the total cross-sectional area of the material to such an extent that the overall stress, defined on the basis of the total cross-sectional area, decreases with increasing applied stress whereas the stress defined on the basis of the solid cross-section may, in fact, continue to increase. Such a process eventually leads to disintegration of the element of concrete and complete loss of its load carrying capacity.

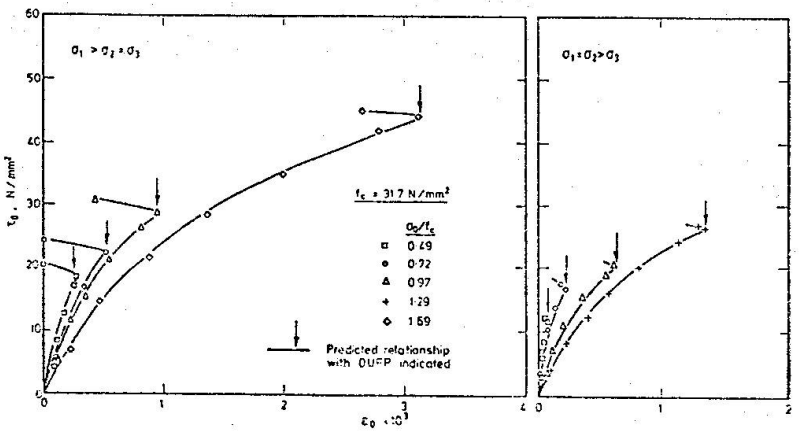


Fig. 2 Typical variation of $\varepsilon_o$ with $\tau_o$ for concrete under various levels of $\sigma_o$

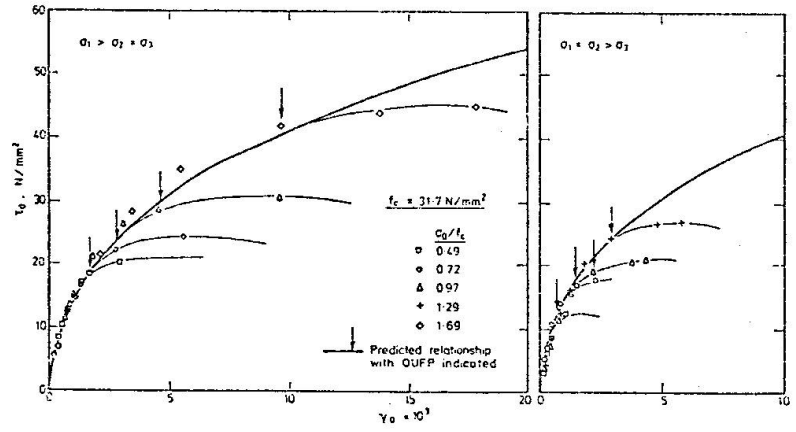


Fig. 3 Typical variation of $\gamma_o$ with $\tau_o$ for concrete under various levels of $\sigma_o$

## 2.3 Components of Deformational Behaviour

Based on the considerations discussed in the preceding sections the deformational behaviour of concrete may be decomposed into the following nonlinear components:-

(a) a component defined by the mechanical properties of concrete assumed as a solid continuum,

(b) a component expressing the effect of the internal stress state caused by the fracture processes, and

(c) a component expressing the effect of void formation.

To quantify the above components using available experimental information appears to be an impossible task since, as discussed in sections 2.1 and 2.2, most of the stress-strain data describe overall material behaviour. It will be shown in the following, however, that the use of these concepts can form a sound basis for the mathematical description of the deformational behaviour.

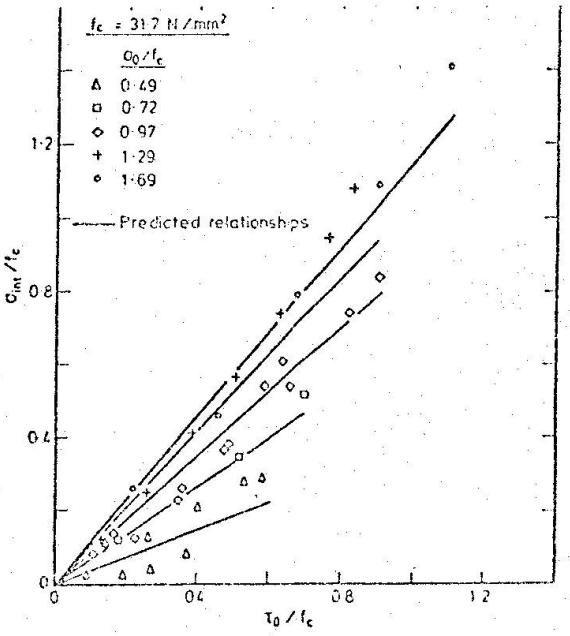


Fig. 4 Typical variation of $\sigma_{int}$ with increasing applied stress

## 3. MODELLING OF CONCRETE BEHAVIOUR

For the mathematical description of the deformational behaviour of concrete a model material with the strength properties of concrete has been introduced such that the fracture processes of the model are qualitatively similar to those of concrete [5]. The deformational behaviour of the model has been considered to consist of three nonlinear components similar to those described for concrete i.e.

component A - defined by the mechanical properties of the model assumed as a solid isotropic continuum,

component B - dictated by the internal stress state caused by the fracture processes, and

component C - expressing the effect of void formation occurring during the fracture processes.

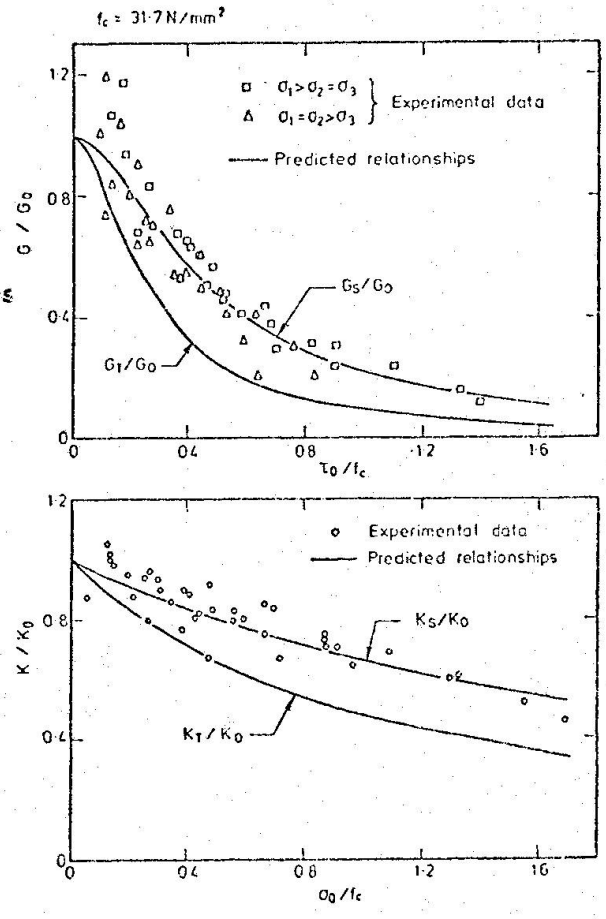


Fig. 5 Typical variations of the secant and tangent values of the bulk and shear moduli with increasing applied stress

## 3.1 Mechanical Properties of the Model

The model material has been devised such that its mechanical properties, when it is

considered as a solid isotropic continuum, are completely defined by the $\sigma_o$-$\varepsilon_o$ and $\tau_o$-$\gamma_o$ relationships obtained for concrete under stress increasing up to OUFP (see Figures 1 and 3, respectively). These relationships have been found to be unique and independent of the third stress invariant and stress path effects [1,5]. Independence of the third stress invariant is considered to indicate that the relationships are independent of any 'damage induced' anisotropy. Such behaviour is consistent with the assumption that these relationships can be used to describe the mechanical properties of a solid isotropic continuum. Furthermore, the $\sigma_o$-$\varepsilon_o$ and $\tau_o$-$\gamma_o$ relationships have been described mathematically by a regression analysis of available experimental data which have been obtained in previous investigations of the behaviour of concrete under multiaxial stress states [5].

Using the above relationships the tangent and secant values of the bulk ($K_t$,$K_s$) and shear ($G_t$,$G_s$) moduli can be easily derived as described elsewhere [1]. Graphical representations of the variations of the above moduli with increasing applied stress for a typical concrete are given in Figure 5.

Having established the bulk and shear moduli the tangent and secant values of the modulus of elasticity (E) and Poisson's ration ($\nu$) can be easily onbtained from the well-known formulae of linear elasticity, $K=E/3(1-2\nu)$ and $G=E/2(1+\nu)$.

### 3.2 Effect of Internal Stresses

The internal stress state caused by the fracture processes of the model is taken to be equivalent to the hydrostatic component of the internal stress state which develops within concrete when subjected to deviatoric stress. Nominal values of the internal stress state $\sigma_{int}$ can be evaluated as described in section 2.1. A graphical representation of the variation $\sigma_{int}$ with increasing applied stress for a typical concrete is shown in Figure 4.

By comparing available experimental data obtained from tests using various states of stress and stress paths [6], it has been found that the relationships shown in Figure 4 are effectively independent of the third stress invariant and stress path effects [1]. The independence of $\sigma_{int}$ on the third stress invariant is expected since $\sigma_{int}$ represents the hydrostatic component of the internal stress state developing within concrete under pure deviatoric stress.

The effect of $\sigma_{int}$ on deformation is apparently equivalent to the deformational response of the model subjected to three principal stresses $\sigma_1=\sigma_2=\sigma_3=\sigma_{int}$.

### 3.3 Effect of Void Formation

The void formation processes occurring within the model are assumed to be similar to those occurring within concrete. They are caused by crack propagation processes which occur in the direction of the maximum principal compressive stress and thus affect predominantly the deformation in the orthogonal directions. Such an effect should be reflected on the ratios of the incremental strains corresponding to the two principal stresses orthogonal to the direction of crack propagation with respect to the incremental strain in the direction of crack propagation.

If it is assumed, therefore, that the volume dilation which begins at the OUFP level is caused entirely by void formation, then the effect of void formation on deformation can be defined by the variations of the volume strain and the above incremental strain ratios with stress changes beyond the OUFP level. A mathematical expression of these changes has been based on theoretical considerations of the fracture mechanism of concrete which have indicated that void formation

within concrete is predominantly dependent on the current stress state, material characteristics and, for stress levels beyond ultimate, on the state of stress at the ultimate strength level [2,3,5].

In contrast to the mathematical description of the mechanical properties of the model and the effect of the internal stress state on deformation, the mathematical description of the effect of void formation on deformation is dependent on the third stress invariant and this dependence reflects the 'damage induced' anisotropy which is inherent in concrete.

## 4. COMPARISON OF PREDICTED AND EXPERIMENTAL STRESS-STRAIN BEHAVIOUR

Figure 6 shows typical representations of the stress-strain relationships predicted for concrete under various states of triaxial axisymmetric stress. The figure also includes experimental values obtained from tests on concrete carried out at Imperial College [5] and show a very close correlation between predicted and experimental relationships.

Figure 7 shows the stress-strain relationships predicted for concrete under biaxial stress conditions together with experimental values obtained at the Technical University of Munich [7]. It is apparent from the figure that the predicted relationships provide a good fit to the data.

The stress-strain relationships predicted for concrete under uniaxial compression has also been found to provide a very close fit to experimental values obtained by other investigators [8]. Furthermore, for concretes with $f_c$>40 N/mm$^2$, they correlate very closely with empirical relationships between applied stress and the corresponding strain in the direction of loading proposed elsewhere for such a stress state [9]. The above relationships are shown in Figure 8.

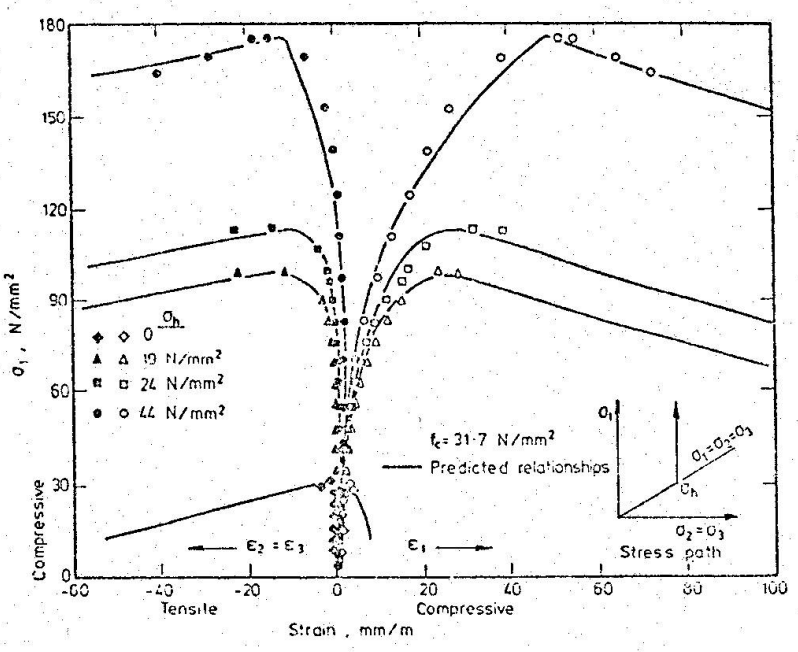


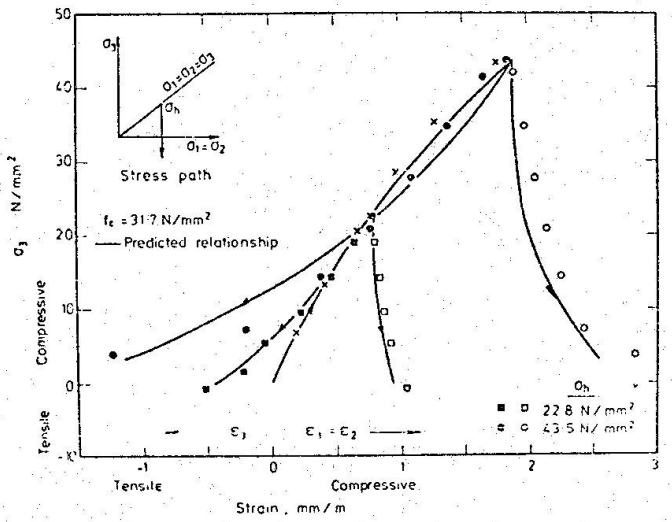


Fig. 6 Typical stress-strain relationships for concrete under triaxial axisymmetric stress states

## 5. CONCLUSIONS

1. The nonlinear deformational behaviour of concrete is considered to be dictated mainly by internal fracture processes occurring under increasing stress. These processes create voids within the body of concrete and reduce high tensile stress concentrations.

2. For the mathematical description of the deformational behaviour of concrete a model material with the strength properties of concrete has been devised such that its fracture processes are qualitatively similar to those of concrete.

3. The deformational behaviour of the model consists of the following components:-

Component A - defined by the mechanical properties of the model assumed as a solid isotropic continuum.

Component B - dictated by the reduction of the high tensile stress concentrations caused by the fracture processes, and

Component C - expressing the effect of void formation occurring during the fracture processes.

4. Components A and B have been found by experiment to be independent of 'damage induced' anisotropy whereas component C essentially expresses the effect of 'damage-induced' anisotropy on deformation.

5. The mathematical description of components A and B has been based on an analysis of experimental data obtained for concrete under multiaxial stress states whereas that of component C has been based on theoretical considerations of the fracture mechanism of concrete.

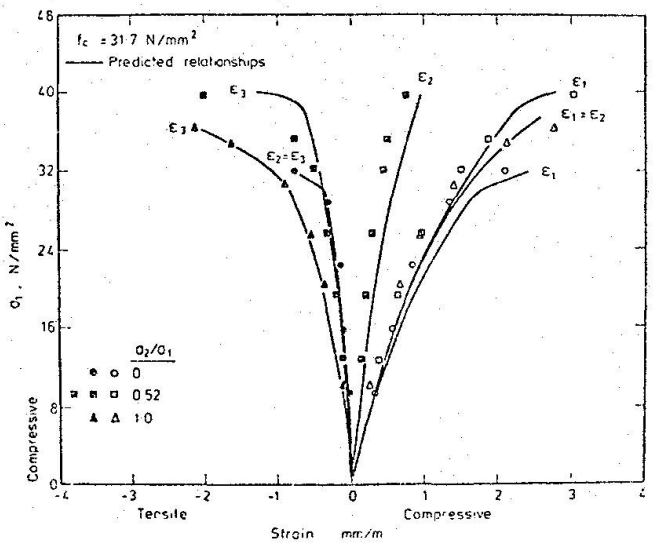


Fig. 7 Typical stress-strain relationships for concrete under biaxial compression

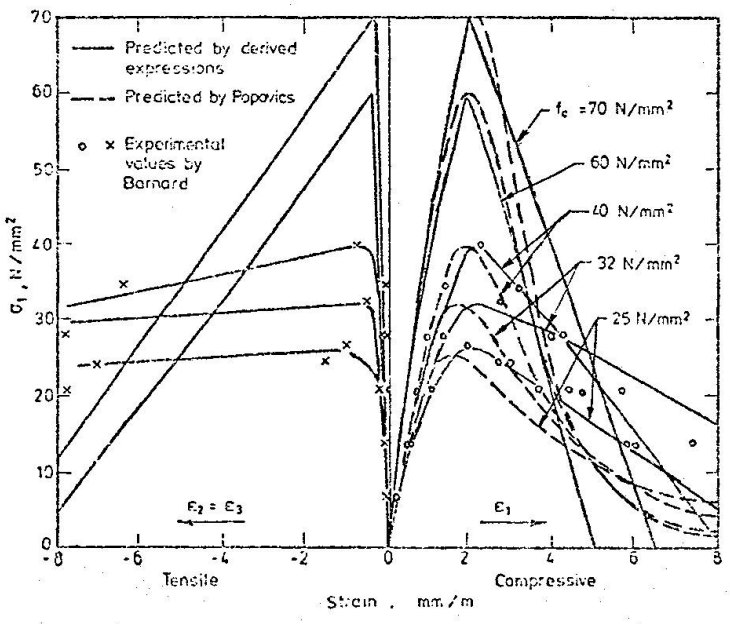


Fig. 8 Typical stress-strain relationships for various concretes under uniaxial compression.

REFERENCES

1. KOTSOVOS, M.D. and NEWMAN, J.B., "Generalised Stress-Strain Relations for Concrete", Journal of the Engineering Mechanics Division, ASCE, V. 104, No. EM4, August 1978, pp. 845-856.

2. KOTSOVOS, M.D. and NEWMAN, J.B., "A Mathematical Description of the Deformational Behaviour of Concrete under Complex Loading", Magazine of Concrete Research, V. 31, No. 107, June 1979.

3. KOTSOVOS, M.D. and NEWMAN, J.B., "Mathematical Description of Deformational Behaviour of Concrete under Generalised Stress Beyond Ultimate Strength", submitted for publication in the ACI Journal.

4. KOTOSOVOS, M.D. and NEWMAN, J.B., "Behaviour of Concrete under Multiaxial Stress", ACI Journal, Proceedings V. 74, No. 9, September 1977, pp. 443-446.

5. KOTSOVOS, M.D., "Mathematical Description of Deformational Behaviour of Concrete under Generalised Stress States", Interim report, SRC Grant GR/A44114, Civil Engineering Department, Imperial College, 1979, 242 pp.

6. KOTSOVOS, M.D. "Effect of Stress Path on the Behaviour of Concrete under Triaxial Stress States", ACI Journal, Proceedings V. 76, No. 2, February 1979. pp. 213-223.

7. KUPFER, H., HILSDORF, H.K. and RUSCH, H., "Behaviour of Concrete under Biaxial Stresses", ACI Journal, Proceedings V. 66, No. 8, August 1969, pp. 656-666.

8. BARNARD, P.R., "Researches into the Complete Stress-Strain Curve for Concrete", Magazine of Concrete Research, V. 16, No. 49, December 1964, pp. 203-210.

9. POPOVICS, S., "A Numerical Approach to the Complete Stress-Strain Curve of Concrete", Cement and Concrete Research, V. 3, No. 5, September 1973, pp. 583-599.

I

# Investigating the Stress-Strain Characteristics of Diagonally Cracked Concrete

Examen des relations entre contraintes et déformations dans le béton fissuré diagonalement

Untersuchung der Spannungs-Dehnungs-Beziehungen von diagonal gerissenem Beton

M.P. COLLINS
Professor
University of Toronto
Toronto, Canada

**SUMMARY**
Experiments aimed at determining the relationships between the average principal compressive strains and the average principal compressive stresses in diagonally cracked reinforced concrete are described. It is demonstrated that these relationships are influenced by the magnitude of the maximum co-existing shear strains.

**RESUME**
Des essais avaient pour but d'examiner les relations entre les déformations principales moyennes de compression et les contraintes principales moyennes de compression dans le béton armé fissuré diagonalement. On montre que ces relations sont influencées par la plus grande valeur des déformations dues au cisaillement.

**ZUSAMMENFASSUNG**
Es werden Versuche beschrieben, die durchgeführt wurden, um die Beziehungen zwischen den mittleren Hauptdruckdehnungen und den mittleren Hauptdruckspannungen in diagonal gerissenem bewehrten Beton zu bestimmen. Es wird gezeigt, dass diese Beziehungen von der Grösse der maximal auftretenden Schiebungen beeinflusst werden.

## 1. INTRODUCTION

Before the load-deformation response of members subjected to shear and/or torsion can be predicted the stress-strain relationships for the reinforcement and for the diagonally cracked concrete must be known.

Because the diagonal cracks cause considerable variations in the values of local strains and stresses it has been found useful [1] to formulate the relationships in terms of average strains and average stresses. The average strains can be thought of as strains measured over a base length which is several times the crack spacing.

Shown in Fig. 1(a) is a typical length of a diagonally cracked reinforced concrete member. The average stress conditions which exist at some point in the diagonally cracked concrete (e.g. at mid-depth) can be represented by a Mohr's circle of stress such as that shown in Fig. 1(b). The average strain conditions which exist at the same point in the diagonally cracked concrete can be represented by a Mohr's circle of strains such as that shown in Fig. 1(c). With reference to Figure 1, the question that will be discussed in this paper is: "What is the relationship between the average principal compressive stress, $f_d$, and the average principal compressive strain, $\varepsilon_d$?"

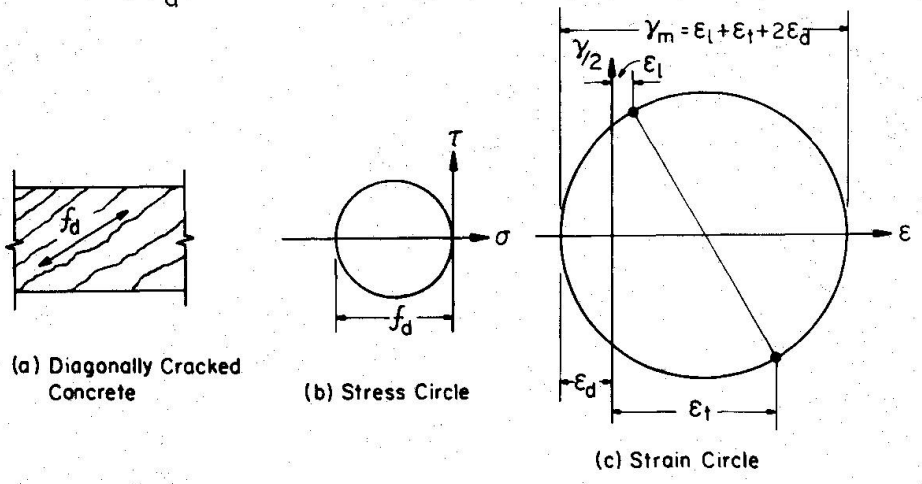


Fig. 1 Stress and Strain Conditions for Diagonally Cracked Concrete

In earlier studies ([2], [3], [4]) it was assumed that $f_d$ could be related to $\varepsilon_d$ by the usual stress-strain curve determined from a cylinder test on the concrete. However, the concrete strain conditions which exist in a cylinder test (see Figure 2) are substantially different from the strain conditions of the diagonally cracked concrete (Figure 1). Will these different strain conditions, which can be described in terms of the ratio of the maximum shear strain, $\gamma_m$ (i.e. the diameter of the strain circle) to the principal compressive strain, $\varepsilon_d$, effect the stress-strain characteristics of the concrete?

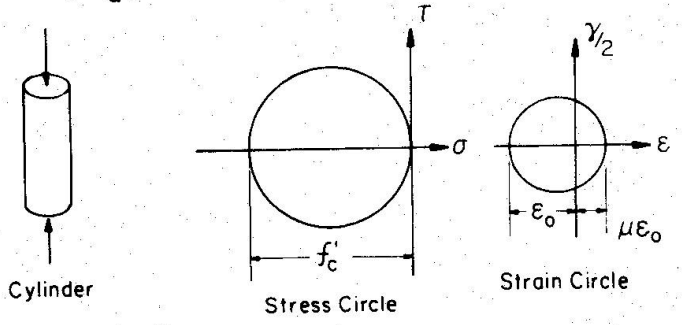


Fig. 2 Stress and Strain Conditions for a Control Cylinder

## 2. EXPERIMENTAL SET-UP

To investigate the effect of the strain ratio, $\gamma_m/\varepsilon_d$, on the relationship between $f_d$ and $\varepsilon_d$ a number of concrete panels were loaded in the manner described in Fig. 3.

Each test set-up consisted of two unreinforced concrete panels cast between three steel columns. The concrete panels, which were 915 mm high, 255 mm wide and 32 mm thick, were attached to the steel columns by being cast around steel teeth which in turn had shear studs attached (see Fig. 3).

The panels were loaded by jacking upwards the central steel column while calibrated inclined tension links held down the outer two steel columns. The lines of action of the hold down forces passed through the centre point of each panel.

The horizontal expansion of the panels was controlled by two hydraulic jacks which loaded two sets of external horizontal calibrated rods. The

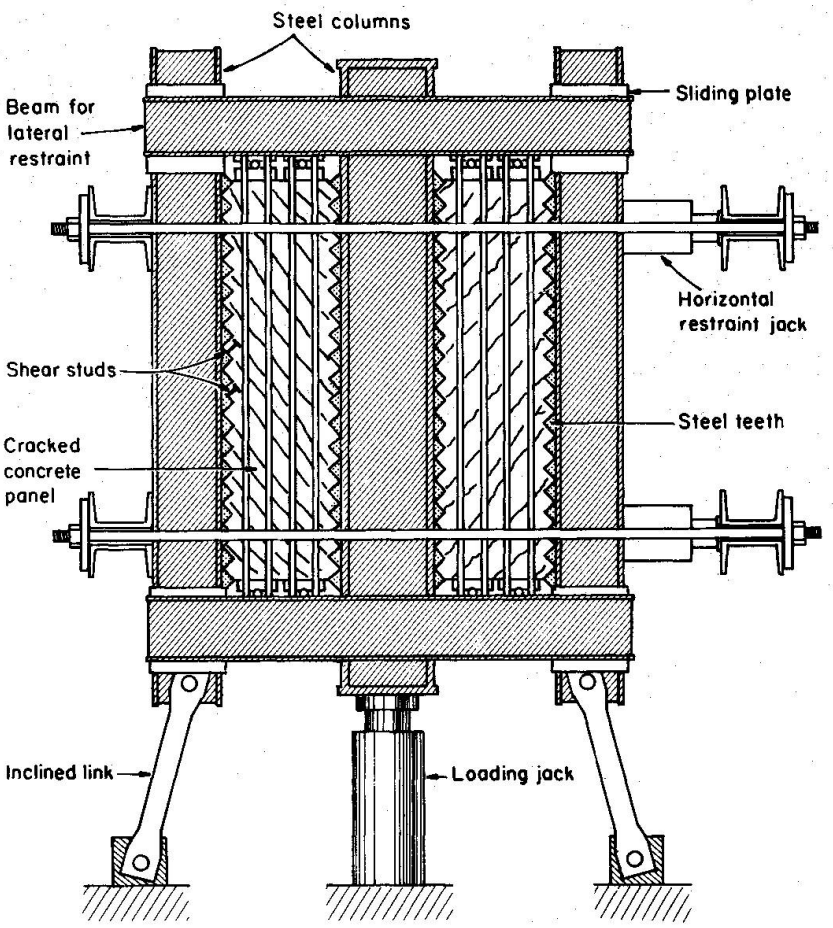


Fig. 3 Test Rig for Loading Panels in Shear

vertical expansion of each panel was controlled not only by the steel columns but also by eight 19 mm diameter external vertical steel rods.

By adjusting the force applied by the horizontal jacks it was possible to change the average horizontal strain in the panel, and hence it was possible to change the ratio of shear strain to horizontal strain. This strain ratio was the prime variable between the different test panels.

The average strain in the concrete panels was determined by measuring the relative movements of the steel columns. These average strain readings were complemented by a series of local strain readings using a demountable mechanical strain gauge with targets located on steel plugs cast in the concrete.

During the test external diagonal steel braces were mounted over one of the two concrete panels. This enabled each panel to be tested separately.

## 3. EXPERIMENTAL RESULTS

The results for four panel tests are summarized in Table 1.

Panels 3 and 3A were cast at the same time from the same concrete mix. At the time of testing the compressive strength of this concrete, $f'_c$, as determined from three 75 mm x 75 mm x 300 mm prisms, was 17.3 MPa and this stress was attained at a compressive strain, $\varepsilon_o$, of $2.0 \times 10^{-3}$. For Panels 4 and 4A, $f'_c$ was 31.7 MPa and $\varepsilon_o$ was $2.4 \times 10^{-3}$.

The shear stress, v, and the horizontal compressive stress, $\sigma_h$, acting on the central vertical plane of each panel at each load stage (L.S.) are listed in Table 1. These stresses were calculated from the measured forces in the horizontal rods and the inclined tension links by means of the free body diagram shown in Fig. 4.

The average change in angle between the originally horizontal and vertical lines (i.e. shear strain $\gamma_{vh}$) and the average horizontal tensile strain, $\varepsilon_h$, are also listed in Table 1. These strain values were calculated from the measured deformations of the panel illustrated in Fig. 5. From the local strain readings it was found that the average vertical strain $\varepsilon_v$, remained essentially at zero.

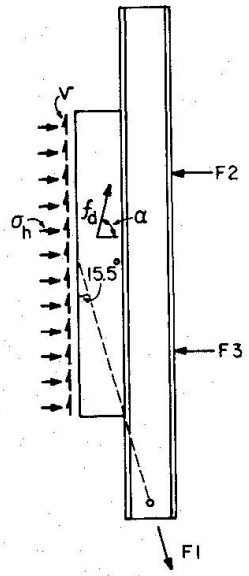


Fig. 4 Forces and Stresses

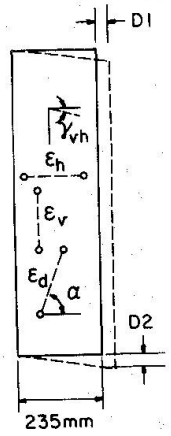


Fig. 5 Deformations and Strains

For each load stage the average value of the principal compressive strain in the concrete, $\varepsilon_d$, the angle of inclination, α, of this principal compressive strain, and the average value of the maximum shear strain, $\gamma_m$ were all calculated from the measured values of $\gamma_{vh}$ and $\varepsilon_h$ by using the Mohr's circle of strain shown in Fig. 6.

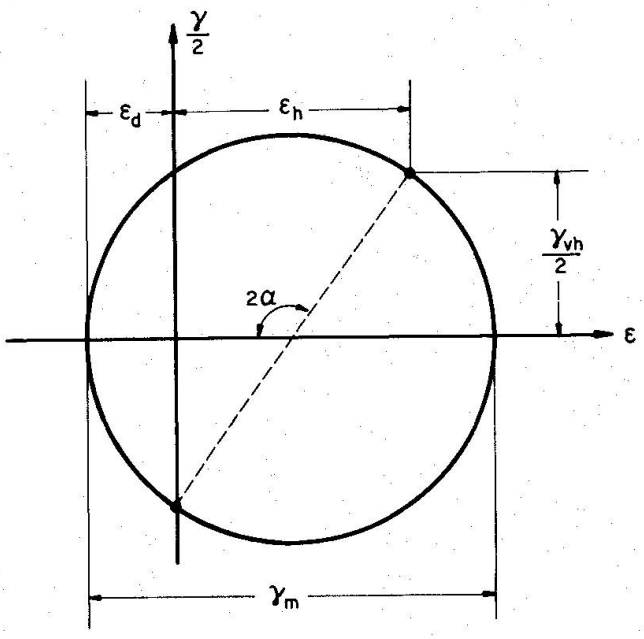


Fig. 6 Strain Relationships for Test Panels

The average value of the principal compressive stress in the concrete, $f_d$, listed in Table 1, was calculated from the measured values of v and α by the relationship:

$$f_d = v\left(\tan\alpha + \frac{1}{\tan\alpha}\right) \quad \ldots (1)$$

This equation is based on the assumptions that there are no tensile stresses in the concrete and that the angle of inclination of the principal compressive stress is equal to the angle of inclination of the principal compressive strain.

If it is assumed that tensile stresses can exist in the cracked concrete then the tabulated values of $\sigma_h$, v and $\alpha$ can be used to calculate the principal tensile stress in the concrete, $f_t$, from the relationship:

$$f_t = \frac{v}{\tan\alpha} - \sigma_h \quad \ldots (2)$$

and the principal compressive stress then becomes:

$$f_d = v\left(\tan\alpha + \frac{1}{\tan\alpha}\right) - f_t \quad \ldots (3)$$

Obviously the value of principal compressive stress calculated from Eq. (3) will be less than the value calculated from Eq. (1). As would be expected neglecting the tensile stresses causes a more significant change for the early load stages. Thus for Panel 4 at load stage 1 the value of $f_d$ given by Eq. (3) would be 0.76 MPa as opposed to the 1.45 MPa given by Eq. (1), whereas at load stage 9 the two estimates of $f_d$ would be 14.26 MPa and 15.06 MPa. Because it is desired not to over-estimate any loss in stiffness due to shear strain the higher estimates of $f_d$ (i.e. those given in Table 1) will be used in the remainder of this paper.

During each test an attempt was made to control the strain ratio $\gamma_m/\varepsilon_d$. Each test started by jacking upwards the central steel column while at the same time having only a minimum force in the horizontal restraining rods. While the panels remained uncracked they had no tendency to expand laterally and hence $\varepsilon_h$ remained zero and the value of the ratio $\gamma_m/\varepsilon_d$ remained at two. Once cracking commenced the panels tended to expand laterally as the central load was increased. This expansion was allowed to occur until the desired value of $\gamma_m/\varepsilon_d$ was reached. Thereafter the magnitudes of the horizontal restraining forces were continuously adjusted in an attempt to maintain a constant value of the ratio $\gamma_m/\varepsilon_d$. However, as can be seen from Table 1, it did not prove possible to maintain $\gamma_m/\varepsilon_d$ at a truly constant value.

For Panels 3, 3A and 4, the crushing failure of the concrete was relatively gradual, enabling "post-peak" readings to be taken (for 3 the peak load occurred between LS 8 and 9 at a shear stress of about 5.7 MPa). However, the highly restrained concrete of Panel 4A essentially disintegrated at the peak stress in a failure that was explosively abrupt. A view of one of the more typical failures is given in Fig. 7.

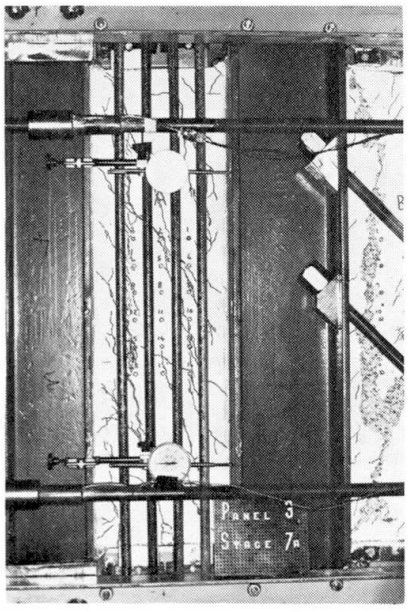


Fig. 7 Panel 3A at Failure

## 6. OBSERVED STRESS-STRAIN CHARACTERISTICS

The observed relationships between the principal compressive stress, $f_d$, and the principal compressive strain, $\varepsilon_d$, for Panels 3 and 3A and for a control prism cast from the same concrete are shown in Fig. 8. The numbers written above the curves in Fig. 8 are the measured values of the strain ratio $\gamma_m/\varepsilon_d$.

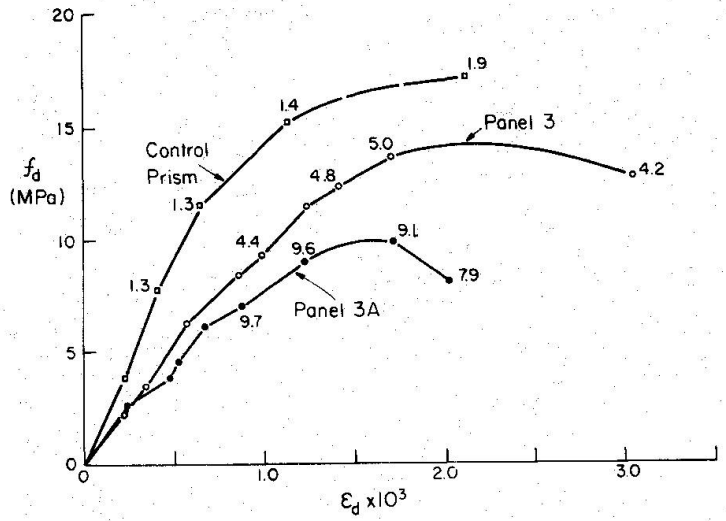


Fig. 8 Observed Stress-Strain Characteristics - Panels 3 and 3A

From Fig. 8 it would appear that the relationship between $f_d$ and $\varepsilon_d$ depends on the strain ratio $\gamma_m/\varepsilon_d$. For a given value of $\varepsilon_d$ the higher the value of $\gamma_m/\varepsilon_d$ the lower the value of $f_d$. Furthermore, the maximum value of $f_d$ that can be attained also appears to be a function of $\gamma_m/\varepsilon_d$.

Fig. 9 shows the relationships between $f_d$ and $\varepsilon_d$ for Panels 4 and 4A and for a control prism cast from the same concrete. It is worthy of note that for Panel 4A the calculated value of $f_d$ reached 97% of $f'_c$. This corresponded to an applied shear stress which was 47% of $f'_c$.

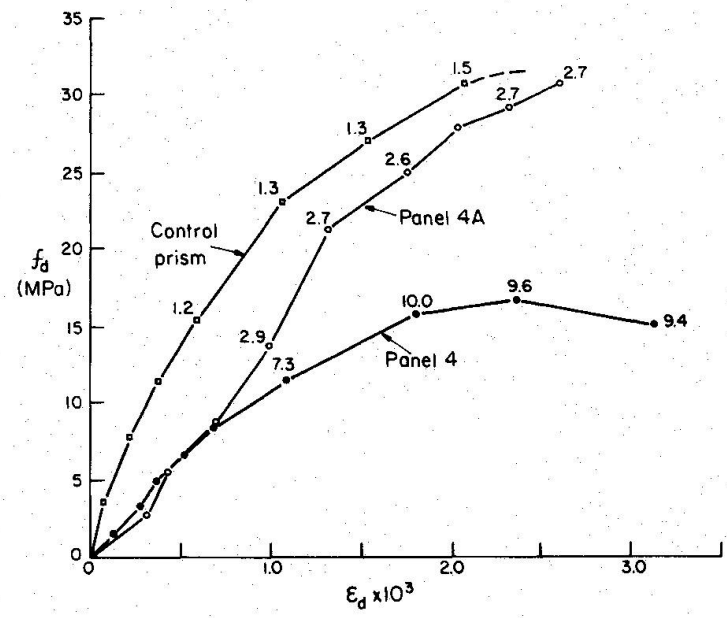


Fig. 9 Observed Stress-Strain Characteristics - Panels 4 and 4A

On the basis of the small number of tests reported in Figures 8 and 9, it appears that the value of $\varepsilon_d$ at which $f_d$ reaches its peak value is not greatly influenced by the value of $\gamma_m/\varepsilon_d$. Further, for any given value of $\gamma_m/\varepsilon_d$ it seems that the $f_d$ versus $\varepsilon_d$ curve could be approximated by a parabola. Based on these observations the following relationship is tentatively proposed:

$$\frac{f_d}{f'_c} = \frac{5.5}{4 + \gamma_m/\varepsilon_d} \left[ 2 \frac{\varepsilon_d}{\varepsilon_o} - \left(\frac{\varepsilon_d}{\varepsilon_o}\right)^2 \right] \qquad \ldots (4)$$

The predictions of Equation (4) are compared with the experimental results in Fig. 10. In this figure the predicted relationships between $f_d$ and $\varepsilon_d$ for four different values of $\gamma_m/\varepsilon_d$ are shown. Also shown are experimental points corresponding to measured values of $f_d$ and $\varepsilon_d$. The numbers written above the points are the measured values of $\gamma_m/\varepsilon_d$. It can be seen from Fig. 10 that the predictions of Equation (4) are in general conservative for these experiments.

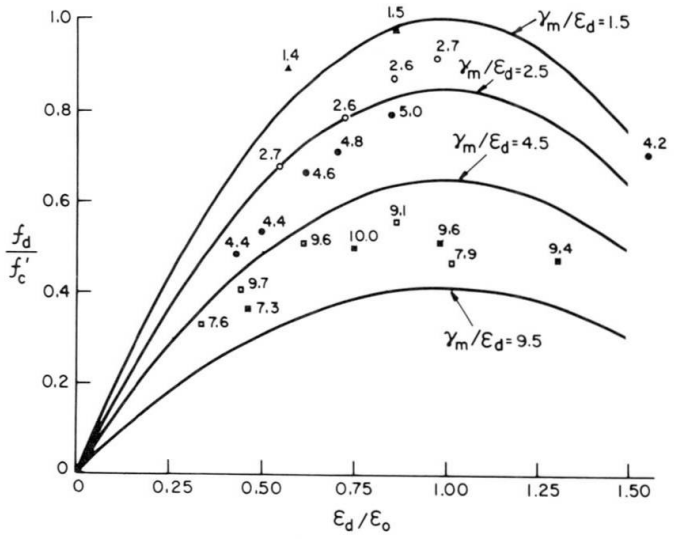


Fig. 10 Predicted and Observed Stress-Strain Relationships

## 7. CONCLUDING REMARKS

The experiments reported in this paper demonstrate that for a given value of principal compressive concrete strain the value of the resulting principal compressive concrete stress depends on the magnitude of the maximum co-existing shear strain. In other words, $f_d$ is a function of both $\varepsilon_d$ and $\gamma_m$.

The particular function suggested in the paper, Eq. (4), was based on only a very limited number of tests and hence should be regarded as tentative.

In an attempt to obtain more extensive data on the stress-strain characteristics of diagonally cracked reinforced concrete a new test rig has recently been installed at the University of Toronto. This rig, which is shown in Fig. 11, will enable 1 m x 1 m x 75 mm panels of reinforced concrete to be tested under a wide variety of stress conditions, including the condition of pure shear.

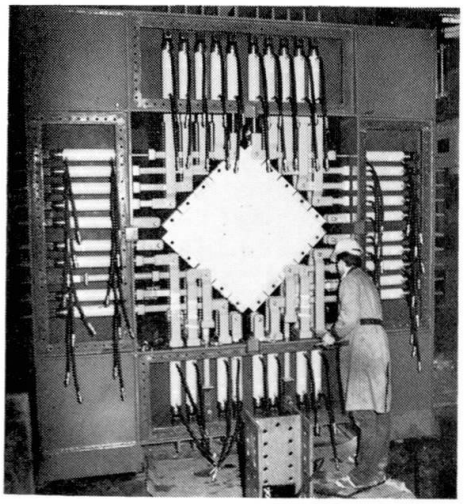

Fig. 11 New Test Rig for Shear Panels

ACKNOWLEDGEMENTS

The experiments reported in this paper were conducted in the laboratories of the Department of Civil Engineering of the University of Canterbury, Christchurch, New Zealand, while the author was on research leave from the University of Toronto. The author is most grateful to the University of Canterbury for all the help which was so generously made available.

TABLE 1: Experimental Results for Four Panels

| SPECIMEN | | L.S. | v (MPa) | $\sigma_h$ (MPa) | $\gamma_{vh} \times 10^3$ | $\varepsilon_h \times 10^3$ | $\alpha$ (°) | $\gamma_m \times 10^3$ | $\varepsilon_d \times 10^3$ | $f_d$ (MPa) | $\gamma_m/\varepsilon_d$ |
|---|---|---|---|---|---|---|---|---|---|---|---|
| $f'_c$ = 17.3 MPa $\varepsilon_o$ = 2.0 x $10^{-3}$ | PANEL #3 | 1 | 1.12 | 0.21 | 0.47 | 0.04 | 47 | 0.47 | 0.22 | 2.24 | 2.2 |
| | | 2 | 1.68 | 0.01 | 0.83 | 0.14 | 50 | 0.84 | 0.35 | 3.41 | 2.4 |
| | | 3 | 2.77 | 0.41 | 1.93 | 1.00 | 59 | 2.18 | 0.59 | 6.28 | 3.7 |
| | | 4 | 3.54 | 0.45 | 3.15 | 2.01 | 61 | 3.74 | 0.86 | 8.34 | 4.4 |
| | | 5 | 3.92 | 0.59 | 3.70 | 2.40 | 61 | 4.41 | 1.00 | 9.24 | 4.4 |
| | | 6 | 4.74 | 0.77 | 4.69 | 3.19 | 62 | 5.67 | 1.24 | 11.45 | 4.6 |
| | | 7 | 4.94 | 0.88 | 5.51 | 3.98 | 63 | 6.80 | 1.41 | 12.21 | 4.8 |
| | | 8 | 5.52 | 1.00 | 6.85 | 5.16 | 63 | 8.57 | 1.71 | 13.66 | 5.0 |
| | | 9 | 5.31 | 1.46 | 11.06 | 6.74 | 61 | 12.95 | 3.11 | 12.52 | 4.2 |
| | PANEL #3A | 1 | 1.37 | 0 | 0.50 | 0 | 45 | 0.50 | 0.25 | 2.76 | 2.0 |
| | | 2 | 1.74 | 0.63 | 1.47 | 0.64 | 57 | 1.60 | 0.48 | 3.83 | 3.3 |
| | | 3 | 1.81 | 0.13 | 2.26 | 1.94 | 65 | 2.98 | 0.52 | 4.76 | 5.7 |
| | | 4 | 2.02 | 0.08 | 3.44 | 3.75 | 69 | 5.09 | 0.67 | 6.03 | 7.6 |
| | | 5 | 2.13 | 0.17 | 5.22 | 6.83 | 71 | 8.60 | 0.88 | 6.93 | 9.7 |
| | | 6 | 2.74 | 0.27 | 7.19 | 9.32 | 71 | 11.77 | 1.23 | 8.90 | 9.6 |
| | | 7 | 3.01 | 0.32 | 9.88 | 12.32 | 71 | 15.80 | 1.74 | 9.79 | 9.1 |
| | | 8 | 2.68 | 0.44 | 10.62 | 11.88 | 69 | 15.93 | 2.03 | 8.00 | 7.9 |
| $f'_c$ = 31.7 MPa $\varepsilon_o$ = 2.4 x $10^{-3}$ | PANEL #4 | 1 | 0.72 | 0.04 | 0.34 | 0 | 45 | 0.34 | 0.17 | 1.45 | 2.0 |
| | | 2 | 1.45 | 0.03 | 0.87 | 0.37 | 57 | 0.95 | 0.29 | 3.17 | 3.3 |
| | | 3 | 2.12 | 0.07 | 1.33 | 0.83 | 61 | 1.57 | 0.37 | 5.00 | 4.3 |
| | | 4 | 2.76 | 0.12 | 1.90 | 1.22 | 61 | 2.26 | 0.52 | 6.48 | 4.3 |
| | | 5 | 3.42 | 0.26 | 2.80 | 2.21 | 64 | 3.57 | 0.68 | 8.69 | 5.3 |
| | | 6 | 4.01 | 0.43 | 5.48 | 5.77 | 68 | 7.96 | 1.09 | 11.55 | 7.3 |
| | | 7 | 4.62 | 0.57 | 11.00 | 14.70 | 72 | 18.40 | 1.80 | 15.72 | 10.0 |
| | | 8 | 5.06 | 0.69 | 13.85 | 17.99 | 71 | 22.70 | 2.36 | 16.45 | 9.6 |
| | | 9 | 4.63 | 0.81 | 18.15 | 23.13 | 71 | 29.40 | 3.14 | 15.06 | 9.4 |
| | PANEL #4A | 1 | 1.40 | 0 | 0.59 | 0 | 45 | 0.59 | 0.31 | 2.83 | 2.0 |
| | | 2 | 2.85 | 0.05 | 1.06 | 0.13 | 49 | 1.07 | 0.47 | 5.72 | 2.3 |
| | | 3 | 4.18 | 0.31 | 1.93 | 0.63 | 54 | 2.03 | 0.70 | 8.79 | 2.9 |
| | | 4 | 6.52 | 2.52 | 2.76 | 0.91 | 54 | 2.90 | 1.00 | 13.72 | 2.9 |
| | | 5 | 10.39 | 4.34 | 3.47 | 0.94 | 53 | 3.59 | 1.32 | 21.52 | 2.7 |
| | | 6 | 12.04 | 4.86 | 4.45 | 1.06 | 52 | 4.57 | 1.76 | 24.76 | 2.6 |
| | | 7 | 13.46 | 5.37 | 5.24 | 1.30 | 52 | 5.39 | 2.05 | 27.72 | 2.6 |
| | | 8 | 14.08 | 5.40 | 6.06 | 1.57 | 52 | 6.26 | 2.34 | 29.10 | 2.7 |
| | | 9 | 14.86 | 5.45 | 6.84 | 1.87 | 53 | 7.09 | 2.61 | 30.83 | 2.7 |

REFERENCES


1. Collins, Michael P., "Towards A Rational Theory for RC Members in Shear", Journal of the Structural Division, American Society of Civil Engineers, Vol. 104, No. ST4, April, 1978, pp. 649-666.
2. Mitchell, Denis, and Collins, Michael P., "Diagonal Compression Field Theory - A Rational Model for Structural Concrete in Pure Torsion," American Concrete Institute Journal, Vol. 71, Aug. 1974, pp. 396-408.
3. Rabbat, Basile G., and Collins, Michael P., "A Variable Angle Space Truss Model for Structural Concrete Members Subjected to Complex Loading," Douglas McHenry International Symposium on Concrete and Concrete Structures, American Concrete Institute, Publication SP-55, Detroit, 1978, pp. 547-587.
4. Onsongo, Winston M., "The Diagonal Compression Field Theory for Reinforced Concrete Beams Subjected to Combined Torsion, Flexure and Axial Load," thesis presented to the University of Toronto, Canada, in 1978, in partial fulfilment of the requirements for the degree of Doctor of Philosophy.

I

# On the Effectiveness Factor in Plastic Analysis of Concrete

Le facteur d'efficacité et l'analyse plastique du béton

Zur wirksamen Festigkeit und der plastischen Berechnung von Beton

H. EXNER
Civil Engineer
TU of Denmark
Lyngby, Denmark

**SUMMARY**
When an uncorrected classic theory of plasticity is used to calculate the carrying capacity of a concrete structure, we may obtain a value that is on the unsafe side. In practical applications, therefore, we reduce the compression strength by an empirically determined effectiveness factor $\nu$ before using it in a plastic analysis. The article describes how we can, on the basis of our knowledge of the stress-strain curve for concrete in uniaxial compression, employ theoretical means to arrive at a reliable $\nu$-value. The theoretical $\nu$-value is compared with the empirical $\nu$-value for various concrete strengths.

**RESUME**
La charge ultime d'une structure en béton armé peut être surestimée si on utilise la théorie de la plasticité classique sans modification. C'est pourquoi on introduit un facteur d'efficacité $\nu$ pour diminuer la résistance du béton. Habituellement les facteurs $\nu$ sont déterminés expérimentalement. L'article décrit comment on peut calculer une valeur $\nu$ sur la base d'une relation connue entre les contraintes et les déformations du béton obtenue à partir d'un essai simple de compression. Des valeurs $\nu$ théoriques sont comparées avec des valeurs empiriques pour des qualités différentes de béton.

**ZUSAMMENFASSUNG**
Die Traglast von Betontragwerken kann überschätzt werden, wenn die klassische Plastizitätstheorie ohne Modifikation angewendet wird. Deshalb wird für die praktische Anwendung die Betondruckfestigkeit um einen empirisch ermittelten Faktor $\nu$ abgemindert. Der Beitrag zeigt, wie ein Wert $\nu$ auf Grund theoretischer Überlegungen ausgehend vom Spannungs-Dehnungs-Diagramm des Betons unter einachsigem Druck bestimmt werden kann. Für verschiedene Betonfestigkeiten werden theoretische Werte $\nu$ mit empirischen verglichen.

## 1. THE USE OF THE THEORY OF PLASTICITY FOR CONCRETE

The use of the theory of plasticity for the analysis of the carrying capacity of a structure has several advantages.

It gives simpler calculations than an analysis in which the entire behaviour is followed from a purely elastic start to an elastic-plastic stage at which the carrying capacity is not increased by further deformations. The calculations can even sometimes be done manually.

As only the ultimate state is considered, no knowledge of the elastic properties is required, i.e., the carrying capacity can be determined on the basis of less information than is required for a complete elastic-plastic analysis.

However, the theory of plasticity also has a number of disadvantages.

For example, it is based on the very drastic assumption that, for strains of arbitrary magnitude, the material retains its maximum stress, in other words, that the strength is not lost again.

Furthermore, the normality criterion is assumed to apply.

From the lower-bound theorem it follows that these assumptions are the most optimistic assumptions regarding the carrying capacity that can be imagined from a knowledge of the failure criterion. It is therefore obvious that direct use of the theory of plasticity may give results that are on the unsafe side.

## 2. INTRODUCTION OF THE EFFECTIVENESS FACTOR $\nu$

In order to take account of the fact that the assumptions are not always satisfied, a correction is introduced - the effectiveness factor $\nu$ less than or equal to 1, see for instance [78.1], by which the characteristic strength values of the material are multiplied before they are used for calculation of the carrying capacity of a structure.

We can find this correction for a specific type of structure by comparing theoretically calculated capacities for the structure with the capacities measured in tests.

There is, however, another method by means of which we can, on certain assumptions, calculate an effectiveness factor on the safe side, on the basis of our knowledge of the material's stress-strain relationship. This method is demonstrated in the following.

## 3. THEOREM FOR DETERMINATION OF SAFE STRESS-STRAIN CURVES

### 3.1 Formulation

Let us imagine two structures (1) and (2) with identical geometry. The structures are subjected to the same, proportionally increasing load with the load parameter P, and it is assumed that the strain increments at each point have the same signs during the entire development of the load.

With these assumptions we can relate a strain-energy function W to each point of each structure, whereby the stresses $\sigma_{ij}$ can be obtained from the strains $\varepsilon_{ij}$ by derivation:

$$\sigma_{ij} = \frac{\partial W(\varepsilon_{ij})}{\partial \varepsilon_{ij}}$$

It is now assumed that as long as the strains lie within certain bounds $f(\varepsilon_{ij}) \leq 0$ or, written symbolically, $\varepsilon \leq \varepsilon_g$ we have:

$$W_1 \geq W_2$$

The carrying capacities $P_1$ and $P_2$ of the structures are each defined as the maximum value P can reach during loading.

We now wish to prove that

$$P_1 \geq P_2$$

provided that the strain in structure (1) does not exceed $\varepsilon_g$ at any point for $P \leq P_1$.

## 3.2 Proof

For an arbitrary displacement field that satisfies the geometrical boundary conditions, we get the potential energy:

$$\Pi_{p1} = \int_V (W_1 + \varphi) dV + \int_{A_T} \psi \, dA$$

$$\Pi_{p2} = \int_V (W_2 + \varphi) dV + \int_{A_T} \psi \, dA$$

where $\varphi$ and $\psi$ are the conservative volume and surface-load potentials, V is the volume of the structure, and $A_T$ is the part of the boundary with given surface loads.

For displacements lying within certain bounds determined by $\varepsilon \leq \varepsilon_g$ throughout, written symbolically $u \leq u_g$, the following applies:

$$W_1 \geq W_2$$

and thus

$$\Pi_{p1} \geq \Pi_{p2}$$

If $P < P_2$, then $\Pi_{p2}$ has a minimum. From this it follows that $\Pi_{p1}$, whose possible minimum lies within $u \leq u_g$, has a lower bound. This implies that $P \leq P_1$, for if P were bigger than $P_1$, $\Pi_{p1}$ could reach arbitrarily low values.

It should be noted that, theoretically, the minimum for $\Pi_{p1}$ can occur for unbounded values of u, corresponding to (1) having become a mechanism, but this means that $P = P_1$, so we still have $P \leq P_1$.

It is thus demonstrated that if $P < P_2$ then $P \leq P_1$, and thus

$$P_1 \geq P_2$$

## 4. THE REAL STRESS-STRAIN DIAGRAM

The measurement of stress-strain curves for concrete in uniaxial compression when the maximum stress has been exceeded and the stress decreases with increasing strains presents problems since the field will be unstable unless the testing machine or other parts of the test arrangement are sufficiently stiff to prevent the elastic energy in the arrangement from being released in a sudden failure. The literature therefore contains very little information on such tests.

At the University of Illinois, Wang, Shah and Naaman have carried out some compression tests on concrete cylinders, in which the stresses were measured for strains up to 6‰ [78.2]. The stiffness of the test arrangement was increased by placing a steel pipe around the concrete cylinder, whereby the pipe was subjected to the same deformations as the concrete.

The authors of [78.2] propose an analytical expression for the stress-strain curve of the form

$$Y = \frac{AX + BX^2}{1 + CX + DX^2}$$

where Y is the stress in relation to the maximum stress, $\sigma/\sigma_c$ and X is the strain in relation to the strain for maximum stress, $\varepsilon/\varepsilon_0$. A, B, C and D are constants. For each concrete strength, two sets of constants are determined, one for the rising branch $\varepsilon \leq \varepsilon_0$ and one for the falling branch $\varepsilon \geq \varepsilon_0$. The constants are determined on the basis of certain selected information, viz. that the slope for $\varepsilon = 0$ and the secant slope for $\sigma = 0.45\ \sigma_c$ both must be the secant slope to $\sigma = 0.45\ \sigma_c$ measured in the test. Further, that $\sigma = \sigma_c$ and $d\sigma/d\varepsilon = 0$ for $\varepsilon = \varepsilon_0$, and that the falling branch must pass through two specific points: the point at which the test curve has the inflexion $(\varepsilon_i, \sigma_i)$ and the point at which $\varepsilon = \varepsilon_{2i} = 2\varepsilon_i - \varepsilon_0$.

On the basis of the tests, the necessary information is found by statistical methods solely as a function of the concrete strength $\sigma_c$. A curve is thereby obtained for each value of $\sigma_c$ (in the interval 21 to 77 MPa covered by the tests).

The authors themselves think that the curves can be extended someway past the 6‰, and they show an example of this in which $\sigma_c = 41$ MPa. However, this extension is only possible for values of $\sigma_c$ in a narrow zone around $\sigma_c = 40$ MPa, since the limit value of $\sigma$ for $\varepsilon \to \infty$, viz., $\sigma_c B/D$ is approximately zero here, whereas it is positive for smaller strength values and negative for higher strength values.

For example, we obtain:

$\sigma \to 13.4$ MPa for $\varepsilon \to \infty$ and $\sigma_c = 20$ MPa

$\sigma \to -10.0$ MPa for $\varepsilon \to \infty$ and $\sigma_c = 70$ MPa

A curve that is to be used for relatively large strains must satisfy the reasonable requirement that it has the asymptotic value zero and that negative values must not occur. Here, therefore, the calculations are not based directly on the curve shown in [78.2] drawn in full line in fig. 1, but on a curve obtained by substituting the requirement that the curve shall pass through the point $(\varepsilon_i, \sigma_i)$ by the requirement that it shall have the asymptotic value zero, the dashed curve in fig. 1. In the interval $0 < \varepsilon < 6‰$, the deviations between the two curves are insignificant compared with the deviations between the analytical curves and the measured curves, see fig. 1.

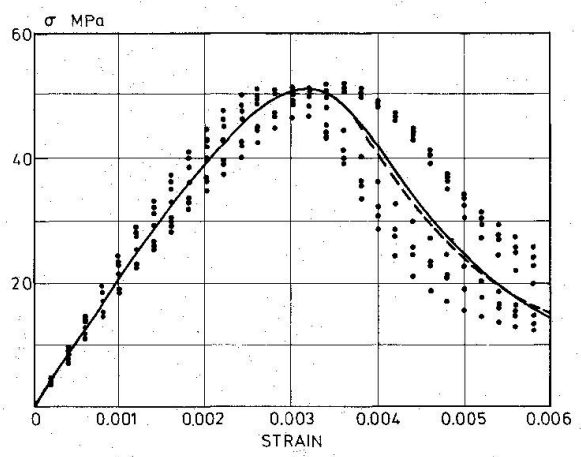


Fig. 1. Measured stress-strain curves and
——— : the analytical curve from [78.1].
------- : the modified curve with the asymptotic value zero.

## 5. THEORETICAL DETERMINATION OF ν

We now wish to use the theorem for the case of uniaxial compression of concrete. From the curve found in section 4, the area below it, i.e. the strain energy for $\varepsilon = \varepsilon_g$, $W(\varepsilon_g)$ is determined for different values of the boundary strain $\varepsilon_g$. For a curve consisting of two straight lines, a linear-elastic branch with the secant modulus mentioned earlier as slope and a plastic branch with constant stress, we then calculate the plastic stress which gives the same value of $W(\varepsilon_g)$, see fig.2.

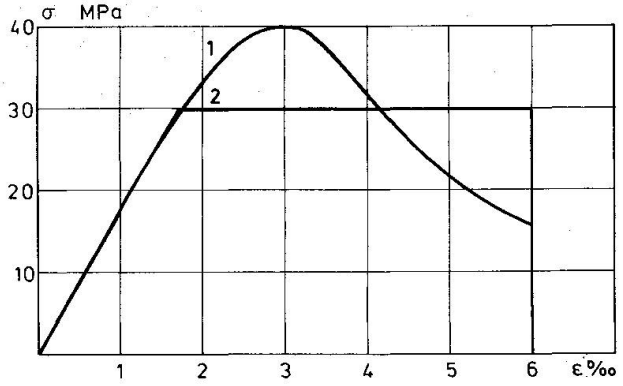


Fig. 2. 1:The analytical stress-strain curve.
2:The corresponding linear-elastic, perfectly plastic stress-strain curve.

With one insignificant exception around the transition between the elastic and the plastic branch, we find that

$$W_1(\varepsilon) \geq W_2(\varepsilon) \qquad \text{for} \qquad \varepsilon \leq \varepsilon_g$$

where the index 1 refers to the curve found in the tests, and the index 2 refers to the linear-elastic, perfectly plastic curve.

The ratio between the maximum stress on curve 2 and that at curve 1 is ν.

With the assumptions of our theorem, and provided the elastic strains are sufficiently small in relation to $\varepsilon_g$, we now know that a value for the carrying capacity of a structure calculated in accordance with the theory of plasticity with the compression strength $\nu\,\sigma_c$ will give a safe value for the actual structure. We have thus arrived at a method of calculating the effectiveness factor directly on the basis of a concrete compression test.

The calculation of ν as a function of $\varepsilon_g$ and $\sigma_c$ gives the result shown in fig. 3. The curves fall with increasing value of $\sigma_c$, since it has been found that the stress-strain curves for a strong concrete fall relatively more rapidly after passing the peak than in the case of weak concrete.

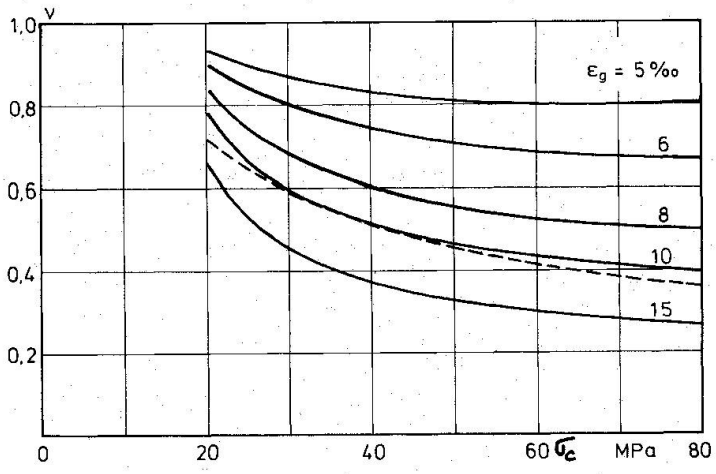


Fig. 3. $\nu$ as a function of $\varepsilon_g$ and $\sigma_c$. The dashed curve is the curve $\nu = 3.2/\sqrt{\sigma_c}$, $\sigma_c$ in MPa from fig.4.

## 6. COMPARISON WITH TESTS

The question is now: which limit strain is the right one? This question requires detailed investigation and cannot be finally answered here. In the investigations in [67.1], measurements are taken of the strains in the web of concrete beams loaded to shear failure. In some cases the measurements showed a compressive strain of up to 8‰, and these measurements were interrupted before failure.

A comparison with empirically determined $\nu$-values can be carried out by means of the results in [79.1]. Here, $\nu$ is determined for the shear strength of beams without shear reinforcement. In one of the test series [62.2], the only varying parameter is $\sigma_c$.

The test results group themselves as shown in fig. 4, in which the curve $\nu = 3.2/\sqrt{\sigma_c}$, $\sigma_c$ in MPa is included.

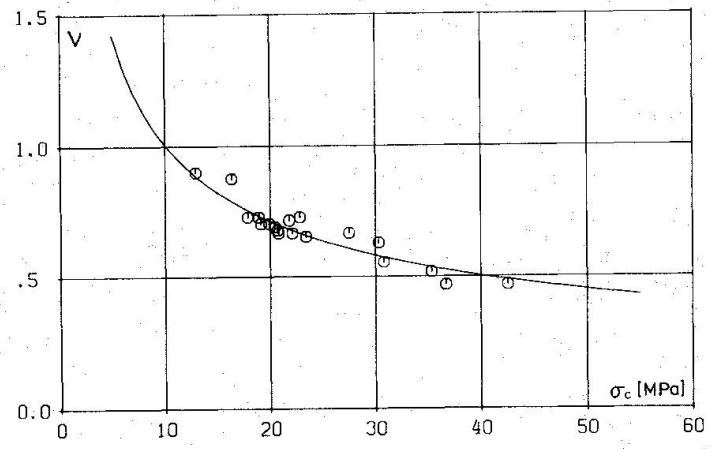


Fig. 4. Empirically determined $\nu$-curve: $\nu = 3.2/\sqrt{\sigma_c}$, $\sigma_c$ in MPa and test results from [79.1]

This curve is also shown dashed in fig. 3. It will be seen that these test results correspond well with the $\nu$-curves for $\varepsilon_g \sim 10‰$.

## 7. REMAINING THEORETICAL ASSUMPTIONS FOR USE OF THEORY OF PLASTICITY

The theory of plasticity assumes strains of arbitrary magnitude, i.e. of arbitrary magnitude in relation to the elastic strains.

In the stress-strain diagram found, there is a finite relationship between the plastic and the elastic strains. This limited yield capacity naturally results in a lower ultimate strength than calculated using the theory of plasticity, but with reasonably selected limit strains, this reduction will be of little significance. Nevertheless, in principle, it must be taken into account in another way.

As the validity of the theorem is not limited by the use of different limit strains at different points of the structure, a higher limit strain and thus a lower effective stress can be used at places where particular big strains can be expected, for instance near corners. If the highest strain here was used as the limit strain for the whole construction, the effective stress would be unnecessarily low.

## 8. EFFECT OF REINFORCEMENT ON THE $\nu$-VALUE

In a compression test on a concrete cylinder reinforced against strain in the direction perpendicular to the load, this reinforcement will somewhat increase the stiffness on the rising branch of the stress-strain curve. On the falling branch, where the concrete has a tendency during crushing to get very big strains in directions perpendicular to the direction of the compression, the reinforcement will get big stresses and will thus to a great degree limit the reduction of the concrete stress.

With the method of calculation introduced here, this will result in an increase in $\nu$. In other words, it is possible to determine the relationship between the effectiveness factor and the degree of reinforcement on the basis of tests on reinforced concrete cylinders.

## 9. CONCLUSION

It may seem very risky to use the optimistic assumptions of the theory of plasticity for calculating the carrying capacity of a structure made of a material like concrete. In practice, however, the applicability of this method of analysis has been demonstrated in many cases in [78.1]. This article shows that its use can also be justified theoretically provided a suitable effectiveness factor is introduced.

It is shown that the reason why the full compression strength of the concrete cannot be utilized in the theory of plasticity is to be found in the falling stress-strain curve of the concrete.

The empirically found decrease of the effectiveness factor with the strength of the concrete is directly explained on the basis of compression tests on concrete cylinders.

A method is given for calculating the effectiveness factor on the basis of the maximum strain. However, here we need to know more about the size of the strains that occur in a structure when the ultimate strength is reached. We also need measurements of the stress-strain curves for concrete strains of 10-15‰.

However, on account of other assumptions made in the analysis of certain types of structure, we cannot expect the introduction of a $\nu$-factor, determined as described here, to remove all systematic discrepancies between test results and theoretical results.

## 10. REFERENCES

[62.1] Van den Berg, F.J.: Shear Strength of Reinforced Concrete Beams without Web Reinforcement, part 2 - Factors Affecting Load at Diagonal Tension Cracking. Journal of the ACI - Proceedings, Vol. 59, pp 1587, Nov. 1962.

[67.1] Ozden, K.: An Experimental Investigation on the Shear Strength of Reinforced Concrete Beams. Faculty of Civil Engineering, Technical University of Istanbul, 1967.

[78.1] Nielsen, M.P., Bræstrup, M.W., Jensen, B.C. and Bach, F.: Concrete Plasticity. Danish Society for Structural Science and Engineering, 1978.

[78.2] Wang, P.T., Shah, S.P. & Naaman, A.E.: Stress-Strain Curves of Normal and Lightweight Concrete in Compression. Journal of the American Concrete Institute, November 1978, No. 11, Proceedings V.75, pp 603-611.

[79.1] Roikjaer, M., Pedersen,C., Bræstrup, M.W., Nielsen, M.P. and Bach, F.: Bestemmelse af ikke-forskydningsarmerede bjælkers forskydningsbæreevne. Structural Research Laboratory, Technical University of Denmark, 1979.

I

# A General Yield Criterion for Orthogonally Reinforced Concrete Slab Elements

Critère général d'écoulement pour des éléments de plaques en béton armé avec armature orthogonale

Eine allgemeine Fliessbedingung für orthogonal bewehrte Betonplattenelemente

P.J. COOKSON
Project Engineer
Burks Green & Partners
Newark, England

**SUMMARY**
A general criterion for orthogonally reinforced concrete slab elements yielding under combined bending, twisting and membrane forces is derived. An upper yield surface is obtained in parametric form, and an approximate closed form criterion is proposed. The approximate criterion reduces to the commonly accepted criteria for membrane forces, and bending and twisting moments, when acting alone as special cases.

**RESUME**
Un critère général d'écoulement est développé pour des éléments de plaques en béton armé avec armature orthogonale sollicités par des actions combinées de flexion et de membrane. Une surface d'écoulement circonscrite est obtenue sous forme paramétrique et un critère approché est proposé. Pour les actions isolées de flexion ou de membrane, le critère approché est semblable aux critères généralement acceptés dans ces cas.

**ZUSAMMENFASSUNG**
Eine allgemeine Fliessbedingung für orthogonal bewehrte, durch kombinierte Biege- und Membrankräfte beanspruchte Betonplattenelemente wird entwickelt. Eine umschriebene Fliessfläche wird in parametrischer Form dargestellt, und eine Näherung dafür in analytisch geschlossener Form wird vorgeschlagen. Die Näherung führt für reine Beanspruchung durch Membrankräfte beziehungsweise durch Biege- und Drillungsmomente auf die allgemein anerkannten entsprechenden Bedingungen.

## 1. INTRODUCTION

Reinforced concrete structures composed of thin-walled elements often carry external loads which produce membrane forces in the plane of the elements in combination with bending and twisting moments about axes in the plane. To be able to apply plasticity theory to such structures at the ultimate limit state it is necessary to know the yield criterion of a slab element under combined stress resultants.

This paper is concerned with obtaining such a yield criterion for a concrete slab element which has been reinforced orthogonally with layers of steel in the (x,y) directions parallel to the slab mid-plane. The sign convention for the stress resultants per unit width is shown in figure(1), for rectangular coordinates (n,t) rotated $\theta$ clockwise from the (x,y) directions.

It will be assumed that the transverse shear forces (Vt,Vn) and stresses normal to the plane of the element have negligible effect on the strength. The general yield criterion is then defined by six independent stress resultants, and may be represented by a closed convex yield surface in six-dimensional space. Previous work on such yield criteria is described by Morley[1].

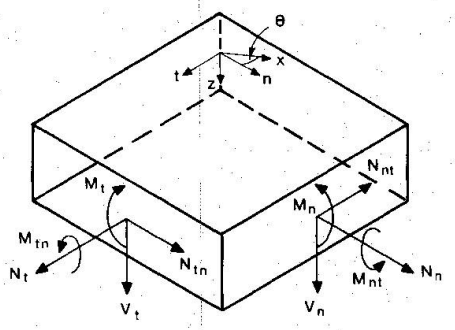


Fig.1 Sign Convention for Stress Resultants

The commonly accepted criterion for yielding to occur under bending and twisting alone is that the bending moment on a given cross-section should reach a value which is a function of the yield moments in the x and y directions alone. This "normal moment criterion", which was adopted by Johansen for his yield line theory, has been adequately justified by a method which considers the respective contributions of the steel and the concrete to the stress resultants for a specified set of strain rates. (see e.g. ref[2]).

A suitable criterion for combined bending, twisting and membrane forces which is analagous to the normal moment criterion is not obvious. In order to obtain such a criterion recourse is made to the method of postulating a set of strain rates, and from an evaluation of the contribution of each layer of material in the slab, the stress resultants are obtained by integrating across the slab thickness.

A yield criterion using this approach has been obtained [3] for a set of strain and curvature rates $\dot{\varepsilon}_t$, $\dot{\varkappa}_{nt}$, $\dot{\varkappa}_t = 0$ and $\dot{\varepsilon}_{nt}$, $\dot{\varepsilon}_n$, $\dot{\varkappa}_n \neq 0$, where $\dot{\varepsilon}_n$, $\dot{\varepsilon}_t$, $\dot{\varepsilon}_{nt}$ are the mid-depth strain-rates, and $\dot{\varkappa}_{nt}$, $\dot{\varkappa}_n$, $\dot{\varkappa}_t$ are the curvature rates: positive directions corresponding to the positive direction of the appropriate stress resultant. These strain rates describe classical yield lines, but with the additional possibility of in-plane shear deformation in the yield line. A relationship $\Phi(Mn,Nn,Nnt) = 0$ is obtained between the bending moment, normal force and in-plane shear force acting in combination on a yielding cross-section of the slab. If Mn,Nn,Nnt

are then expressed in terms of Mx,My,Mxy,Nx,Ny,Nxy and $\theta$ ,the angle between the x and n axes(fig.1) a one parameter set of hyperplanes is defined in (Mx.....Nxy) space.The hypersurface enveloped by this one parameter family represents an "upper yield surface",which is a convex surface circumscribing the actual yield surface of the body,and is defined by the set of hyperplanes which touch the true yield surface.Mathematically the envelope is obtained by eliminating $\theta$ between the expressions for $\Phi = 0$ and $\partial\Phi/\partial\theta = 0$.Braestrup[4] and Save[5] have obtained upper yield surfaces in this manner for the yielding of plates under bending and twisting alone.

The six-dimensional yield surface obtained represents a total yield surface in (Mx....Nxy) space,even though it is based on a strain rate field having one principal curvature rate and one strain rate in the direction of zero curvature rate equal to zero.The generalisation is valid because other combinations of strain rate and curvature rate can be described when the flow rule is applied to the intersections of the hypersurfaces which constitute the upper yield surface.

In the following a yield criterion in parametric form is derived,a safe approximation to this criterion is proposed,and finally the approximate surface is transposed into (Mx....Nxy) space.No rigorous proof of the continuity or the convexity of the yield surface is given.

## 2.PARAMETRIC YIELD CRITERION

The yield criterion derived below in parametric form is described in more detail elsewhere[3,6],but a brief outline is included here for completeness.

If it is assumed that transverse shear and stresses normal to the slab plane are unimportant,then the yield criteria for the steel and the concrete are required in plane stress.The steel is taken to carry stresses only in the original bar directions,and it yields at a stress $\pm\sigma_y$ .The concrete is taken to be an isotropic rigid plastic material with negligible tensile strength,and with a square principal stress yield criterion as shown in figure(2).

Under an applied set of stress resultants the element is taken to be yielding with a strain rate set defined by $\dot{\varepsilon}_{nn}$, $2\dot{\varepsilon}_{nt}$, $\dot{\varkappa}_{nn}$,as the only non-zero strain rates.Under such conditions,assuming plane sedtions remain plane,the strain rates at a distance z from the median plane(fig.1)are given by:

$$\dot{e}_t = \dot{\varepsilon}_{tt} = 0$$

$$\dot{e}_{nt} = \dot{\varepsilon}_{nt} = \text{constant}$$

$$\dot{e}_n = \dot{\varepsilon}_{nn} + \dot{\varkappa}_{nn}.z$$

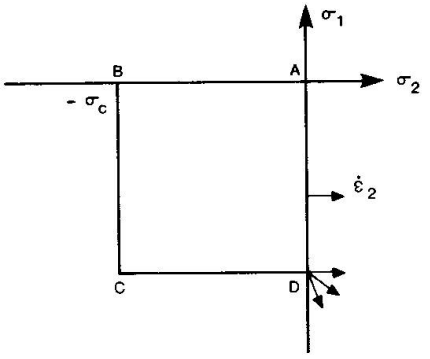


Fig.2 Yield Criterion for Concrete

From an examination of Mohr's circle it can be seen that for these conditions the principal strain rates are non-zero and of opposite sign.Therefore from the normality law the corresponding

stress states in the concrete must be defined by corners B and D of the yield criterion.Assuming that the concrete is isotropic the principal directions of stress and strain rate coincide,and the stress values at level z can be defined as follows:

$$\sigma_n = -\frac{\sigma_c}{2}\left[1 - \frac{\dot{e}_n}{\sqrt{(\dot{e}_n^2 + 4\dot{e}_{nt}^2)}}\right] \qquad \tau_{nt} = \sigma_c \cdot \frac{\dot{e}_{nt}}{\sqrt{(\dot{e}_n^2 + 4\dot{e}_{nt}^2)}}$$

The contribution of the concrete to the stress resultants can now be found from the integrals:

$$M_n^c = \int_{-h/2}^{h/2} \sigma_n z.dz \qquad N_n^c = \int_{-h/2}^{h/2} \sigma_n dz \qquad N_{nt}^c = \int_{-h/2}^{h/2} \tau_{nt} dz$$

Similar uniquely defined expressions exist for $M_t^c, N_t^c, M_{nt}^c$, as $\sigma_t$ is uniquely determined when $\dot{e}_{nt} \neq 0$.
It can then be shown that

$$M_n^c = \sigma_c \cdot \left(\frac{h}{2}\right)^2 \cdot \left[\frac{\varphi - \psi - \chi(\lambda+\mu)}{(\lambda-\mu)^2}\right]$$

$$N_n^c = \sigma_c \cdot \frac{h}{2} \cdot \left[\frac{\chi}{\lambda-\mu} - 1\right]$$

$$N_{nt}^c = \sigma_c \cdot \frac{h}{2} \cdot \frac{\psi}{\lambda-\mu}$$

where $\lambda = (\dot{e}_n / 2\dot{e}_{nt})$ at $z = +h/2$ and $\mu = (\dot{e}_n / 2\dot{e}_{nt})$ at $z = -h/2$
and

$$\chi = [1+\lambda^2]^{1/2} - [1+\mu^2]^{1/2} \qquad \varphi = \lambda[1+\lambda^2]^{1/2} - \mu[1+\mu^2]^{1/2}$$

$$\psi = \log_e\left[\frac{\lambda + (1+\lambda^2)^{1/2}}{\mu + (1+\mu^2)^{1/2}}\right]$$

Again similar parametric equations can be defined for the reactions $M_t^c, N_t^c, M_{nt}^c$. In order to obtain a closed form expression for the yield criterion in generalized stress space it would be necessary to eliminate $\lambda, \mu$ from the above expressions,and then add the steel contribution to obtain the total stress resultants.It would be difficult to eliminate $\lambda$ and $\mu$ directly so a simple conservative approximation to the parametric surface is sought.

Approximations which are within 10% of the values given by the parametric surface are discussed elsewhere[3].However in the following an alternative approximation is proposed which is more conservative,but which allows a simple transformation of the yield surface into (Mx....Nxy) space.

## 3 APPROXIMATE YIELD CRITERION

The following conditions are used as an approximate relationship between the concrete stress resultants:

$$N_{nt}^{c2} + N_n^c.[\sigma_c h + N_n^c] + 2M_n^c.\sigma_c = 0 \qquad \text{for } \dot{e}_n \geq 0 \quad ....(1)$$

$$N_{nt}^{c2} + N_n^c.[\sigma_c h + N_n^c] - 2M_n^c.\sigma_t = 0 \qquad \text{for } \dot{e}_n \leq 0$$

The two paraboloids defined by equations (1) correspond to the approximation suggested by Janas and Sawczuk[7] for a material with a maximum normal stress condition at failure.These relationships are plotted for given values of $N^c_{nt}$ in fig.(3) together with the values obtained from the parametric equations for the same values of $N^c_{nt}$ .It can be seen that under certain combinations of $N^c_{nt}$ , $M^c_n$ ,the approximate surface is very conservative.For $N^c_{nt}=0$ or $M^c_n=0$,however,the parametric values and the approximate relationships coincide:but the approximate surface has a corner when $M^c_n=0$ whilst the parametric surface is smooth.

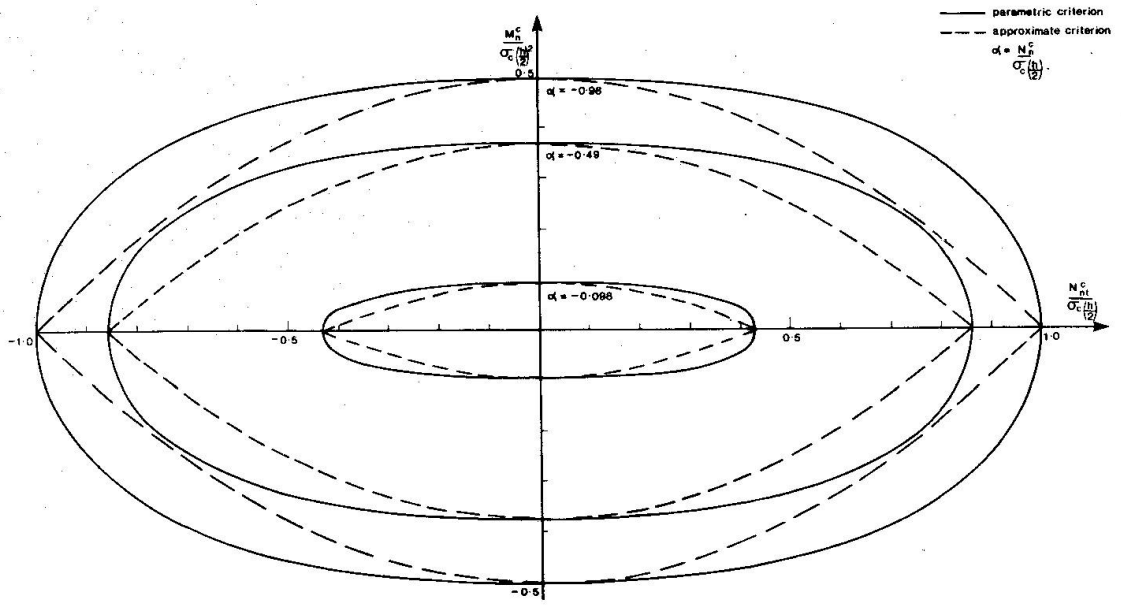


Fig.3 Yield Surfaces for Concrete Stress Resultants

The total stress resultants are obtained by adding the steel contributions $M^s_n$ , $N^s_n$ , $N^s_{nt}$ ,and equations (1) become:

$$(N_{nt}-N^s_{nt})^2 + (N_n-N^s_n).[\sigma_c h+(N_n-N^s_n)] + 2(M_n-M^s_n).\sigma_c = 0 \quad ...(2a)$$

$$(N_{nt}-N^s_{nt})^2 + (N_n-N^s_n).[\sigma_c h+(N_n-N^s_n)] - 2(M_n-M^s_n).\sigma_c = 0 \quad ...(2b)$$

It is noted that equations (2a,2b) are also valid for $\dot{\varepsilon}_{nt}=0$ i.e. a convential yield line.Under these circumstances $\sigma_n$ at a given depth z is $-\sigma_c$ or 0,but $\sigma_t$ is indeterminate as the stress states are no longer confined to the corners in fig.(2) and $M^c_t$ is therefore unknown.$M^c_{nt}$ ,on the other hand,is known to be zero.

## 4.TRANSFORMATION OF THE YIELD CRITERION TO (Mx,My...Nxy) SPACE

To define the yield locus in (Mx...Nxy) space Mn etc.are first expressed in terms of (Mx,My,.....Nxy,$\theta$) ,giving a function $\Phi=0$.A yield surface envelope is then obtained by eliminating$\theta$between the equations $\Phi=0$ and $\partial\Phi/\partial\theta=0$.
The steel reinforcement is treated as plates of constant thickness at the level of the bar centres which are only able to carry stress in the original bar directions,and which yield at a stress $\pm\sigma_y$.The slab has k layers of reinforcement in the x direction,each layer of area $a_i$ per unit length and at depth $z=d_i$ from the median plane.$A_x$ and $H_x$ are defined by:

$$A_x = \sum_k a_i r_i \qquad H_x = \sum_k d_i a_i r_i$$

where $r_i$ is the ratio of the stress in layer (i) to the yield stress $\sigma_y$ .The ratio $r_i$ when determinate takes the value of ±1.Similar expressions also define $A_y$ and $H_y$ .The steel contributions can now be defined:

$$N_n^s = \sigma_y(A_x\cos^2\theta + A_y\sin^2\theta) \qquad N_{nt}^s = \sigma_y(A_x - A_y).\sin\theta\cos\theta$$

$$M_n^s = \sigma_y(H_x\cos^2\theta + H_y\sin^2\theta) \qquad M_{nt}^s = \sigma_y(H_x - H_y).\sin\theta\cos\theta$$

Substitution of these values into equation(2a),together with the known expressions for Nn etc.in terms of Nx,Ny,Nxy,θ gives,with some rearrangement:

$$\Phi = [N_{xy}^2 + \sigma_c h(N_x - A_x\sigma_y) + (N_x - A_x\sigma_y)^2 + 2(M_x - H_x\sigma_y)\sigma_c]\cos^2\theta$$
$$+ [N_{xy}^2 + \sigma_c h(N_y - A_y\sigma_y) + (N_y - A_y\sigma_y)^2 + 2(M_y - H_y\sigma_y)\sigma_c]\sin^2\theta$$
$$- [N_{xy}.\{(N_x - A_x\sigma_y) + (N_y - A_y\sigma_y) + \sigma_c h\} + 2M_{xy}\sigma_c]\sin 2\theta = 0 \qquad ..(3)$$

Elimination of θ between the expression for $\Phi$ and $\partial\Phi/\partial\theta = 0$ gives:

$$[N_{xy}^2 + \sigma_c h(N_x - A_x\sigma_y) + (N_x - A_x\sigma_y)^2 + 2(M_x - H_x\sigma_y)\sigma_c].[N_{xy}^2 + \sigma_c h(N_y - A_y\sigma_y)$$
$$+ (N_y - A_y\sigma_y)^2 + 2(M_y - H_y\sigma_y)\sigma_c] = [N_{xy}.\{(N_x - A_x\sigma_y) + (N_y - A_y\sigma_y) + \sigma_c h\}$$
$$+ 2M_{xy}\sigma_c]^2 \qquad .....(4a)$$

and for hogging principal curvature the equivalent expression is:

$$[N_{xy}^2 + \sigma_c h(N_x - A_x\sigma_y) + (N_x - A_x\sigma_y)^2 - 2(M_x - H_x\sigma_y)\sigma_c].[N_{xy}^2 + \sigma_c h(N_y - A_y\sigma_y)$$
$$+ (N_y - A_y\sigma_y)^2 - 2(M_y - H_y\sigma_y)\sigma_c] = [N_{xy}.\{(N_x - A_x\sigma_y) + (N_y - A_y\sigma_y) + \sigma_c h\}$$
$$- 2M_{xy}\sigma_c]^2 \qquad ....(4b)$$

The general yield criterion defined by equations (4a,4b)can be used to determine which combinations of the six stress resultants (Mx,My,Mxy,Nx,Ny,Nxy) will cause yielding of a given orthogonally reinforced concrete slab element.

## 5.SPECIAL CASES FROM THE GENERAL YIELD CRITERION

### 5.1.Nx = Ny = Nxy = 0

Under these conditions equation (4a) reduces to:

$$[M_x - \sigma_y\{H_x + A_x(\tfrac{h}{2} - \tfrac{A_x\sigma_y}{2\sigma_c})\}].[M_y - \sigma_y\{H_y + A_y(\tfrac{h}{2} - \tfrac{A_y\sigma_y}{2\sigma_c})\}] = M_{xy}^2$$

which with Ax,Ay,Hx,Hy,constant for all values of θ,becomes:

$$(Mpx - Mx).(Mpy - My) = M_{xy}^2 \qquad .....(5a)$$

where Mpx,Mpy are the ultimate moments for simple bending in the x and y directions respectively.The corresponding expression for negative bending is:

$$(M'px + Mx).(M'py + My) = M_{xy}^2 \qquad .....(5b)$$

where M'px,M'py are the ultimate hogging moments in the x and y directions.

Equations (5a) and (5b) are the commonly accepted expressions for the yield criterion under bending alone.But it should be noted that $\dot{\varepsilon}_{nt} \neq 0$ on the yield line.

5.2.Mx,My,Mxy=0

If Hx=Hy=0 (which could occur for equal top and bottom reinforcement in a plate)then equations (4a,4b) become:

$$[N_{xy}^2 + \sigma_c h(N_x - A_x\sigma_y) + (N_x - A_x\sigma_y)^2] \cdot [N_{xy}^2 + \sigma_c h(N_y - A_y\sigma_y) + (N_y - A_y\sigma_y)^2]$$
$$= N_{xy}^2 [(N_x - A_x\sigma_y) + (N_y - A_y\sigma_y) + \sigma_c h]^2$$

which reduces to:

$$[(N_x - A_x\sigma_y)(N_y - A_y\sigma_y) + \sigma_c h\{(N_x - A_x\sigma_y) + (N_y - A_y\sigma_y) + \sigma_c h\} - N_{xy}^2]$$
$$\cdot [(N_x - A_x\sigma_y)(N_y - A_y\sigma_y) - N_{xy}^2] = 0$$

thus either $N_{xy}^2 = (N_x - A_x\sigma_y) \cdot (N_y - A_y\sigma_y)$ .....(6a)

or $N_{xy}^2 = [(N_x - A_x\sigma_y) + \sigma_c h] \cdot [(N_y - A_y\sigma_y) + \sigma_c h]$ ...(6b)

Equations (6a,6b) correspond to the yield criteria for in plane forces derived by Nielsen[8].It should be noted that these equations coincide with the parametric equations and are therefore exact as they satisfy equilibrium,yield and are kinematically admissible.Nielsen derived them on the basis of static admissibility.

6.DISCUSSION OF THE GENERAL YIELD CRITERION

The values to be used for Ax,Ay,Hx,Hy,in equations (4a,4b) are various.When a layer of steel is in tension or compression then the contribution to Ax etc.is clearly defined.However when the strain rate in a given steel layer is zero the steel stress is indeterminate,lying in the range $-\sigma y \leqslant \sigma s \leqslant +\sigma y$.When this occurs the corresponding value of Ax,Ay,Hx,orHy is not uniquely defined for the given set of strain rates.Consequently "flat" zones are produced in the yield surface in 6-D space as each steel layer undergoes a stress change from $-\sigma y$ to $+\sigma y$.

In most practical cases two layers of steel will be provided in the x and y directions;top steel and bottom steel.To consider every combination of tensile,compressive or indeterminate stress would lead to an extremely complex yield surface.It is therfore suggested that a restricted set of steel stresses be considered when a slab has known amounts of top and bottom steel.(The restrictions are unnecessary when using the yield criterion for provision of strength formulae).It is proposed that the top steel is taken to be $+\sigma y$ in both directions,or $-\sigma y$ in both directions,and similarly for the bottom steel.The four permutations which can be introduced into equations (4a,4b) will give eight relationships which define a yield surface in (Mx....Nxy) space.The range of validity of the eight relationships will be defined by the boundaries created from the intersection of each of the eight hypersurfaces.The yield locus thus derived either coincides with,or circumscribes,the locus which would be obtained if proper account were taken of the other

combinations of stresses occurring in the steel.Consequently the above assumptions about the steel are unsafe in some circumstances in that they overestimate the resistance of the slab element to certain combinations of applied stress resultants.However for practical reinforcement percentages the error involved will not be great,and will often be offset by the conservatism introduced by the safe approximation of the concrete contributions relative to the parametric values.

The parametric yield criterion was derived by considering a strain rate field which had one principal curvature rate,and one strain rate in the direction of zero curvature rate,equal to zero.Nevertheless the yield criterion obtained for (Mx...Nxy) space is valid for any combination of strain rates and curvature rates because the flow rule applied at the intersection of the surfaces composing the yield criterion will describe the other combinations of strain and curvature rates.The six-dimensional surface thus derived represents an upper yield surface for an orthogonally reinforced concrete plate,when transverse shear and stresses normal to the plane of the plate can be taken to have negligible influence.

The simplified approximate yield criterion could be used for calculations using assumed collapse mechanisms by applying the normality law,but such computation does not strictly represent an upper bound calculation as the yield criterion used is a lower bound approximation.Results for collapse loads thus obtained could therefore be less than or greater than the true collapse load,and subsequent comparison with experiments could give a misplaced confidence in the accuracy of the theory.For upper bound calculations it may be preferable to use approximations closer to the parametric yield surface.Such computation is feasible (see[3]) as the yield surface does not need to be defined in (Mx...Nxy) space in these circumstances.

The range of validity of a lower bound approximation to an upper yield surface is debatable.Nevertheless the parametric equations represent the true yield surface for a useful set of strain rates i.e. generalized yield lines,and the suggested approximations are not too crude for most practical cases.Therefore sufficient grounds exist to accept the resulting yield surface as a useable criterion.The proposed yield criterion is more likely to be of use for lower bound calculations,and in particular for deriving formulae for the provision of reinforcement in slabs.

1. MORLEY, C.T. "Yield Criteria for Elements of Reinforced Concrete Slabs in Plasticity in Reinforced Concrete, Introductory Report." IABSE Colloquium 1979
2. MORLEY, C.T. "On the Yield Criterion of an Orthogonally Reinforced Concrete Slab Element." J.Mech.Phys.Solids.14,1966 pp 33-47
3. COOKSON, P.J. "Generalized Yield Lines in Reinforced Concrete Slabs." To be published in J.Struct.Mechanics
4. BRAESTRUP, M.W. "Yield-Line Theory and Limit Analysis of Plates and Slabs" Mag.Conc.Res.Vol.27 No.71 pp99-106
5. SAVE, M. "A Consistent Limit Analysis Theory for Reinforced Concrete Slabs" Mag.Conc.Res.Vol.19 No.58 pp3-12
6. COOKSON, P.J. "Collapse of Concrete Box Girders involving Distortion of the Cross-Section." PhD Thesis Cambridge 1976 p.227
7. JANAS, M. & SAWCZUK, A. "Influence of Positions of Lateral Restraints on Carrying Capacity of Plates." C.E.B.Bulletin No.58 1966 pp164-189
8. NIELSEN, M.P. "On the Strength of Reinforced Concrete Discs." Acta Polytechnica Scandinavica. Ci 70, 1971 p.261

I

## Yield Polyhedron of R.C. Shear Walls under Combined Forces

Polyèdre d'écoulement pour des voiles en béton armé sollicités par des actions combinées

Fliesspolyeder für Schubwände aus Stahlbeton unter kombinierter Beanspruchung

M. YAMADA
Professor of Structural Engineering
Kobe University
Kobe, Japan

H. KAWAMURA
Research Associate Dr.-Ing.
Faculty of Engineering
Kobe University
Kobe, Japan

K. MASUO
Research Member, M.Eng.
General Building Research Cooperation
Fujishirodai, Suita
Osaka, Japan

**SUMMARY**
N-M-Q Yield Polyhedron of reinforced concrete unit shear walls subjected to the combined action of axial force, bending moment and shear force, is clarified analytically through the idealization of shear wall into a truss model. Calculated moment-shear force interaction is compared with test results. It becomes clear that there are two types of fracture modes of reinforced concrete shear walls, i.e. flexural yield and shear failure modes. On this yield polyhedron of shear wall it becomes possible to analyse the ultimate states of reinforced concrete structures with cantilever-type shear walls.

**RESUME**
En remplaçant un voile en béton armé par un treillis, on obtient un polyèdre d'écoulement soumis à l'action combinée d'un moment de flexion, d'un force axiale et d'une force de cisaillement. Des résultats d'essais sont comparés avec l'interaction calculée entre le moment de flexion et la force de cisaillement. Il y a deux types de rupture distincts: la rupture par flexion et la rupture par cisaillement. Le polyèdre d'écoulement peut former la base de l'examen de la charge ultime des structures en béton armé avec des voiles en porte-à-faux.

**ZUSAMMENFASSUNG**
Mit Betrachtungen an einem Ersatzfachwerk wird ein Fliesspolyeder für Schubwände aus Stahlbeton ermittelt, welche durch kombiniert wirkende Biegung, Normalkraft und Querkraft beansprucht werden. Der berechneten Interaktion zwischen Biegemoment und Querkraft werden Versuchsergebnisse gegenübergestellt. Zwei Versagensarten sind zu unterscheiden, nämlich Biegebrüche und Schubbrüche. Das Fliesspolyeder kann der Untersuchung der Grenztragfähigkeit von Stahlbetontragwerken mit kragträgerartigen Schubwänden zu Grunde gelegt werden.

## 1. INTRODUCTION

It has been long recognized that cantilever shear walls in multistory reinforced concrete structures are effective resisting elements against such lateral loads as earthquakes and wind loads. Many researchers [1][2][3][4][5][6] have been carried out their researches to make clear the elasto-plastic deformation and fracture behaviors of shear walls experimentally as well as analytically. As a base of deformation and fracture analysis of such structures as cantilever shear wall structures, it is desirable to develop the yield and plastification conditions of unit shear walls, which are one span and one story in cantilever shear walls.

In order to present such a base of the ultimate state analysis of structures, the senior author [7] had presented the N-M-Q yield polyhedron of rectangular and wide flange sections of elasto-plastic materials. In this paper, the yield polyhedron of unit shear walls subjected to axial force, bending moment and shear force at the upper and lower boundaries of them is developed through the idealizations of unit shear walls into a truss system. Then, moment-shear force interaction calculated for shear walls under constant axial force is compared with experimental results.

## 2. IDEALIZATIONS OF SHEAR WALLS

### 2.1 Truss Model of Shear Walls

Shear walls in multistory cantilever shear wall structures are subjected to axial force, bending moment and shear force at the upper and lower boundaries of them. These shear walls may be idealized into a truss model [8], which is composed of two vertical column elements and two diagonal brace elements hinged at the upper and lower boundaries in consequence of the observation of cracking patterns and fracture modes of tested shear walls, as shown in Fig. 1.

### 2.2 Equilibrium Equation of Truss Model

Axial force (N), bending moment (M) and shear force (Q), which act on the upper boundary of a truss model are in equilibrium with axial forces ($N_{c_1}$,$N_{c_2}$,$N_{b_1}$,$N_{b_2}$) in all elements of the truss model, as follows:

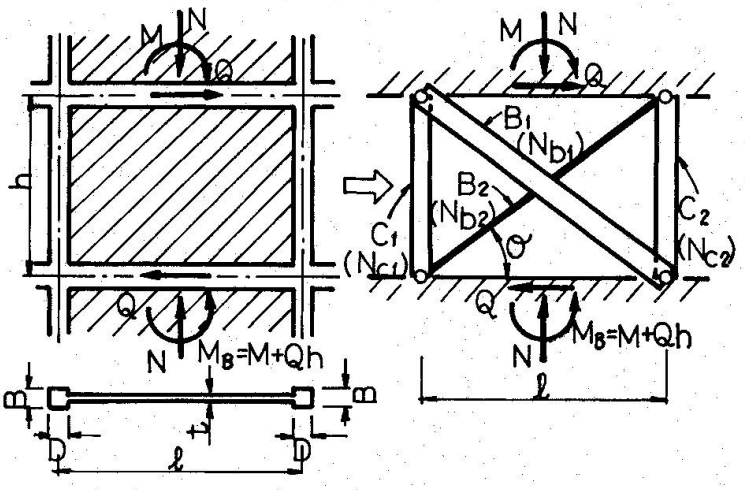


Fig. 1 Truss Model

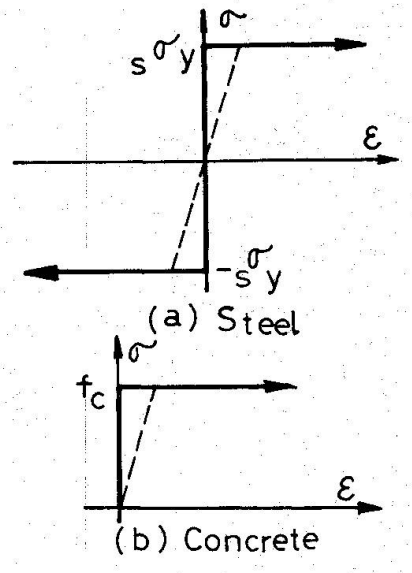


Fig. 2 σ-ε Relation

$$\begin{Bmatrix} N \\ M \\ Q \end{Bmatrix} = \begin{bmatrix} 1 & 1 & \sin\theta & \sin\theta \\ -\ell/2 & \ell/2 & -(\sin\theta)/2 & \ell(\sin\theta)/2 \\ 0 & 0 & \cos\theta & -\cos\theta \end{bmatrix} \begin{Bmatrix} N_{c_1} \\ N_{c_2} \\ N_{b_1} \\ N_{b_2} \end{Bmatrix} \tag{1}$$

## 2.3 Assumptions of Characteristics of Materials

Stress-strain relationships of concrete and reinforcing steel are assumed such as shown in Fig. 2, that is, tensile resistance of concrete is neglected and concrete shows somewhat flow after yielding.

## 2.4 Yield Axial Forces of Each Element in Truss Model

### 2.4.1 Column Elements

Side columns of shear walls are idealized into column elements. The tensile and compressive yield axial forces ($N^-_{cy}$,$N^+_{cy}$) of these elements are:

$$\begin{cases} N^-_{cy} = -\, a_c\, {}_s\sigma_y \\ N^+_{cy} = a_c\, {}_s\sigma_y + f_c\, A_c \end{cases} \tag{2}$$

where $f_c$ : compressive strength of concrete,
$A_c$ : gross area of column element (= B D),
$a_c$ : cross sectional area of longitudinal reinforcements in column,
${}_s\sigma_y$ : yield stress of reinforcing steel.

### 2.4.2 Brace Elements

Infill concrete panels with wall reinforcements are idealized into two diagonal brace elements in the following two cases:

(a) In case I, one of brace elements carry tension and the other compression. So, the infill concrete panels are idealized into a diagonal brace element which carries only compression with a definite effective width and the wall reinforcements are idealized into a diagonal brace element which carries only tension. The cross sectional area ($a_d$) of this latter element is assumed:

$$a_d = p_{wh}\, h\, t \cos\theta + p_{wv}\, \ell\, t \sin\theta \tag{3}$$

where $p_{wh}$: horizontal reinforcement ratio in wall,
$p_{wv}$: vertical reinforcement ratio in wall.

Therefore, the tensile and compressive yield axial forces ($N^-_{by_1}$,$N^+_{by_1}$) are:

$$\begin{cases} N^-_{by_1} = -\, a_d\, {}_s\sigma_y \\ N^+_{by_1} = B_e\, t\, f_c \end{cases} \tag{4}$$

where $B_e$ : effective width of concrete brace element.

(b) In case II, both of brace elements carry either tension or compression alternatively. In the former, then, the infill concrete panels are neglected. In the latter, however, they are idealized into two diagonal brace elements which carry only compression with a definite effective width defined in the case I. The wall reinforcements are idealized into two diagonal brace elements which

carry either tension or compression. It is assumed that the cross sectional areas of these elements are equal to $a_d/2$. Therefore, the tensile and compressive yield axial forces ($N^-_{by_2}$,$N^+_{by_2}$) are:

$$\begin{cases} N^-_{by_2} = -\dfrac{a_d}{2}\, s\sigma_y \\ N^+_{by_2} = \dfrac{a_d}{2}\, s\sigma_y + B_e\, t\, f_c \end{cases} \tag{5}$$

## 3. N-M-Q INTERACTION OF SHEAR WALLS

Truss model shows four modes of collapse mechanisms such as shown in Fig. 3. In these collapse mechanisms, interactions constructed for external loads applying the truss model are expressed as planes in N-M-Q space based upon the principle of virtual work, as follows.

$$\begin{cases} \text{Mode I} & : -N\dfrac{\ell}{2} + M + Q\,h = -\left( N^-_{cy}\,\ell + N^-_{by_1}\, h\cos\theta \right), \text{ for } B_1 : \text{comp.} \\ \text{Mode II} & : Q = \left( N^+_{by_1} - N^-_{by_1} \right) h\cos\theta \\ \text{Mode III} & : M + \dfrac{Q}{2}\, h = \left( N^+_{cy} - N^-_{cy} \right)\dfrac{\ell}{2} \text{ for } B_1 : \text{comp. and } B_2 : \text{tens.} \\ \text{Mode IV} & : N\dfrac{\ell}{2} + M + Q\,h = N^-_{cy}\ell + N^+_{cy_1}\, h\cos\theta, \text{ for } B_2 : \text{tens.} \end{cases} \tag{6}$$

Then, the N-M-Q polyhedral interaction are expressed as the inner surface of foregoing planes corresponding to four modes of collapse mechanisms as shown in Fig. 4, that is, this N-M-Q interaction is obtained through the upper bound theorem. On the other hand, in Fig. 4, all the combinations of yield forces of all elements are shown on the surfaces, consequently, the lower bound theorem is satisfied.

In actual calculations of N-M-Q interaction, this is composed of points, which are obtained by means of substituting the stress states described in Table 1 into Eq. (1). Because infill concrete panels with reinforcements are idealized into brace elements with two different areas $a_d$ mentioned in the section 2.4.2, two lines of $N_{b_1} = 0$, two lines of $N_{b_2} = 0$ and two lines of $Q = 0$ on the N-M-Q interaction are obtained as boundaries. Then, 3-8-13-4, 3-8-15, 2-15-16 and 1-2-16-19 planes correspond to the case II.

## 4. M-Q INTERACTION OF SHEAR WALLS UNDER CONSTANT AXIAL FORCES

In the design of actual structures, axial forces acting on shear walls are restricted to be lower than the balanced axial force above which a compressive column element begins to yield. An axial load is kept to be constant and lateral loads are applied incrementally in the experiments of shear walls. In order to compare experimental results with analytical values, N-M interaction under constant axial force is illustrated in Fig. 5(a) from N-M-Q interaction. The characteristic points on this M-Q interaction are obtained from Eq. (1), as:

$$\begin{cases} M_a = \left( \dfrac{N}{2} - N^-_{cy} - N^-_{by_1}\sin\theta \right)\ell & M_c = \left( \dfrac{N}{2} - N^-_{cy} \right)\ell \\ M'_a = \left( \dfrac{N}{2} - N^-_{cy} - N^-_{by_2}\sin\theta \right)\ell & Q_c = -N^-_{by_1}\cos\theta \\ Q_y = \left( N^+_{by_1} - N^-_{by_1} \right)\cos\theta \end{cases} \tag{7}$$

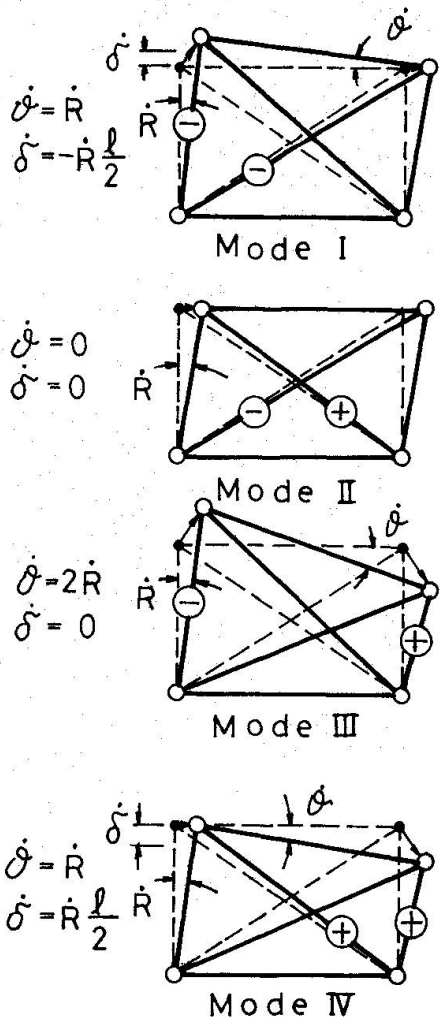


Fig. 3 Collapse Mechanisms

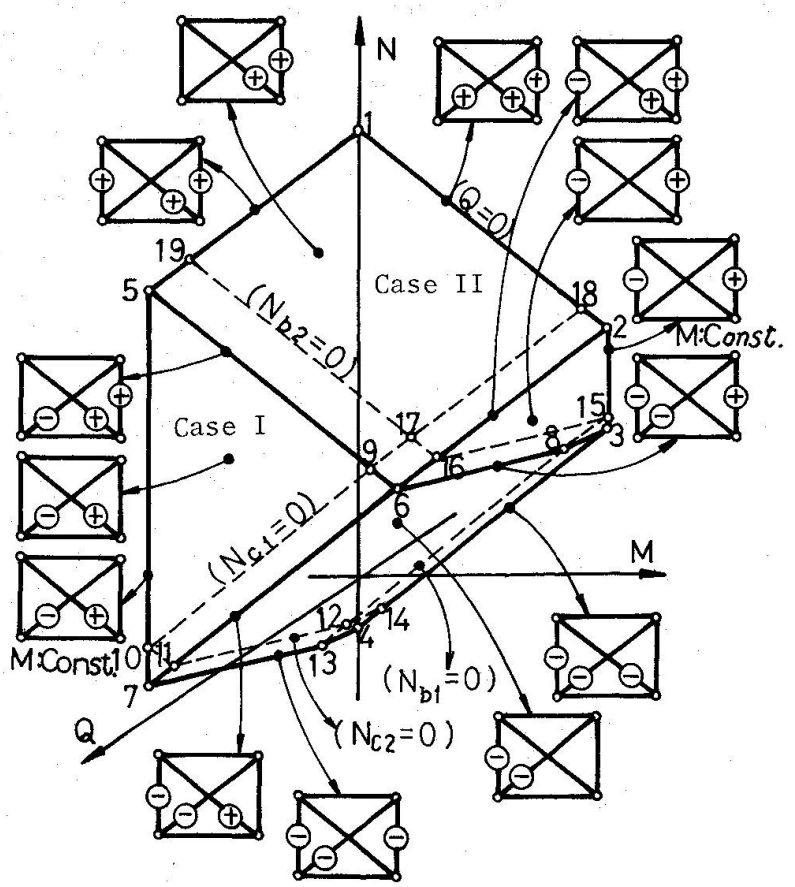


Fig. 4 N-M-Q Interaction

Table 1 Points of Intersection on N-M-Q Interaction

| Points of Intersection | | Stress States of All Elements of Truss Model | | | |
|---|---|---|---|---|---|
| | | Column Elements | | Brace Elements | |
| | | $N_{c1}$ | $N_{c2}$ | $N_{b1}$ | $N_{b2}$ |
| All Elements Yield. | 1 | $N^{-}_{cy}$ | $N^{+}_{cy}$ | $N^{+}_{by2}$ | $N^{+}_{by2}$ |
| | 2 | $N^{-}_{cy}$ | $N^{+}_{cy}$ | $N^{-}_{by2}$ | $N^{-}_{by2}$ |
| | 3 | $N^{-}_{cy}$ | $N^{+}_{cy}$ | $N^{-}_{by2}$ | $N^{-}_{by2}$ |
| | 4 | $N^{-}_{cy}$ | $N^{-}_{cy}$ | $N^{-}_{by2}$ | $N^{-}_{by2}$ |
| | 5 | $N^{+}_{cy}$ | $N^{+}_{cy}$ | $N^{+}_{by1}$ | $N^{-}_{by1}$ |
| | 6 | $N^{-}_{cy}$ | $N^{+}_{cy}$ | $N^{+}_{by1}$ | $N^{-}_{by1}$ |
| | 7 | $N^{-}_{cy}$ | $N^{-}_{cy}$ | $N^{+}_{by1}$ | $N^{-}_{by1}$ |
| One Element is "0", Another Elements Yield. | 8 | $N^{-}_{cy}$ | $N^{+}_{cy}$ | 0 | $N^{-}_{by1}$ |
| | 9 | 0 | $N^{+}_{cy}$ | $N^{+}_{by1}$ | $N^{-}_{by1}$ |
| | 10 | 0 | 0 | $N^{+}_{by1}$ | $N^{-}_{by1}$ |
| | 11 | $N^{-}_{cy}$ | 0 | $N^{+}_{by1}$ | $N^{-}_{by1}$ |
| | 12 | $N^{-}_{cy}$ | 0 | 0 | $N^{-}_{by1}$ |
| | 13 | $N^{-}_{cy}$ | $N^{-}_{cy}$ | 0 | $N^{-}_{by1}$ |
| | 14 | $N^{-}_{cy}$ | 0 | $N^{-}_{by2}$ | $N^{-}_{by2}$ |
| | 15 | $N^{-}_{cy}$ | $N^{+}_{cy}$ | 0 | 0 |
| | 16 | $N^{-}_{cy}$ | $N^{+}_{cy}$ | $N^{+}_{by1}$ | 0 |
| | 17 | 0 | $N^{+}_{cy}$ | $N^{+}_{by1}$ | 0 |
| | 18 | 0 | $N^{+}_{cy}$ | $N^{+}_{by2}$ | $N^{+}_{by2}$ |
| | 19 | $N^{+}_{cy}$ | $N^{+}_{cy}$ | $N^{+}_{by1}$ | 0 |

Then, a relation between bending moment of the upper boundary of unit shear walls and that of the lower is $M_B = M + Q\,h$, as shown in Fig.1. $M_B/M_a$ - $Q/Q_y$ interaction in which $M_B$ and $Q$ are the maximum bending moment and the ultimate shear capacity of individual shear walls is shown in Fig.5(b). When the case in which two diagonal brace elements carry only tension is neglected, this interaction is represented with two solid lines. The thick broken line illustrated in Fig.5(b) classifies shear walls into two fracture modes, i.e. flexural yield mode and shear failure mode.

## 5. EFFECTIVE WIDTH OF CONCRETE BRACE ELEMENTS IN TRUSS MODEL

The effective width of concrete brace elements is determined on the basis of experimental results [2][3] which are obtained with the loading of shearing type (diagonal loading) excluding bending moment from external loads at the upper and lower boundaries of shear walls. Then, the shear capacity of concrete brace elements ($Q_w$) is expressed:

$$Q_w = Q_u - Q_s \tag{8}$$

where $Q_u$ : ultimate shear capacity of tested shear walls,
$Q_s$ : shear capacity of wall reinforcements ( $= a_d\, {}_s\sigma_y \cos\theta$ ).

The effective width of concrete brace elements is expressed as:

$$B_e = \frac{Q_w}{f_c\, t \cos\theta} = \frac{\tau_w}{f_c}\,\frac{\ell}{\cos\theta} \tag{9}$$

where $\tau_w$ : nominal shear stress ( $= Q_w/\ell\, t$ ).

Tested results [2][3] are plotted in $\tau_c/f_c$ - $\beta_s p_w$ relation, as shown in Fig.6, where $\beta_s p_w = ( {}_s\sigma_y/f_c )\, p_w$ : reinforcing index, $p_w = p_{wh} = p_{wv}$.

It is able to recognized that $\tau_w/f_c$ is nearly equal to 0.2 independently of reinforcing index in Fig.6. Therefore, it is assumed that the effective width of concrete brace elements is equivalent to $0.2\,\ell / \cos\theta$.

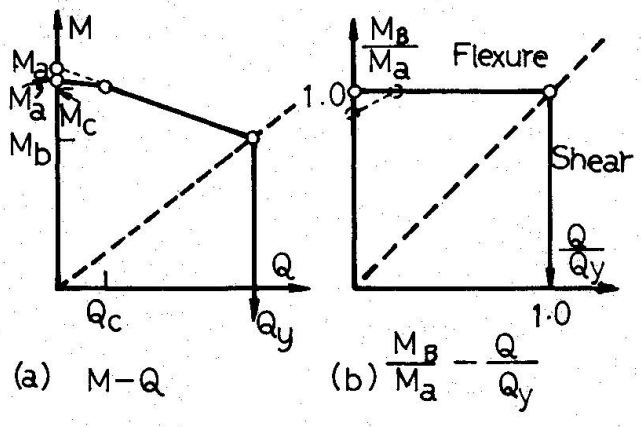


Fig. 5 Moment-Shear Force Interaction

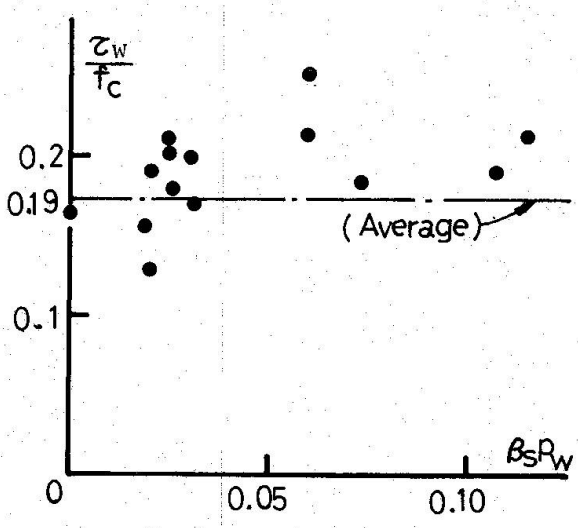


Fig. 6 $\frac{\tau_w}{f_c}$ - $\beta_s p_w$ Relation

## 6. COMPARISON OF EXPERIMENTAL RESULTS WITH CALCULATED VALUES

In the analysis of foregoing chapters, although the tensile ultimate strength of reinforcing steel is neglected, calculations for reference are carried out in consideration of them. However, the compressive ultimate strength of steel is neglected.

Tested results [4][5][6] of flexural type loading of shear walls are plotted on M-Q planes, as shown in Fig.7. Since the ultimate strength of reinforcements is not described in the original document [5], it is assumed that that of column reinforcements equal to 1.5 $_{s}\sigma_{y}$ and that of wall reinforcements equal to 1.1 $_{s}\sigma_{y}$.

It is considered that the broken line in Fig.7(a) classifies flexural yield mode and shear failure mode of shear walls. Similarly, the broken line in Fig.7(b) represents the boundary of following two failure modes of shear walls. In the first mode, shear walls may fail in shear after the yielding of reinforcements of a tensile column. In the other mode, these may not fail in shear.

The tested values of ultimate bending moment are somewhat higher than calculated yield bending moment, but coincide well with calculated ultimate bending moment for the shear walls of flexural yielding type.

The ratio of ultimate shear capacities between tested and calculated shear failure type scatter widely than the flexural yielding type. This scattering may be caused by ignoring of the confining effects [3] of side columns on infill wall panels. So, if the effective width $B_e$ of a diagonal brace element is assumed adequately, these scattering may become smaller.

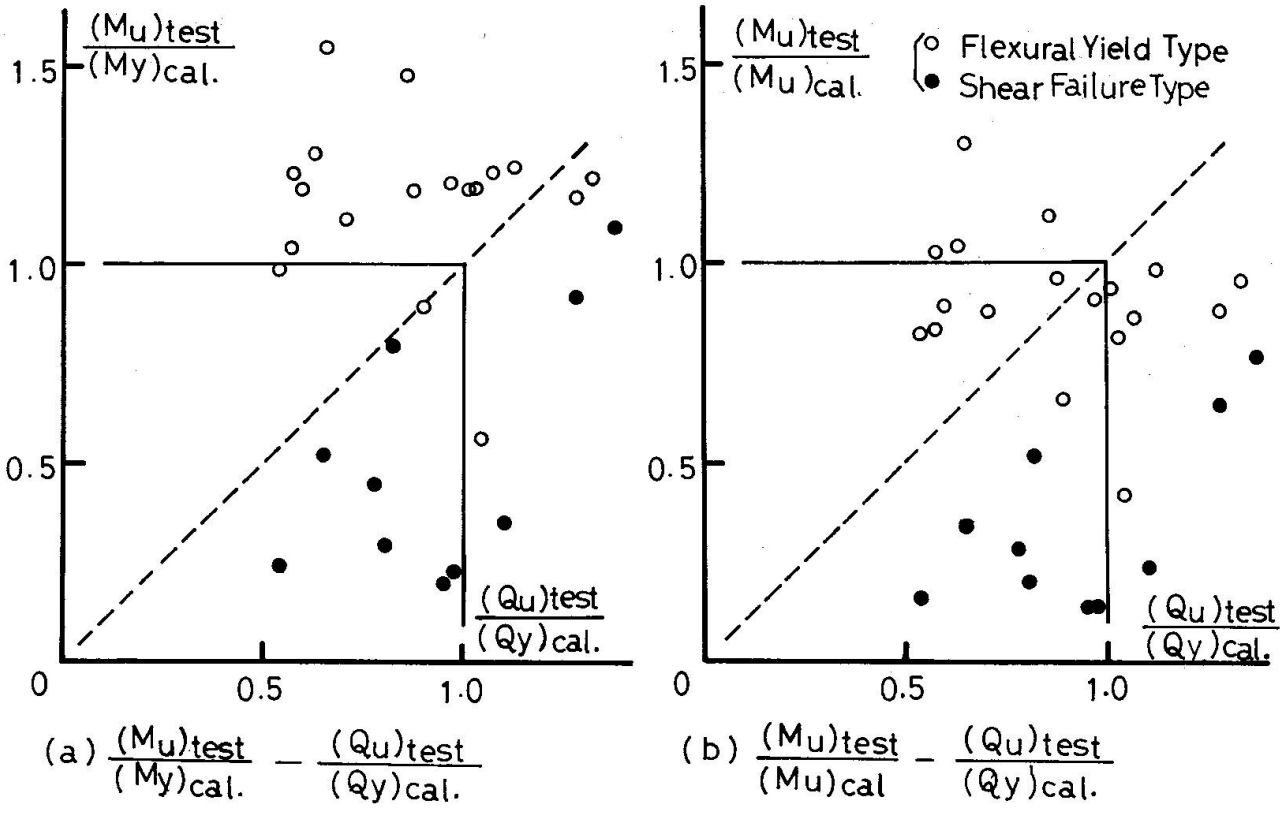


Fig. 7 Comparison of Experimental Results with Calculated Values

## 7. CONCLUDING REMARKS

Reinforced concrete shear walls subjected to the combined action of axial force, bending moment and shear force are idealized into truss model, such as shown in Fig.1. Then, the yield polyhedron of such shear walls is clarified analytically. In the analysis, the effective width of concrete brace elements is assumed to be $0.2\ell / \cos\theta$, on the basis of the experimental results of shear walls which are obtained by shear loading tests. The calculated moment-shear force interactions are compared with the experimental results of shear walls which are obtained by lateral loading tests under constant axial loads. From this analysis, therefore, possible to predict flexural yield mode and shear failure mode of shear walls and to estimate the ultimate shear resistance and bending moment of them.

## REFERENCES

1 MARTI,P.: "Plastic Analysis of Reinforced Concrete Shear Walls",Introductory Report of IABSE Colloquium Kopenhagen 1979, Plasticity in Reinforced Concrete, Oct. 1978, pp.51-69.

2 YAMADA,M., KAWAMURA,H., KATAGIHARA,K.: "Reinforced Concrete Shear Walls Without Opening; Test and Analysis", ACI Special Publication 42, Shear in Reinforced Concrete, Vol.2, 1974, pp.539-558.

3 YAMADA,M., KAWAMURA,H., INADA,A.: "Analysis of R. C. Shear Walls by Multi Brace Element Method", IABSE Colloquium, Copenhagen, 1979, Session 4, (in subscription).

4 BARDA,F., HANSON,J.M., CORLEY,W.G.: "Shear Strength of Low-Rise Walls with Boundary Elements", ACI Special Publication 53, Reinforced Concrete Structures in Seismic Zones, 1977, pp.149-202.

5 YAMAGUCHI,I., SUGANO,S., HIGASHIBATA,Y., et al: "An Experimental Study on Reinforced Concrete Shear Walls Subjected to Bending Moment, Shear and Axial Loads, (in Japanese)", (Part 1 Outline and Experimental Results), (Part 2 Discussion of Experimental Results), Rep.,Annual Meeting.,AIJ, Oct.1975,pp.1189-1192.

6 ENDOU,T., HIROSAWA,M., OZAKI,M., et al: "A Study on Effects on Protection against Collapse of Building by Shear Walls, (in Japanese)", Reseach Work for the Period 1st April 1971 - 31st March 1972, Building Research Institute, Ministry of Construction, Goverment of Japan, 1972, pp.625-632.

7 KLÖPPEL,K., YAMADA,M.: "Fließpolyeder des Rechteck- und I-Querschnittes unter der Wirkung von Biegemoment, Normalkraft und Querkraft", Der Stahlbau, 27. Jahrg. H.11, Nov. 1958, s.284-290.

8 YAMADA,M., KAWAMURA,H.: "Aseismic Capacity of Buildings --- Based upon Resonance - Fatigue - Characteristics ---, (in Japanese)", Proceedings of the Fourth Japan Symposium of Earthquake Engineering, Nov. 1975, pp.567-574.

I

# Plasticity and Endochronic Inelasticity in Finite Element Analysis of Reinforced Concrete

Plasticité et inélasticité endochronique dans l'analyse du béton armé par éléments finis

Plastizität und endochronische Inelastizität bei der Berechnung von Stahlbeton mittels finiter Elemente

S.I. SØRENSEN
Dr. ing.
The Norwegian Institute of Technology
Trondheim, Norway

**SUMMARY**
Plane reinforced concrete members subjected to monotonic and cyclic loading are analyzed by the finite element method, using different material models for concrete under compression; plasticity and endochronic inelasticity. Numerical results are compared with test results. For monotonic loading the observed behaviour is approximated equally well with both models, while the endochronic model seems to give a more realistic representation of the cyclic behaviour.

**RESUME**
Des éléments plans en béton armé sollicités par des charges monotoniques et cycliques sont analysés à l'aide de la méthode par éléments finis. Deux modèles différents sont utilisés pour le béton: plasticité et inélasticité endochronique. Des résultats numériques sont comparés avec des résultats expérimentaux. Tandis que le comportement sous une charge monotonique est bien décrit avec les deux modèles, le modèle endochronique semble donner une représentation plus réaliste du comportement sous une charge cyclique.

**ZUSAMMENFASSUNG**
Ebene Stahlbetonträger unter monoton wachsender und zyklischer Belastung werden mittels finiter Elemente untersucht. Für den Beton werden einerseits plastische und andererseits endochronisch inelastische Modelle verwendet. Numerische Resultate werden mit Versuchsergebnissen verglichen. Beide Modelle ergeben eine etwa gleich gute Näherung für das Verhalten unter monoton wachsender Belastung. Für zyklische Belastung führt das endochronische Modell zu einer realistischeren Wiedergabe des Verhaltens.

## 1. INTRODUCTION

In nonlinear analysis of reinforced concrete structures, the real behaviour of concrete in compression can be approximated by several theories. Commonly used are nonlinear elasticity and flow theory of plasticity. Several refinements have been introduced in these theories, enabling them to give a better representation of different effects in the nonlinear concrete behaviour [1-6].
A new approach, which is an important step in the direction of developing a more unified and comprehensive material model for concrete was proposed by Bazant and Bhat [7,8]. This formulation, termed endochronic inelasticity, is based on an extensive set of functions which fit most of the experimental observed effects in nonlinear concrete behaviour.

This paper deals with finite element analyses of plane reinforced concrete members, where the concrete behaviour in compression is approximated by a simple plasticity approach and endochronic inelasticity. Several numerical examples are presented and discussed.

## 2. MATHEMATICAL MODELLING OF REINFORCED CONCRETE

### 2.1 Concrete in compression

#### 2.1.1 Plasticity

The stress-strain behaviour is approximated by an elastic-strain hardening plastic approach, see Fig. 1a. The stress-strain response is assumed to be linearly elastic below the stability limit, while linear strain-hardening is assumed after the initial yielding.

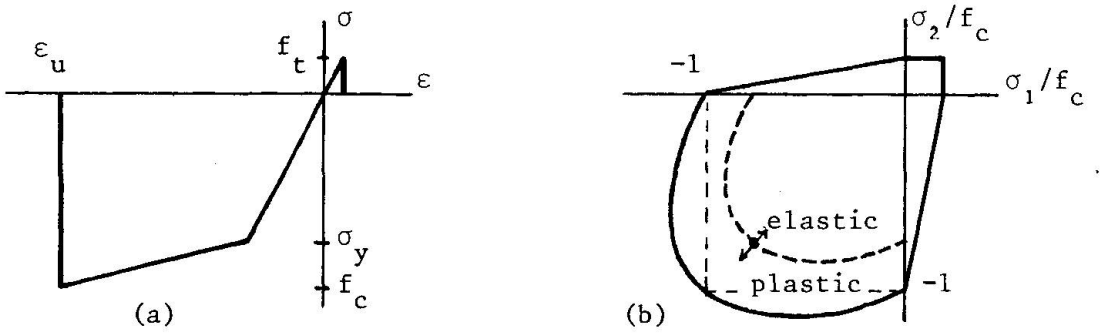


Fig.1 Plasticity model

Since only plane states of stress are considered the biaxial compressive strength is approximated by a failure envelope according to von Mises, see Fig. 1b. This is a very simple approach, and no increase of strength for equal compression in two directions is achieved. Compression failure (crushing) is assumed to occur when the compressive strength is reached.

#### 2.1.2 Endochronic Inelasticity

The endochronic theory for concrete, with material parameters as given in Ref. [7] is used in the present study. Good agreement between theory and experiments has been demonstrated; it appears that effects like nonlinear stress-strain response, inelastic dilatancy, cyclic behaviour and multiaxial strength can be represented by the endochronic model. Fits of experimental stress-strain curve and biaxial strength are shown in Fig. 2. A detailed derivation of the theory, with fits of numerous experimental data can be found in Ref. [7].

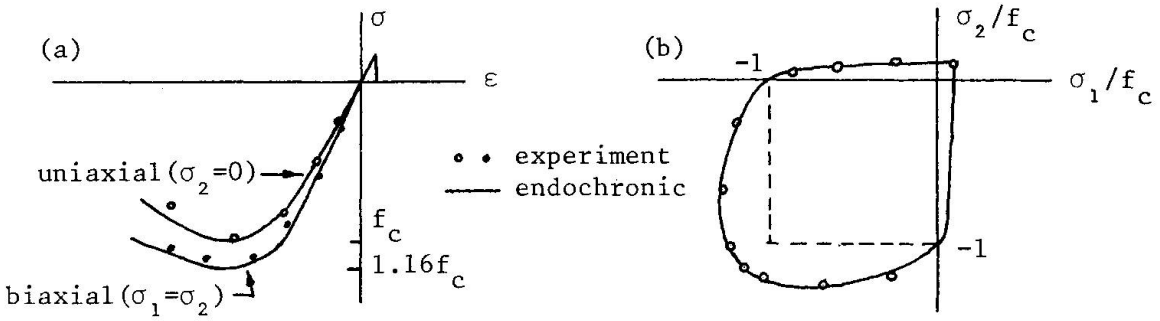


Fig.2 Endochronic model

## 2.2 Concrete in Tension

In the plasticity approach the tension cracking process is controlled by a maximum tensile stress criterion, while a combined stress and strain criterion is used in the endochronic approach. Cracks are assumed to open perpendicular to the highest principal stress or strain direction when the failure envelopes in tension regions in Figs. 1b and 2b are reached. At this point there are of course no shear stresses to be transferred across the crack. By further straining, however, shear strains may occur parallel to the crack. This raises the question of whether aggregate interlocking is capable of transferring shear stress over the crack. Shear transfer is taken into account by assuming that a "cracked" shear modulus is retained through a factor $0 \leq \alpha \leq 1$ times the elastic shear modulus. In the plasticity approach this factor is made dependent upon average crack widths computed in the program, while a constant value after cracking is used in the endochronic approach, see Fig. 3. In the endochronic approach, criteria for closing and reopening of cracks are introduced as demonstrated by Fig. 4.

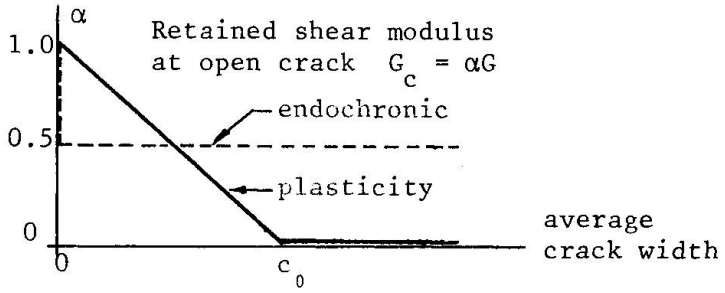


Fig.3 Shear retention factor

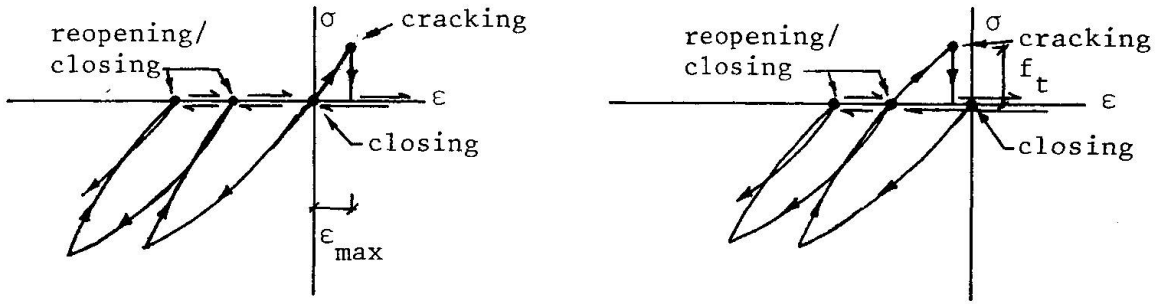


(a) First loading in tension (b) First loading in compression

Fig.4 Criteria for opening,closing and reopening of cracks

### 2.3 Reinforcement Steel Behaviour

The reinforcement steel behaviour is approximated by a uniaxial stress-strain relationship. A plasticity formulation is used, assuming linear, isotropic strain hardening after initial yielding. The stress-strain curve is assumed to be the same in tension and compression.

## 3. NUMERICAL SOLUTION TECHNIQUES

### 3.1 Finite Element Approximations

The concrete is modelled by quadrilateral, isoparametric finite elements, based on the assumption of linear interpolation functions in terms of displacements. The quadrilateral has four corner nodes with two translational degrees of freedom each. In the endochronic approach regular 2x2 Gaussian integration is used for computation of the strain energy, while the concept of selective integration according to Doherty et al [9] is used in the plasticity approach; i.e the shear strain is sampled at the centroid, but used in accumulation of strain history at the four Gaussian points. This approach improves the bending performance of the element. The reinforcement bars are modelled by simple two-noded bar elements with linear displacement interpolation. Compatibility between concrete and reinforcement is assured at common nodal points.

### 3.2 Solution Procedures

Incremental solution procedures are used in both approaches. In the plasticity program, an incremental (tangential) procedure is combined with a Newton-Raphson type iteration process. In reality, a modified version of the original Newton-Raphson process is used, since it is made possible to choose at what iteration steps the stiffness matrix is updated or kept constant.

In the computer program constructed around the endochronic model, a similar type of solution procedure is used. Errors due to incremental linearization are eliminated by carrying out equilibrium iterations in this case too. However, it should be noted that the endochronic formulation is not a tangential one. Special care must be taken in the equilibrium iteration process, since the parameters which account for inelastic effects are path dependent, and a wrong path may be followed during the equilibrium iterations. Such problems can be avoided by using a solution procedure as proposed in Ref.[10]. The iteration is terminated when the displacement corrections become sufficiently small, measured in terms of a modified displacement norm, see Bergan and Clough [11], or when a prescribed minimum number of cycles has been reached.

## 4. NUMERICAL APPLICATIONS

### 4.1 Monotonically Loaded Members

#### 4.1.1 Bending Failure

A simply supported beam was tested by Burns and Siess [12] . The behaviour under monotontically increasing load is analyzed by the plasticity and endochronic models. The test specimen failed by yielding of reinforcement at 156 kN. Figure 5 shows finite element idealization, midspan load deflection curves and computed crack patterns. It appears that both models approximate degredation of stiffness due to cracking, and ultimate load with fairly good accuracy.

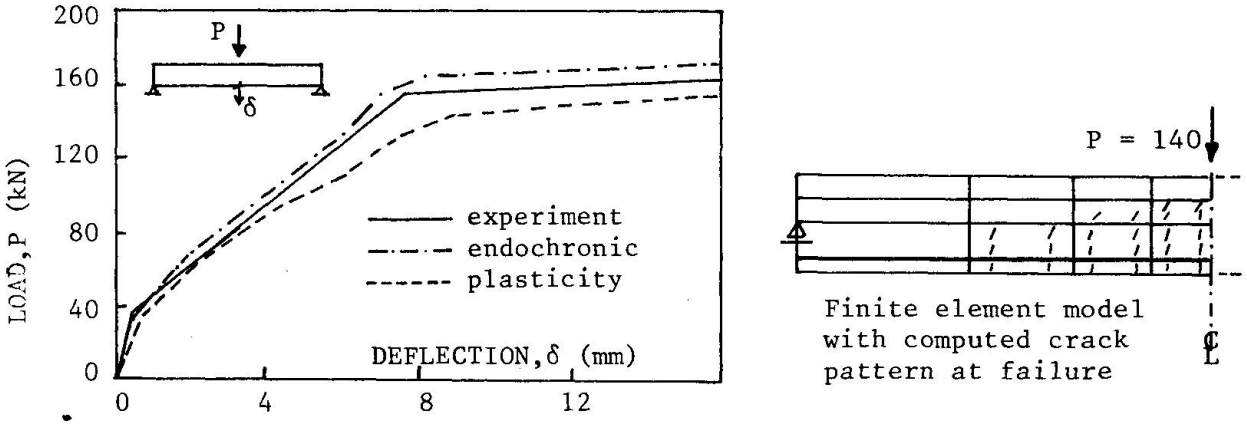


Fig.5 Results from analyses, Burns-Siess beam

### 4.1.2 Diagonal Tension Failure

A beam, tested by Bresler and Scordelis [13], is also analyzed using both material models. The test specimen failed by a rapid diagonal tension failure mechanism at a load level of 258,1 kN. Figure 6 shows experimental and numerical load-deflection curves. Both models show good agreement with the test with respect to cracked stiffness. As regards ultimate load at failure, no such load can be seen from the endochronic approach. The plasticity approach, however, indicated a failure load of approximately 230 kN, which is about 10 percent below the experimental value.

The different results can be explained by the different assumptions of shear retention after cracking, and the differences in the numerical integrations which are used. This is discussed in Ref. [14].

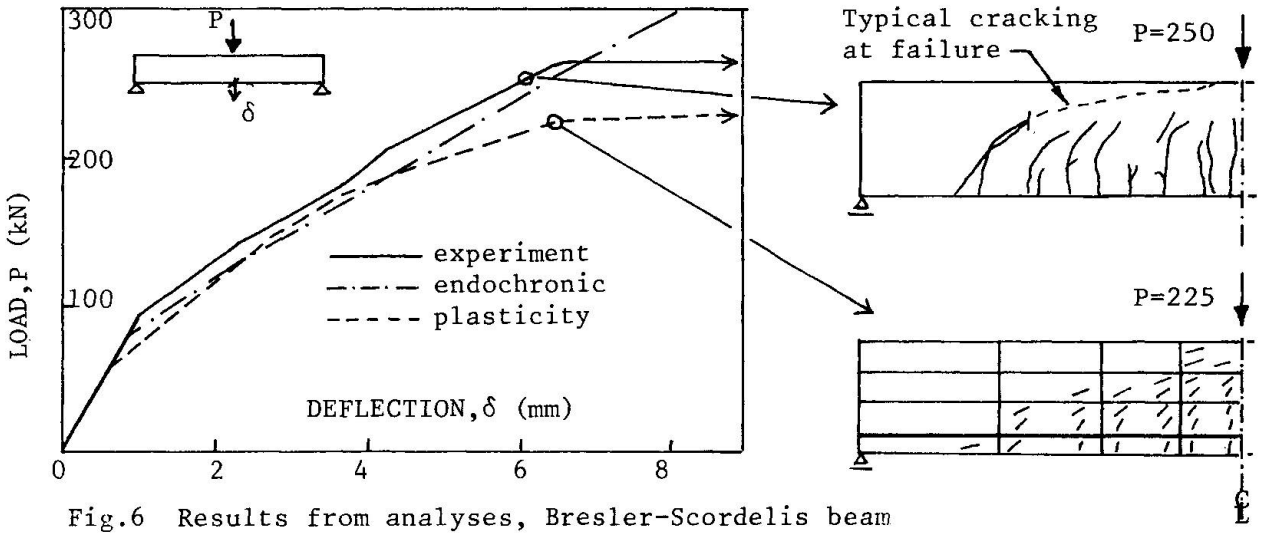


Fig.6 Results from analyses, Bresler-Scordelis beam

### 4.2 Cyclically loaded Members

A shear panel subjected to cyclic loading was tested by Cervenka [15]. The specimen was first subjected to two load cycles with amplitude P=±53,4 kN, which is approximately 46 percent of an analytically predicted monotonic failure load. Tension cracking is the dominant nonlinear effect within this load range, which may be termed "elastic cycling". Further, the specimen was subjected to load cycles with amplitude P = ± 102,3 kN, which is about 88% of the predicted failure load. Yielding of reinforcement and inelasticity of concrete in compression appeared in these cycles, which then may be termed "plastic cycling".

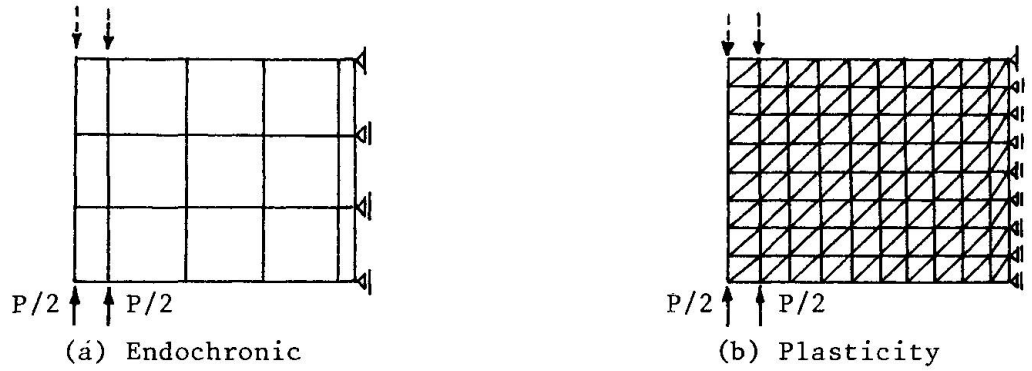


(a) Endochronic (b) Plasticity

Fig.7 Finite element idealizations of Cervenka's shear panel

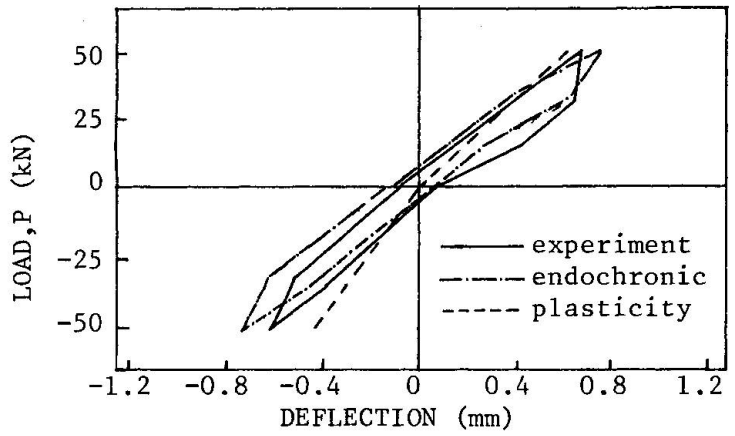


(a) Second load cycle (elastic)

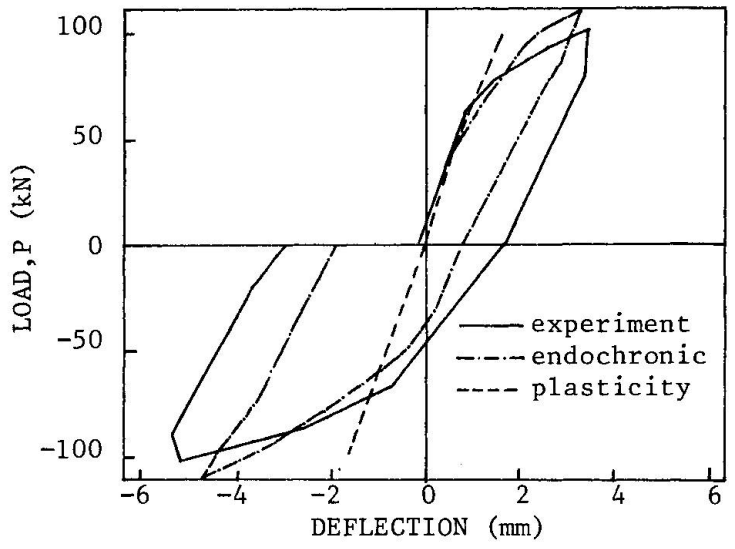


(b) Third load cycle (plastic)

Fig.8 Results from analyses, Cervenka's shear panel

The endochronic model is used to analyze the behaviour during the three first cycles (two elastic and one plastic). A detailed description is given in Ref. [10]. The finite element model is shown in Fig. 7a. For comparison, numerical results obtained by Cervenka, using a plasticity model similar to the one in the present study are presented [15, 16, 17]. Fig. 7b shows the finite element model (triangular elements) used in the plasticity approach.

Fig. 8 a-b shows experimental and numerical load-deflection curves. It appears that the results obtained by the endochronic model compare favourably with the experiments. This is probably due to a better representation of cyclic stress-strain behaviour in the endochronic model, but also, as pointed out by Cervenka and Gerstle [17], because a crack mode with two cracks opened simultaneously at a point must be included. This possibility is not taken into account in Cervenka's analysis, while it is included in the endochronic model.

## 5. CONCLUSIONS

On the basis of the limited amount of results presented, the following conclusions may be drawn:

- As could be expected, the simple plasticity model and the endochronic model are both capable of approximating the behaviour of monotonically loaded members in a plane stress situation with fairly good accuracy.
- As regards cyclically loaded members, the endochronic model seems to give better results than the plasticity model used in this study.
  The possibility of having two cracks open simultaneously at a point should be included when cyclic behaviour is considered.

If triaxial states of stress were considered, the endochronic model must be expected to be superior to the simple plasticity model in compression, where the sensitivity to hydrostatic pressure is neglected. However, more refined plasticity models as proposed in Refs.[4, 5, 6] have to be compared numerically to the endochronic model before any general conclusions can be drawn.

## 6. REFERENCES

[1] KUPFER, H.B. and GERSTLE, K.H.: "Behaviour of Concrete under Biaxial Stresses", ASCE Jorun. Eng. Mechn. Div., Vol. 99, No. EM4, August 1973, pp. 853-866.

[2] CEDOLIN, L, CRUTZEN, Y.R.J. and DEI POLI, S.: "Stress-Strain Relationship and Ultimate Strength of Concrete under Triaxial Loading Conditions", Costuzioni in Cemento Armato, Studi & Rendiconti, Vol. 13, 1976, pp. 123-137.

[3] GERSTLE, K.H. et al.: "Behaviour of Concrete under Multiaxial Stress States", Paper presented at the ASCE Annual Convention, Chicago, Illinois, Oct. 1978.

[4] ARGYRIS, J.H. et al.: "Recent Developments in the Finite Element Analysis of Prestressed Concrete Reactor Vessels", ISO-Report No. 151, Stuttgart, 1973.

[5] WILLIAM, K.J. and WARNKE, E.P.: "Constitutive Model for the Triaxial Behaviour of Concrete", Seminar on Concrete Structures subjected to Triaxial Stresses, ISMES, Bergamo, Italy, May 1974.

[6] CHEN, A.C.T. and CHEN, W.F.: "Constitutive Relations for Concrete", ASCE Journ. Eng. Mech. Div., Vol. 101, No. EM4, August 1975, pp.465-481.

[7] BAZANT, Z.P. and BHAT, P.: "Endochronic Theory of Inelasticity and Failure of Concrete", ASCE Journ. Eng. Mech. Div., Vol. 102, No. EM4, August 1976, pp. 701-702.

[8] BAZANT, Z.P. and BHAT, P.: "Prediction of Hysteresis of Reinforced Concrete Members", ASCE Journ. Struct. Mechn. Div., Vol. 103, No. ST1, Jan. 1977, pp. 156-167.

[9] DOHERTY, P.W., WILSON, E.L. and TAYLOR, R.L.: "Stress Analysis of Axi-Symmetric Solids Using Higher Order Quadrilateral Finite Elements", SESM Report No. 69-3, Univ. of California, Berkeley, 1969.

[10] SØRENSEN, S.I.: "Endochronic Theory in Nonlinear Finite Element Analysis of Reinforced Concrete", Report No. 78-1, The Div. of Struct. Mechanics, The Norwegian Inst. of Technology, The University of Trondheim, March 1978.

[11] BERGAN, P.G. and CLOUGH, R.W.: "Convergence Criteria for Iterative Processes", AIAA Journal, Vol. 10, No. 8, 1972, pp. 1107-1108.

[12] BURNS, N.H. and SIESS, C.P.: "Load-deformation Characteristics of Beam-Column Connections in Reinforced Concrete", SRS No. 234, Civil Eng. Studies, Univ. of Illinois, Urbana-Champaign, Illinois, Jan. 1962.

[13] BRESLER, B. and SCORDELIS, A.C.: "Shear Strength of Reinforced Concrete Beams - Series II", SESM Report No. 64-2, Univ. of California, Berkely, Dec. 1964.

[14] ARNESEN, A., SØRENSEN, S.I. and BERGAN, P.G.: "Nonlinear Analysis of Reinforced Concrete", Paper presented at Int.Conf. on Engineering Application of the Finite Element Method, A/S COMPUTAS, Oslo, Norway May 9-11, 1979.

[15] CERVENKA, V.: "Inelastic Finite Element Analysis of Reinforced Concrete Panels", Ph.D. Dissertation, Dept. of Civil Engineering, Univ. of Colorado, Boulder, 1970.

[16] CERVENKA, V. and GERSTLE, K.H.: "Inelastic Analysis of Reinforced Concrete Penels: Theory", IABSE Publications, Vol. 31-II, 1971, pp. 31-45.

[17] CERVENKA, V. and GERSTLE, K.H.: "Inelastic Analysis of Reinforced Concrete Panels: Experimental Verification and Application", IABSE Publications, Vol. 32-II, 1972, pp. 25-39.

SUMMARY OF DISCUSSION - SESSION 1

The discussion of the contributions to Session 1 turned in the main about several distinct topics and will be summarized under corresponding headings:

1. Relation between Plasticity Theory and Concrete Behaviour

A. Sawczuk stressed the desirability of following a continuum mechanics approach in formulating failure criteria for concrete, and indicated difficulties arising from cracking, stress histories, etc. He also indicated the need for a stress-strain law at yielding. Z. Sobotka elaborated along similar lines, showing interaction formulae for yielding of orthotropic slabs which include the effects of compressibility.

An exchange between D.H. Clyde and W.F. Chen concerned the effect of assumed tensile concrete strength on the rigour of plasticity theory for concrete.

H. Exner's paper elicited several comments. Clark questioned the applicability of the "effectiveness factor" to narrow plastic shear zones. P. Marti pointed out the inability of the formulation to consider local unloading. He also explained the effectiveness factor as a means of obtaining the average failure stress in a particular strain range. In responding, H. Exner agreed as to the importance of the actual stress- or strain history of the problem.

2. Relation between Plain and Reinforced Concrete Behaviour

S.M. Uzumeri pointed out the difficulty of using plain concrete laws as models for actual situations in reinforced concrete members, such as the effect of confinement. M.P. Collins also observed that the strain field in the vicinity of reinforcement could not easily be represented in tests on plain concrete. W.F. Chen responded that before going on to more complicated problems, we need to know the behaviour of the concrete alone.

3. Tensile Strength

M. Virlogeux enquired into our knowledge of tensile behaviour and was answered by T. Bröndum-Nielsen that tensile stress-strain curves had been obtained in Copenhagen.

K.H. Gerstle commented on the inconsistency of a zero-tension strength assumption for zones of high shear. M.W. Braestrup and M.P. Collins pointed out that even in such cases shear strength without tension strength was possible due to confinement effects.

M.D. Kotsovos, on the other hand, observed that cracking should not only be associated with applied tensile stress but also with internal stress concentrations.

## 4. Shear Transfer Across Cracks

C.T. Morley and R.P. Johnson (in reference to S.I. Sörensen's paper) enquired into shear strength and stiffness across cracks; R.P. Johnson pointed out that the shear stiffness depended on crack width, and therefore crack spacing. S.I. Sörensen explained that in the absence of test data, he had assumed crack widths between 0.0 and 0.5 mm. G. Mehlhorn cited analyses which indicated incompatibility of results with the actual assumed value, other than zero, of the shear stiffness across cracks.

## 5. Endochronic Theory

Great interest was shown in S.I. Sörensen's comparison of results of plasticity and endochronic analyses. J. Blaauwendraad questioned whether equal care had been used in formulating both approaches; S.I. Sörensen's reply indicated that his endochronic model was more refined than his plasticity model. Computer time requirements also played a role in assessing relative merits; at present, work was under way in Trondheim to improve the efficiency of the endochronic analysis.

K.H. Gerstle pointed out that Darwin and Pecknold had obtained results similar to Sörensen's using a simpler approach, whereupon V. Cervenka suggested care in such comparisons; his analysis (on which these comparisons were based) had neglected one important crack mode, which might have made his panel too stiff. M.D. Kotsovos, finally, commented favorably on the fundamental rigour of the endochronic theory compared to the other analyses.

K.H. GERSTLE